

# Discovery of Novel and Potent *N*-Methyl-D-aspartate Receptor Positive Allosteric Modulators with Antidepressant-like Activity in Rodent Models

Zhongtang Li,<sup>||</sup> Guanxing Cai,<sup>||</sup> Fan Fang,<sup>||</sup> Wenchao Li, Minghua Fan, Jingjing Lian, Yinli Qiu, Xiangqing Xu, Xuehui Lv, Yiyang Li, Ruqiu Zheng, Yuxi Wang, Zhongjun Li, Guisen Zhang, Zhenming Liu,\* Zhuo Huang,\* and Liangren Zhang\*



Cite This: *J. Med. Chem.* 2021, 64, 5551–5576



Read Online

ACCESS |



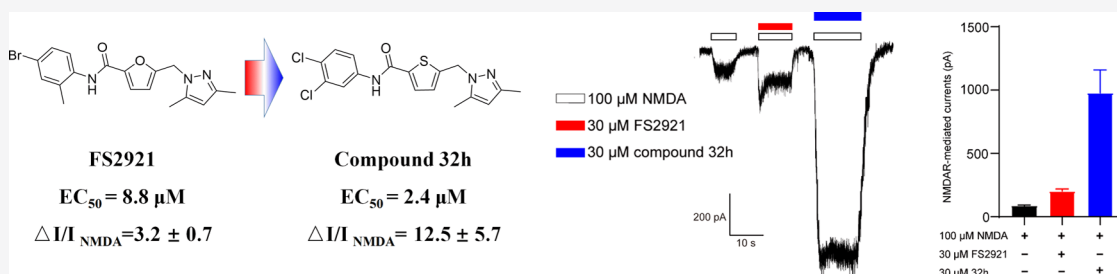
Metrics & More



Article Recommendations



Supporting Information



**ABSTRACT:** *N*-Methyl-D-aspartate receptors (NMDARs) are glutamate-gated  $\text{Na}^+$  and  $\text{Ca}^{2+}$ -permeable ion channels involved in excitatory synaptic transmission and synaptic plasticity. NMDAR hypofunction has long been implicated in the pathophysiology including major depressive disorders (MDDs). Herein, we report a series of furan-2-carboxamide analogues as novel NMDAR-positive allosteric modulators (PAMs). Through structure-based virtual screen and electrophysiological tests, FS2921 was identified as a novel NMDAR PAM with potential antidepressant effects. Further structure–activity relationship studies led to the discovery of novel analogues with increased potentiation. Compound 32h caused a significant increase in NMDAR excitability *in vitro* and impressive activity in the forced swimming test. Moreover, compound 32h showed no significant inhibition of hERG or cell viability and possessed a favorable PK/PD profile. Our study presented a series of novel NMDAR PAMs and provided potential opportunities for discovering of new antidepressants.

## INTRODUCTION

MDDs involve depressed mood, loss of interest and enjoyment, and decreased energy, causing increased global disability and suicide rates.<sup>1</sup> However, the pathogenesis of MDDs remains complicated and unclear. Thus far, the monoamine-deficiency hypothesis is the main pathophysiological explanation of MDDs. However, considering a number of refractory patients, a novel therapeutic mechanism should be proposed.<sup>2</sup>

The recent approval of esketamine by the Food and Drug Administration (FDA) for treating treatment-resistant depression represents an important milestone in MDD drug discovery; indeed, this is the first mechanistically distinct drug approved in the past three decades. Although it is an *N*-methyl-D-aspartate receptor (NMDAR) blocker, esketamine (**1**) can alleviate depressive symptoms in deeply depressive and treatment-resistant patients via complex mechanisms, mainly including synaptic or GluN2B-selective extrasynaptic NMDAR inhibition, inhibition of NMDARs localized on GABAergic interneurons, and inhibition of NMDAR-dependent burst firing of lateral habenula neurons.<sup>3,4</sup> However, there are several apparent limitations of esketamine, including its potential for

abuse, cardiovascular and urinary tract side effects, and its dissociative effects necessitating the hospitalization of patients during the treatment. Therefore, the identification of safer NMDAR modulators is an essential goal in discovering novel antidepressants.<sup>5</sup>

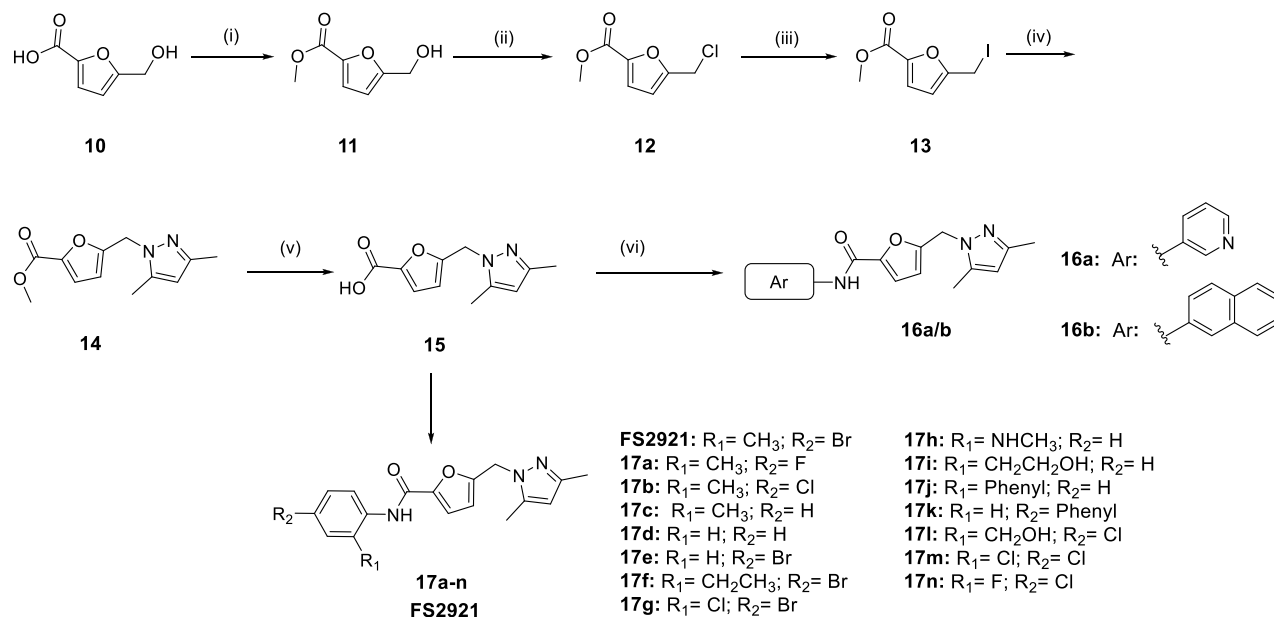
NMDARs are distinct dual-ligand-gated ion channels activated by the brain's primary excitatory neurotransmitter, L-glutamate, and another co-agonist, D-serine or glycine. As a heterotetrameric complex, the NMDAR is assembled by two obligatory GluN1 subunits with either two GluN2 subunits (including GluN2A–GluN2D) or a combination of one GluN2 subunit and one GluN3 subunit (including GluN3A–GluN3B).<sup>6</sup> NMDARs are nonselective to  $\text{Na}^+$ ,  $\text{K}^+$ , or  $\text{Ca}^{2+}$ ;

Received: November 21, 2020

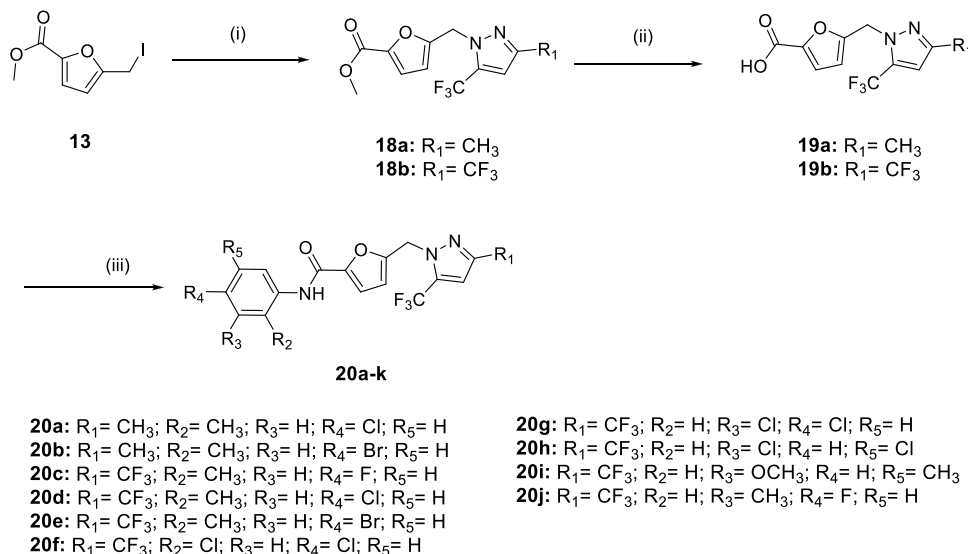
Published: May 3, 2021





Scheme 2. Synthesis of Compounds 16a/b and 17a-n<sup>a</sup>

<sup>a</sup>Reagents and conditions: (i) H<sub>2</sub>SO<sub>4</sub>, MeOH; (ii) SOCl<sub>2</sub>, DMF, CH<sub>2</sub>Cl<sub>2</sub>, 0 °C to r.t., 1 h; (iii) NaI, acetone, reflux, 0.5 h; (iv) 3,5-dimethyl-1H-pyrazole or 3,5-difluoromethyl-1H-pyrazole, K<sub>2</sub>CO<sub>3</sub>, CH<sub>3</sub>CN, 60 °C, 7 h; (v) NaOH, MeOH, 40 °C, 3 h; (vi) 3-aminopyridine for **16a** and 2-naphthylamine for **16b** and substituted aniline for **17a-n** or DIPEA, HATU, CH<sub>2</sub>Cl<sub>2</sub>, 0 °C to r.t., 12 h.

Scheme 3. Synthesis of Compounds 20a-j<sup>a</sup>

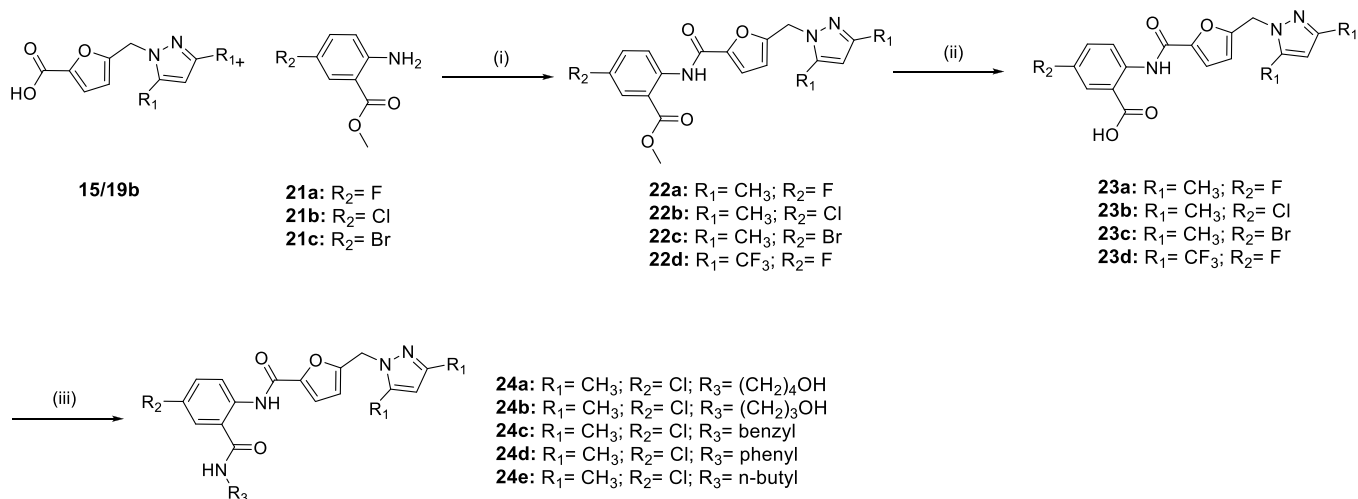
<sup>a</sup>Reagents and conditions: (i) 3-methyl-5-trifluoromethyl-1H-pyrazole or 3,5-difluoromethyl-1H-pyrazole, K<sub>2</sub>CO<sub>3</sub>, CH<sub>3</sub>CN, 60 °C, 7 h; (ii) NaOH, MeOH, 40 °C, 3 h; (iii) substituted aniline, DIPEA, HATU, CH<sub>2</sub>Cl<sub>2</sub>, 0 °C to r.t., 12 h.

## RESULTS AND DISCUSSION

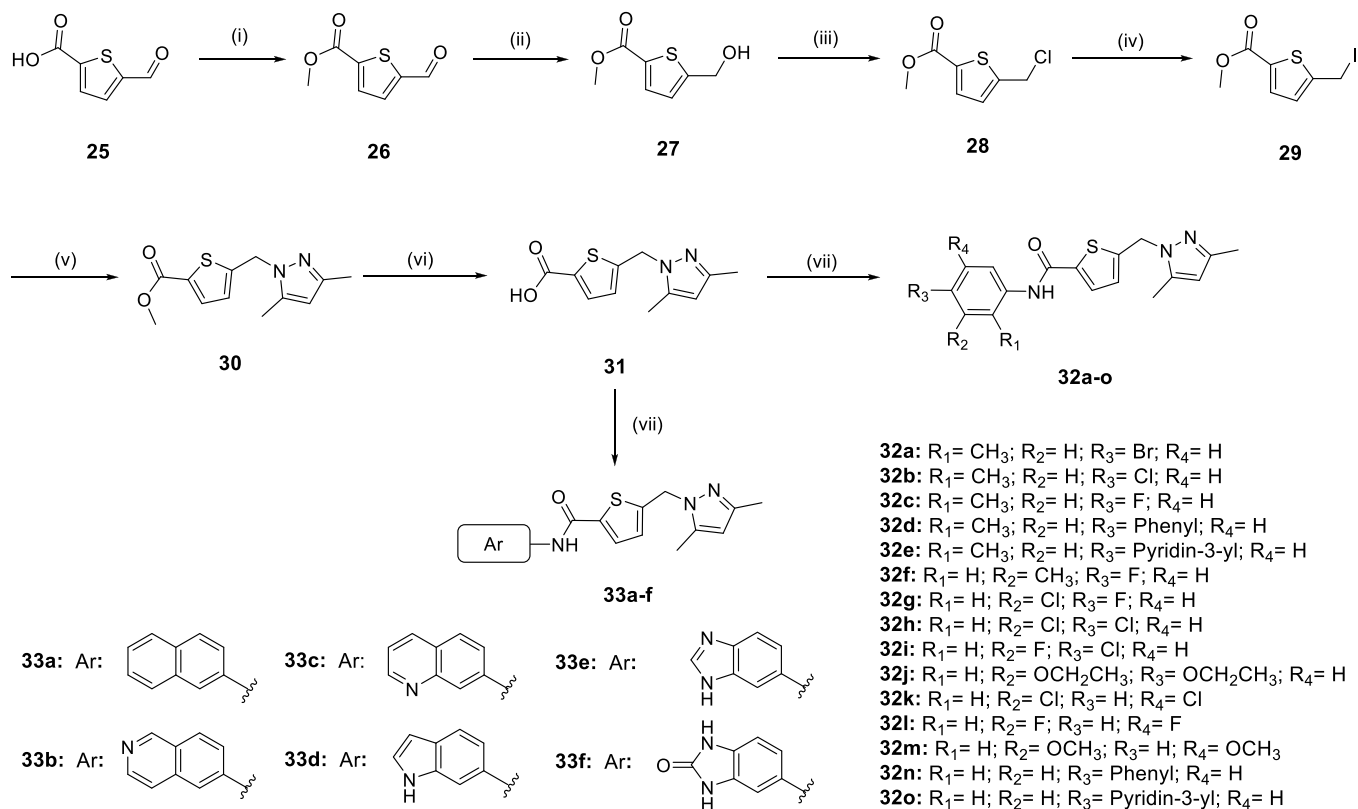
**Structure-Based Virtual Screening and Identification of Two Potential NMDAR PAMs.** Several studies identified an allosteric binding site for GNE series compounds between the GluN2A and GluN1LBDs.<sup>32–35</sup> Our workflow of virtual screening is summarized in the protocol in Figure 1A. One co-crystal structure (PDB ID: 5KDT, Table S1) of GNE0723 was chosen for the virtual screening to identify novel NMDAR ligands. More than 300,000 compounds from the SPECS chemical library and the Chinese National Compound Library of Peking University (PKU-CNCL) were docked onto the crystal structure using the Glide molecular docking module.

Sorted by docking score, all compounds within the top one percent were obtained. Because the residue Val266 of GluN2A at the dimer interface is a key residue for the selectivity of GluN2A-containing NMDARs, compounds interacting with Val266 were isolated using the PoseFilter module in the Maestro platform. Based on compound docking results and physicochemical properties, eight compounds were purchased for further biological activity tests (Table S2). All of the active compounds passed the pan assay interference compound (PAINS) test by PAINS-remover.<sup>36</sup>

The NMDAR currents induced by NMDA in mouse brain slices were detected by patch-clamp experiments. As depicted

Scheme 4. Synthesis of Compounds 24a-e<sup>a</sup>

<sup>a</sup>Reagents and conditions: (i) DIPEA, HATU, CH<sub>2</sub>Cl<sub>2</sub>, 0 °C to r.t., 12 h; (ii) NaOH, MeOH, 40 °C, 3 h; (iii) 4-amino-1-butanol for **24a**, 3-aminopropanol for **24b**, benzylamine for **24c**, aniline for **24d** and butylamine for **24e**; DIPEA, HATU, CH<sub>2</sub>Cl<sub>2</sub>, 0 °C to r.t., 12 h.

Scheme 5. Synthesis Compounds 32a-o and 33a-f<sup>a</sup>

<sup>a</sup>Reagents and conditions: (i) MeI, NaHCO<sub>3</sub>, DMF; (ii) NaBH<sub>3</sub>CN, EtOH; (iii) SOCl<sub>2</sub>, DMF, CH<sub>2</sub>Cl<sub>2</sub>, 0 °C to r.t., 1 h; (iv) NaI, acetone, reflux, 0.5 h; (v) 3,5-dimethyl-1H-pyrazole, K<sub>2</sub>CO<sub>3</sub>, CH<sub>3</sub>CN, 60 °C, 7 h; (vi) NaOH, MeOH, 40 °C, 3 h; (vii) naphthalen-2-amine for **33a**, isoquinolin-6-amine for **33b**, quinolin-7-amine for **33c**, 1H-indol-6-amine for **33d**, 1H-benzo[d]imidazol-6-amine for **33e**, 5-amino-1,3-dihydro-2H-benzo[d]imidazol-2-one for **33f** and substituted aniline, DIPEA, HATU, CH<sub>2</sub>Cl<sub>2</sub>, 0 °C to r.t., 12 h.

in Figure 2C, slight currents induced by 10 μM NMDA were observed. Then, the selected compounds were added in the presence of 10 μM NMDA. Significantly enhanced currents were observed with FS2915 and FS2921 (Figure 2B), representing the most prominent NMDAR sensitization potency with more than 10<sup>3</sup> pA current. Compared with the vehicle, FS2915 enhanced currents by more than 30 folds

( $\Delta I/I_{\text{NMDA}} > 30$ ), while FS2921 exhibited a  $\Delta I/I_{\text{NMDA}}$  value of 19.3. We also calculated the CNS drug-like properties of the selected compounds, with favorable values defined as  $A \log P < 3$ , polar surface area (PSA) < 90 Å<sup>2</sup>, and blood-brain barrier (BBB) permeability with the ADMET\_BBB\_Level < 3. FS2915 showed a higher activity and more favorable  $A \log P$ , but it was predicted to have poor BBB permeability

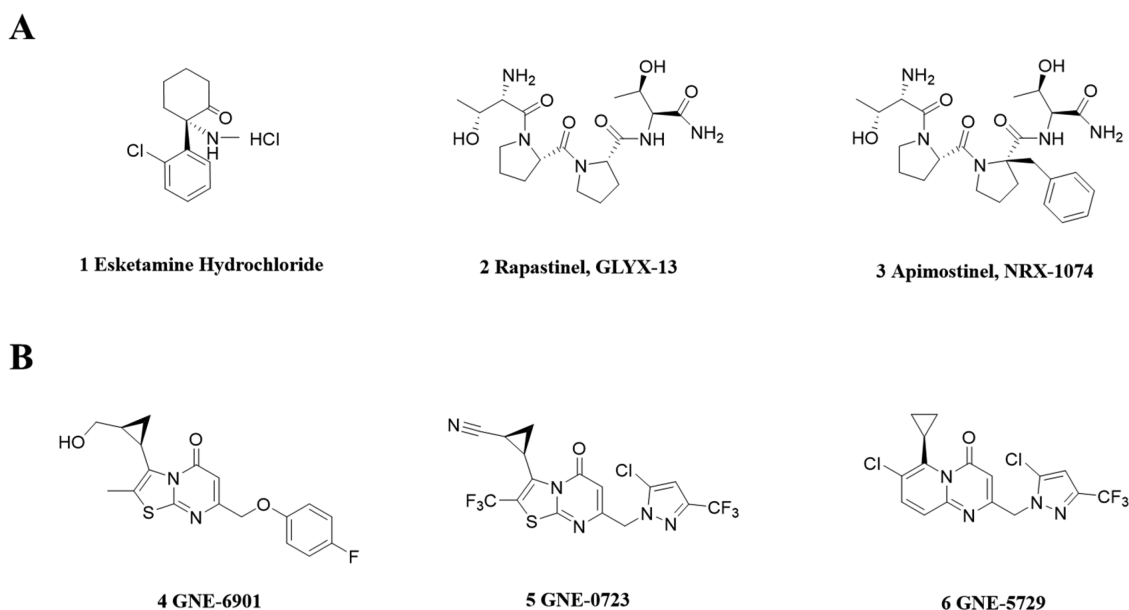


**Figure 1.** Potential antidepressants targeting NMDARs (A) and positive allosteric modulators of NMDARs (B).

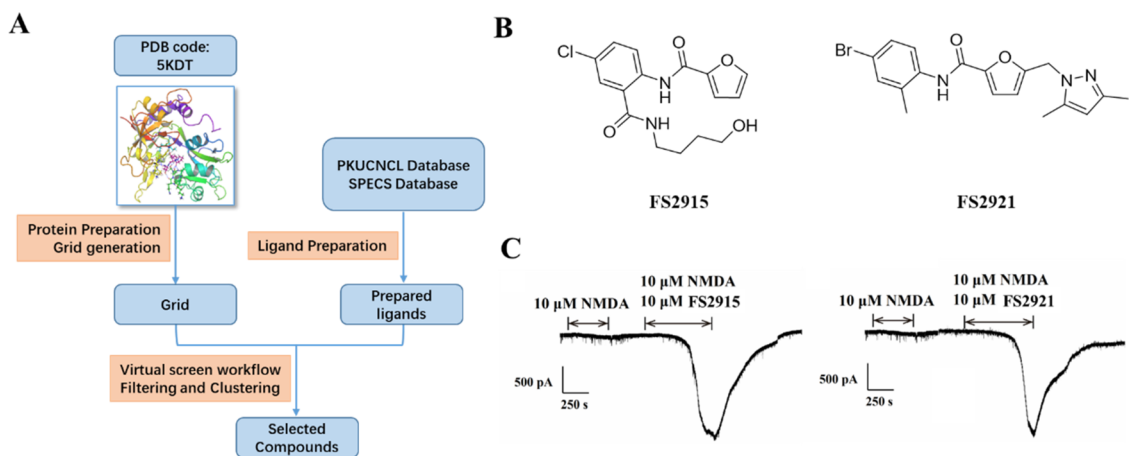


**Figure 2.** (A) Summary of the workflow of virtual screening; (B) chemical structures of two identified NMDAR PAMs; (C) whole-cell recordings of currents evoked by 10 μM NMDA and 10 μM FS2915 or FS2921 on slices of the mouse brain. Scale: X axis = 250 s and Y axis = 500 pA.

**Table 1.** Enhancement Effects on NMDARs and Representative Molecular Properties of the Selected Compounds

compounds	current (pA) <sup>a</sup>	$\Delta I/I_{\text{NMDA}}$ (mean $\pm$ SEM) <sup>b</sup>	MW <sup>c</sup>	$A \log P$ <sup>d</sup>	ADMET_BBB_level <sup>e</sup>	Log BB <sup>f</sup>	PSA <sup>g</sup>
Vehicle	54.6 $\pm$ 4.6	ND <sup>h</sup>	ND	ND	ND	ND	ND
FS2915	1317.0 $\pm$ 297.6	32.8 $\pm$ 13.7	336.8	2.78	3	-1.11	101.9
FS2921	1183.0 $\pm$ 302.9	19.3 $\pm$ 5.2	388.3	4.79	2	-0.18	59.7

<sup>a</sup>NMDAR currents were determined at the saturated concentrations of glutamate. Data are presented as geometric mean values of at least three independent runs. <sup>b</sup>Values are the increased folds of test compound (30 μM) coupled with NMDA (100 μM) over NMDA (100 μM) alone. Data are presented as geometric mean values of at least three independent runs. <sup>c</sup>Molecular weight. <sup>d</sup>Predicted octanol/water partition coefficient using the Maestro 11.5 *Qikprop* module. <sup>e</sup>0: very high; 1: high; 2: medium; 3: low; 4: undefined. <sup>f</sup>Log of the brain/blood partition coefficient (Log BB) using the Maestro 11.5 *Qikprop* module. <sup>g</sup>Topographical polar surface area using the Maestro 11.5 *Qikprop* module. <sup>h</sup>Not determined.

probably because of the higher PSA. FS2921 seemed to possess moderate activity and drug-like properties with the exception of a high  $A \log P$ . Based on the chemical structure characteristics, furan-2-carboxamide was identified as a common scaffold shared by FS2915 and FS2921, which provided a potential starting scaffold for more chemical modifications to improve biological activities and physico-chemical properties (Table 1).

**Allosteric Modulation of NMDARs by FS2921.** To better understand the allosteric modulation of native neuronal NMDARs, we performed the whole-cell patch-clamp experiments on neurons with FS2921. *In vitro* cultured neurons were visibly surrounding by glial cells, and glial cells provided endogenous glycine/D-serine to support neurons. It was expected that the concentration of glycine/D-serine around the cells would increase with the culture time.<sup>37</sup> After culturing for about 7 days, all the young neurons were screened to

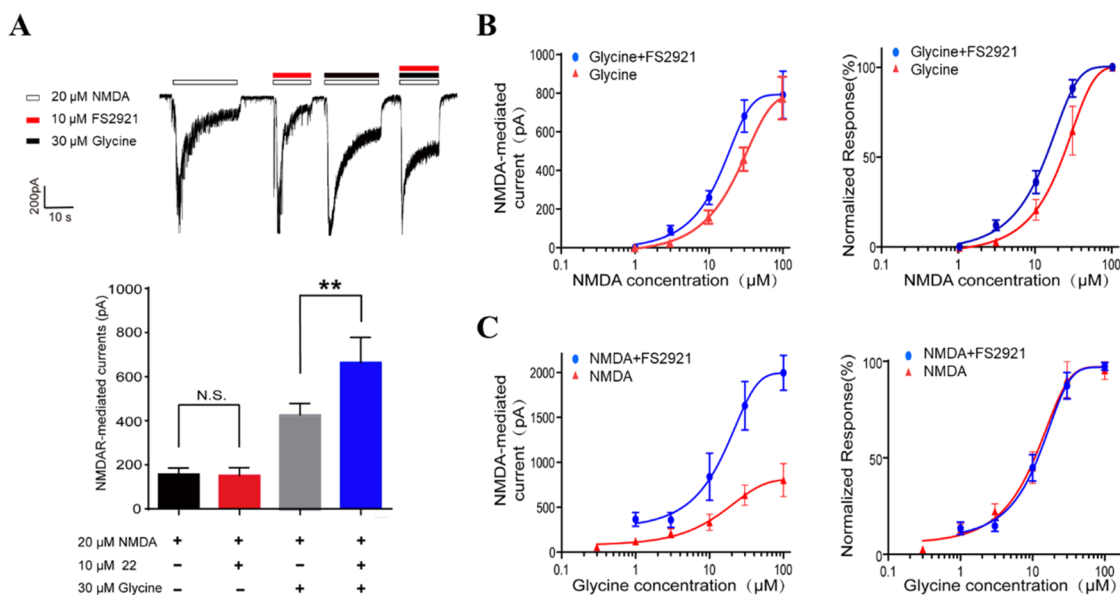


**Figure 3.** Allosteric modulation of NMDARs by FS2921. (A) Representative whole-cell recording from neurons cultured *in vitro* and the statistical results, showing that FS2921 application enhances the response to NMDA + glycine application. (B) Agonist concentration–response curves of NMDA in the presence of 30  $\mu\text{M}$  glycine, indicating that FS2921 acts as a PAM with a shift of the NMDA  $\text{EC}_{50}$  but no altered steady-state currents. (C) Agonist concentration–response curves of glycine in the presence of 100  $\mu\text{M}$  NMDA, indicating that FS2921 acts as a PAM with significant enhancement of steady-state currents but no shift of the glycine  $\text{EC}_{50}$ . Values are expressed as mean  $\pm$  SEM from three independent experiments. The  $p$  value compared to the control group (\*\* $p < 0.01$ ).

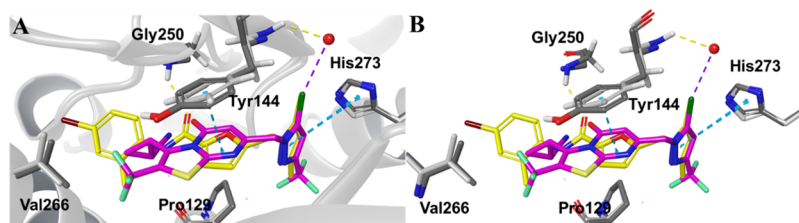


**Figure 4.** Superimposition of the binding modes of FS2921 (yellow) and GNE-0723 (pink) in GluN1/GluN2A LBD (PDB ID: SKDT, gray) with (A) and without (B) protein ribbons. The yellow dotted lines represent hydrogen bonds; the blue dotted lines represent  $\pi$ – $\pi$  interactions; the purple dotted lines represent halogen bonds.

provide neurons with normal reaction by adding NMDA (Figure 4). Due to the low level of endogenous glycine/D-serine, selected neurons gave the weak currents (below 200 pA) induced by 20  $\mu\text{M}$  NMDA alone.<sup>38</sup> When 10  $\mu\text{M}$  FS2921 was added without exogenous glycine/D-serine, the response to 20  $\mu\text{M}$  NMDA was observed to remain unchanged. Therefore, we suspected that FS2921 could not potentiate the NMDAR response induced by 20  $\mu\text{M}$  NMDA because of the low concentration of D-serine produced by glial cells cultured for 7 to 8 days. However, when the primary neurons were treated with exogenous 20  $\mu\text{M}$  NMDA and 30  $\mu\text{M}$  glycine, increased NMDA currents were observed when compared with those in neurons treated with NMDA alone.

When 10  $\mu\text{M}$  FS2921 was continuously present with exogenous 20  $\mu\text{M}$  NMDA and 30  $\mu\text{M}$  glycine, NMDAR currents were significantly enhanced to more than 600 pA. The results suggested that FS2921 could significantly potentiate the NMDAR response in the presence of the co-agonist glycine. Furthermore, a similar electrophysiological experiment was performed on the GluN1/GluN2A overexpressing HEK-293 cells to prove that FS2921 has no activity as a glutamate agonist or a glycine agonist. The GluN1/GluN2A-overexpressing cell line could avoid the endogenous glutamate or

glycine, so that glycine or glutamate alone did not show response, while glycine coupled with glutamate caused apparent currents. FS2921 did not show any response to glycine or NMDA alone, indicating that FS2921 did not act as a glutamate or glycine agonist (Figure S1 in the Supporting Information).

Considering that NMDAR requires to be co-activated by two agonists, two different dose–effect relationship studies were performed to determine the allosteric modulation to NMDA and glycine, separately. Whole-cell recording from neurons cultured *in vitro* showed that NMDA induced the currents in the presence of 30  $\mu\text{M}$  glycine in a dose-dependent manner (Figure 3B); likewise, glycine induced the currents in the presence of 100  $\mu\text{M}$  NMDA (Figure 3C). FS2921 slightly increased NMDA potency from  $23.9 \pm 1.3$  to  $13.6 \pm 1.1$   $\mu\text{M}$ , but it had no influence on the maximum currents induced by saturated NMDA. When the recording was performed in the constant presence of 30  $\mu\text{M}$  FS2921 accompanied by 100  $\mu\text{M}$  NMDA, FS2921 did not alter glycine potency with  $\text{EC}_{50} = 11.8 \pm 1.3$   $\mu\text{M}$  but significantly increased the maximum currents. FS2921 was thought to bind to the allosteric site on the GluN1-GluN2A subunit interface and stabilize the conformation of LBDs to increase the open probability of the channel,

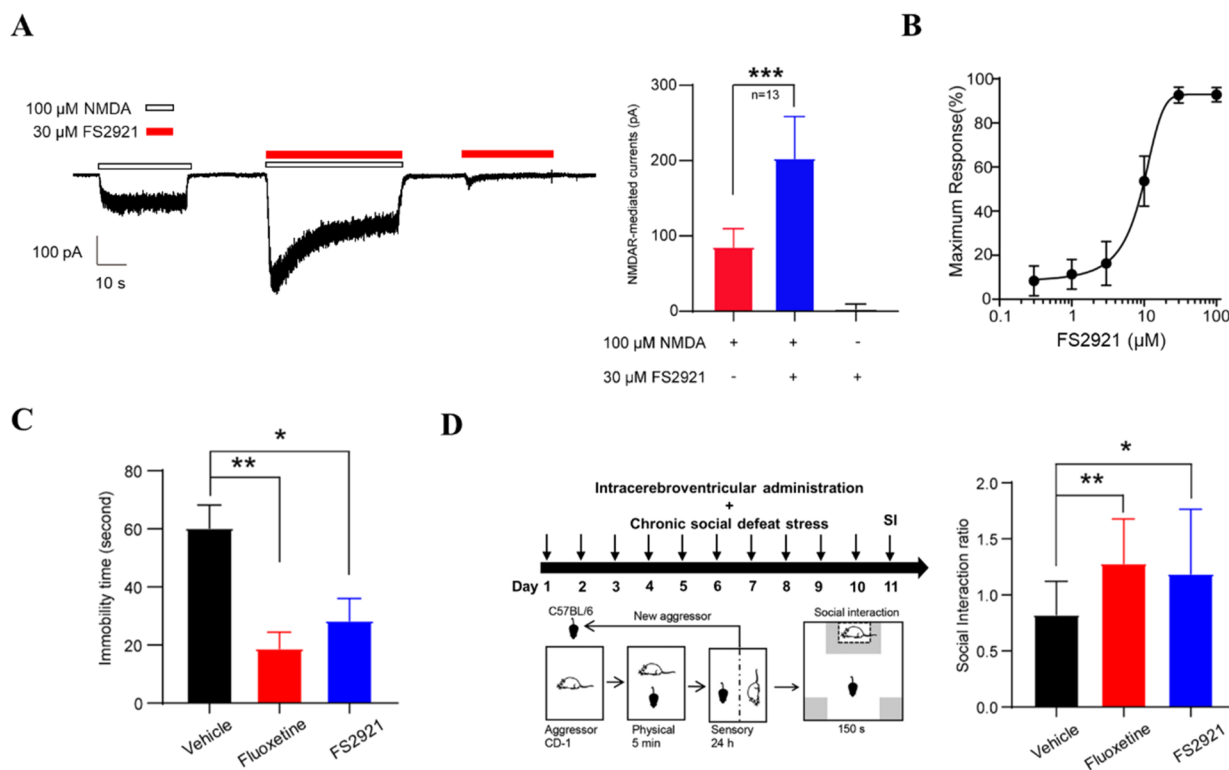


**Figure 5.** (A) Whole-cell recording from neurons cultured *in vitro* and the statistical results, showing that FS2921 application significantly enhanced the response compared to NMDA application alone; Scale: X axis = 10 s and Y axis = 100 pA. (B) Concentration–response curves of FS2921 showing the response to NMDA (100 μM).  $EC_{50}$  values were determined in the presence of saturating glutamate. The values are the mean of at least five experiments. (C) FS2921 reduced immobility duration in the forced swim test (FST) on C57BL/6N mice. (D) FS2921 administration and chronic social defeat stress (CSDS) were both performed daily as indicated by the arrows. FS2921 reversed the reduced social interaction caused by CSDS. Values are expressed as mean  $\pm$  SD from three independent experiments ( $n = 10–11$ ). The  $p$  value compared to the control group (\* $p < 0.05$ , \*\* $p < 0.01$ , \*\*\* $p < 0.001$ ).

even in the presence of saturating NMDA and glycine. It was speculated that FS2921 might affect glycine responses and NMDA affinities due to its interactions with the GluN1 and GluN2A subunits whose LBDs contained ligand-binding pocket of glycine and NMDA, respectively. However, the causes of the differences in allosteric modulation between the two endogenous agonists are still unclear.

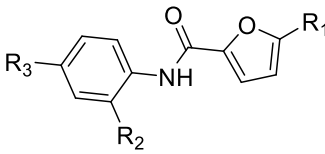
**Binding Modes and Isoform Selectivity Analysis of FS2921.** As depicted in Figure 4, we used induced docking to re-dock FS2921 to the allosteric binding site. Superimposition of the binding modes of GNE-0723 and FS2921 showed many similarities. For example, the imidazole groups on the two compounds superimposed perfectly, and both compounds formed the same  $\pi$ – $\pi$  interaction with His273. The core structure of FS2921 was located at the same position as the thiazolo[3,2-*a*]pyrimidin-5-one structure of GNE-0723, and both exhibited the same  $\pi$ – $\pi$  interaction with Tyr144. The isopropyl group of Val266 was located at the dimer interface of GluN1/GluN2A LBD and had a collision with the 4-bromophenyl group of FS2921. Based on the SAR study of the GNE series compounds, the selectivity to GluN2A against other GluN2 subunits could be attributed to van der Waals interactions between the hydrophobic pocket composed of Val266 and adjacent residues. According to our results, this pocket is occupied by the bulky phenyl of FS2921, suggesting that FS2921 could be a potential GluN2A-selective PAM.

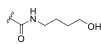
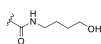
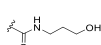
To verify our hypothesis, whole-cell voltage-clamp experiments on HEK-293 cells expressing GluN1/GluN2A, GluN1/GluN2B, GluN1/GluN2C, or GluN1/GluN2D were per-

formed to study the isoform selectivity of FS2921. The results indicated that FS2921 accompanied by both 10 μM NMDA and 30 μM glycine selectively enhanced GluN2A currents but did not affect GluN2B currents. Moreover, we found that FS2921 exhibited slight inhibition of GluN1/GluN2C currents (Figure S2). Our findings demonstrated that FS2921 was a functionally selective GluN1/GluN2A PAM versus GluN1/GluN2B and GluN1/GluN2D. By contrast, FS2921 exhibited a weak NAM effect on GluN1/GluN2C.

To investigate the influence of native AMPA receptors and  $\gamma$ -aminobutyric acid (GABA) receptors on the effect of FS2921, the primary hippocampal neurons cultured for 7–9 days were used. In contrast to the response of AMPA receptors induced by 10 μM AMPA, FS2921 did not have any influence on the currents. Similarly, the responses induced by 10 μM GABA did not differ significantly from those in the presence of FS2921 (30 μM) (Figure S3 in the Supporting Information).

**Enhancement of Currents of FS2921 on Neuronal NMDARs.** When the neurons were cultured for 12–15 days, the concentration of glycine around neurons increased with the expression of serine racemase and growth of glial cells.<sup>39</sup> In the condition of high glycine levels, the responses to NMDA of these neurons were raised significantly by FS2921. However, FS2921 could not induce any response without the addition of NMDA. When 100 μM NMDA and no exogenous glycine were applied, we changed the dose of FS2921 and found that the NMDAR-mediated currents increased in a dose-dependent manner (Figure 5A,B). The  $EC_{50}$  value of FS2921 was  $8.8 \pm 0.9$  μM.  $\Delta I/I_{\text{NMDA max}}$  was calculated to be 3.8, which

Table 2. Chemical Structures and In Vitro Activity of *N*-Phenylfuran-2-carboxamide Analogues with Substituents in the Furyl and Phenyl


Compound	R <sub>1</sub>	R <sub>2</sub>	R <sub>3</sub>	$\Delta I/I_{\text{NMDA}}$ (mean $\pm$ SEM) <sup>a</sup>	LogBB (BBB_level) <sup>b</sup>	PSA <sup>c</sup>
FS2915	H		Cl	3.5 $\pm$ 0.5	-1.1 (3)	101.8
FS2921		CH <sub>3</sub>	Br	3.2 $\pm$ 0.7	-0.13 (2)	59.9
9a	H	CH <sub>3</sub>	Br	-0.2 $\pm$ 0.0	0.15 (1)	43.9
9b	Me	CH <sub>3</sub>	Br	-0.3 $\pm$ 0.2	0.12 (1)	43.7
9c	Cl	CH <sub>3</sub>	Br	1.2 $\pm$ 0.9	0.32 (1)	43.8
24a			Cl	1.7 $\pm$ 0.4	-0.77 (3)	93.9
24b			Cl	2.9 $\pm$ 0.4	-1.48 (3)	118.7
24c			Cl	2.9 $\pm$ 1.1	-0.78 (3)	94.2
24d			Cl	1.2 $\pm$ 0.5	-0.71 (3)	93.1
24e			Cl	-0.6 $\pm$ 0.6	-0.59 (3)	93.6

<sup>a</sup>Values are the increased folds of the test compound (30  $\mu$ M) coupled with NMDA (100  $\mu$ M) over NMDA (100  $\mu$ M) alone. <sup>b</sup>Log of the brain/blood partition coefficient (Log BB) using the Maestro 11.5 *Qikprop* module; 0: very high; 1: high; 2: medium; 3: low; 4: undefined. <sup>c</sup>Polar surface area using the Maestro 11.5 *Qikprop* module.

indicated increased currents induced by the test compound compared to NMDA (100  $\mu$ M) alone. Both parameters were tested to evaluate the activity of other derivatives.

**Antidepressant Effects of FS2921.** To identify the antidepressant effect of FS2921 *in vivo*, we investigated mice behavior using the FST and chronic social defeat stress (CSDS). The FST is widely used to study depressive-like behaviors in rodents; in this test, a rodent's immobility time in water reflects a measure of behavioral despair. In our tests, one intracerebroventricular treatment with FS2921 moderately decreased the immobility time in the FST compared with the control group ( $p < 0.05$ ) (Figure 5C). The fluoxetine group exhibited a significant decrease in the immobility time ( $p < 0.01$ ) at the same dose as FS2921.

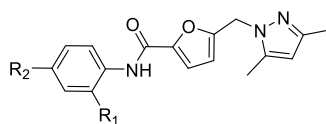
To mimic complicated symptoms of major depression in patients, CSDS is often applied in animals to induce depressive-like behaviors, including decreases in food intake, inhibition of body weight gain, and social-avoidance behavior.

CSDS was performed in accordance with the previously described protocols (Figure 5D).<sup>40</sup> In brief, C57BL/6N mice were pretreated with FS2921 every day before applying CSDS. With intracerebroventricular administration of FS2921 and CSDS repeated for up to 10 days, social interaction tests were performed on day 11. The results showed that FS2921 moderately reversed the reduction in social interactions induced by CSDS and exhibited an equal antidepressant effect compared with that of fluoxetine.

**SAR Analysis.** Based on the structural similarities between FS2915 and FS2921, the furan-2-carboxamide scaffold was determined to be a dominant skeleton for designing analogues. The current-enhancing potency of each compound was measured by a whole-cell patch-clamp assay carried out on neurons cultured *in vitro*. The results are expressed as  $\Delta I/I_{\text{NMDA}}$  values presented in Tables 2–6.

FS2915 and FS2921 were used as starting hits for the first round of structural investigation (shown in Table 2). The

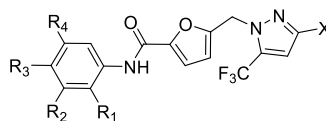
**Table 3. Chemical Structures and In Vitro Activity of 5-((3,5-Dimethyl-1H-pyrazol-1-yl)methyl)-N-phenylfuran-2-carboxamide with Substituents on the Phenyl**



compound	R <sub>1</sub>	R <sub>2</sub>	$\Delta I/I_{\text{NMDA}}$ (mean $\pm$ SEM) <sup>a</sup>	Log BB (BBB_level) <sup>b</sup>	PSA <sup>c</sup>
FS2921	CH <sup>3</sup>	Br	3.2 $\pm$ 0.7	-0.13 (2)	59.9
17a	CH <sup>3</sup>	F	1.9 $\pm$ 0.2	-0.20 (2)	59.9
17b	CH <sup>3</sup>	Cl	3.2 $\pm$ 0.4	-0.14 (2)	59.9
17c	CH <sup>3</sup>	H	1.2 $\pm$ 0.3	-0.31 (2)	59.9
17d	H	H	0.1 $\pm$ 0.1	-0.4 (2)	61.3
17e	H	Br	1.2 $\pm$ 0.6	-0.19 (2)	61.3
17f	CH <sup>2</sup> CH <sup>3</sup>	Br	2.6 $\pm$ 1.2	-0.2 (2)	59.4
17g	Cl	Br	1.7 $\pm$ 0.5	-0.0 (2)	60.2
17h	NHCH <sup>3</sup>	H	0.8 $\pm$ 0.2	-0.5 (3)	73.3
17i	CH <sup>2</sup> CH <sup>2</sup> OH	H	0.4 $\pm$ 0.3	-0.9 (3)	81.4
17j	Phenyl-	H	0.3 $\pm$ 0.1	-0.4 (2)	58.8
17k	H	Phenyl-	6.7 $\pm$ 3.2	-0.4 (2)	61.0
17l	CH <sup>2</sup> OH	Cl	1.1 $\pm$ 0.4	-0.4 (2)	83.1
17m	Cl	Cl	4.7 $\pm$ 2.3	-0.0 (2)	60.2
17n	F	Cl	0.9 $\pm$ 0.3	-0.1 (2)	60.7
22a	COOCH <sub>3</sub>	F	1.5 $\pm$ 0.6	-0.8 (3)	94.2
22b	COOCH <sub>3</sub>	Cl	0.1 $\pm$ 0.2	-0.8 (3)	93.9
22c	COOCH <sub>3</sub>	Br	2.7 $\pm$ 0.6	-0.6 (3)	91.2

<sup>a</sup>Values are the increased folds of the test compound (30  $\mu$ M) coupled with NMDA (100  $\mu$ M) over NMDA (100  $\mu$ M) alone. <sup>b</sup>Log of the brain/blood partition coefficient (Log BB) using the Maestro 11.5 *Qikprop* module; 0: very high; 1: high; 2: medium; 3: low; 4: undefined. <sup>c</sup>Polar surface area using the Maestro 11.5 *Qikprop* module.

**Table 4. Chemical Structures and In Vitro Activity of 5-((5-Trifluoromethyl-1H-pyrazol-1-yl) methyl)-N-phenylfuran-2-carboxamides with Substituents on the Phenyl**



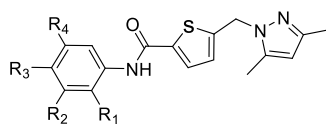
compound	X	R <sub>1</sub>	R <sub>2</sub>	R <sub>3</sub>	R <sub>4</sub>	$\Delta I/I_{\text{NMDA}}$ (mean $\pm$ SEM) <sup>a</sup>	Log BB (BBB_level) <sup>b</sup>	PSA <sup>c</sup>
20a	CH <sub>3</sub>	CH <sub>3</sub>	H	Cl	H	7.7 $\pm$ 3.	0.2 (1)	59.6
20b	CH <sub>3</sub>	CH <sub>3</sub>	H	Br	H	1.2 $\pm$ 0.5	0.2 (1)	59.5
20c	CF <sub>3</sub>	CH <sub>3</sub>	H	F	H	2.4 $\pm$ 1.0	0.4 (1)	58.4
20d	CF <sub>3</sub>	CH <sub>3</sub>	H	Cl	H	0.7 $\pm$ 0.4	0.4 (1)	59.6
20e	CF <sub>3</sub>	CH <sub>3</sub>	H	Br	H	10.7 $\pm$ 3.5	0.4 (1)	59.5
20f	CF <sub>3</sub>	Cl	H	Cl	H	0.4 $\pm$ 0.5	0.6 (0)	60.3
20g	CF <sub>3</sub>	H	Cl	Cl	H	2.9 $\pm$ 0.3	0.6 (0)	61.1
20h	CF <sub>3</sub>	H	Cl	H	Cl	13.8 $\pm$ 4.9	0.6 (0)	60.0
20i	CF <sub>3</sub>	H	OCH <sub>3</sub>	H	OCH <sub>3</sub>	2.5 $\pm$ 1.7	0.1 (1)	76.9
20j	CF <sub>3</sub>	H	CH <sub>3</sub>	F	H	5.5 $\pm$ 2.3	0.4 (1)	61.1
22d	CF <sub>3</sub>	COOCH <sub>3</sub>	H	F	H	1.9 $\pm$ 2.5	-0.1(3)	94.4

<sup>a</sup>Values are the increased folds of the test compounds (30  $\mu$ M) coupled with NMDA (100  $\mu$ M) over NMDA (100  $\mu$ M) alone. <sup>b</sup>Log of the brain/blood partition coefficient (Log BB) using the Maestro 11.5 *Qikprop* module; 0: very high; 1: high; 2: medium; 3: low; 4: undefined. <sup>c</sup>Polar surface area using the Maestro 11.5 *Qikprop* module.

removal of (3,5-dimethyl-1H-pyrazol-1-yl)methyl or 3,5-dimethyl-1H-pyrazol-1-yl in FS2921 (**9a** and **9b**) resulted in a loss of potentiating activity. The chlorine on the furan moiety (**9c**) induced decreased potentiating activity. By merging the scaffold of FS2915 and that of FS2921 to obtain compound **24a** with a Cl atom at the *para*-position of the benzanilide moiety, the potentiating activity was also found to decrease. When the 4-hydroxybutyl group was changed to a truncated 3-hydroxypropyl (**24b**) or a benzyl group (**24c**), the potentiating activity increased slightly compared to that of compound **24a**.

Nevertheless, when the 4-hydroxybutyl group was further changed to a phenyl (**24d**) or *n*-butyl group (**24e**), the potentiating activity decreased significantly compared to that of compound **24a**. The first round of structural investigation determined that both the 3,5-dimethyl-1H-pyrazol-1-yl group and the 4-hydroxybutyl)carbamoyl group are important to the common scaffold and that the potentiating activity persists when both of them are present. However, due to the bulky groups at the R<sub>2</sub> position, the PSA values of compounds **24a-e** were all above 90, resulting in low Log BB permeability. Taken

**Table 5. Chemical Structures and In Vitro Activity of 5-((3,5-Dimethyl-1H-pyrazol-1-yl)methyl)-N-phenylthiophene-2-carboxamide with Substituents on the Phenyl**



compound	R <sub>1</sub>	R <sub>2</sub>	R <sub>3</sub>	R <sub>4</sub>	$\Delta I/I_{\text{NMDA}}$ (mean $\pm$ SEM) <sup>a</sup>	Log BB (BBB_level) <sup>b</sup>	PSA <sup>c</sup>
32a	CH <sub>3</sub>	H	Br	H	1.5 $\pm$ 0.3	0.1 (1)	50.5
32b	CH <sub>3</sub>	H	Cl	H	-0.2 $\pm$ 0.1	0.1 (1)	50.5
32c	CH <sub>3</sub>	H	F	H	10.1 $\pm$ 0.8	-0.1 (2)	50.2
32d	CH <sub>3</sub>	H	phenyl	H	2.8 $\pm$ 1.8	-0.3 (2)	50.8
32e	CH <sub>3</sub>	H	pyridin-3-yl	H	1.8 $\pm$ 1.9	-0.6 (3)	63.8
32f	H	CH <sub>3</sub>	F	H	2.4 $\pm$ 0.5	-0.1 (2)	51.7
32g	H	Cl	F	H	3.5 $\pm$ 1.1	0.1 (1)	51.9
32h	H	Cl	Cl	H	12.5 $\pm$ 5.7	0.1 (1)	51.7
32i	H	F	Cl	H	6.0 $\pm$ 2.4	0.1 (1)	51.6
32j	H	OCH <sub>2</sub> CH <sub>3</sub>	OCH <sub>2</sub> CH <sub>3</sub>	H	2.7 $\pm$ 2.2	-0.6 (3)	66.6
32k	H	Cl	H	Cl	1.2 $\pm$ 0.4	0.1 (1)	51.7
32l	H	F	H	F	5.0 $\pm$ 2.7	0.0 (1)	51.7
32m	H	OCH <sub>3</sub>	H	OCH <sub>3</sub>	0.4 $\pm$ 1.5	-0.4 (2)	68.5
32n	H	H	phenyl	H	2.8 $\pm$ 0.8	-0.4 (2)	52.3
32o	H	H	pyridin-3-yl	H	14.3 $\pm$ 4.8	-0.4 (3)	65.2

<sup>a</sup>Values are the increased folds of the test compound (30  $\mu$ M) coupled with NMDA (100  $\mu$ M) over NMDA (100  $\mu$ M) alone. <sup>b</sup>Log of the brain/blood partition coefficient (Log BB) using the Maestro 11.5 *Qikprop* module; 0: very high; 1: high; 2: medium; 3: low; 4: undefined. <sup>c</sup>Polar surface area using the Maestro 11.5 *Qikprop* module.

together, the 3,5-dimethyl-1H-pyrazol-1-yl group at the R<sub>1</sub> position contributed to the satisfactory activity and the favorable Log BB, which was considered suitable for further SAR exploration.

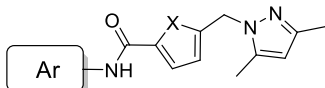
In the next round of structural investigation based on FS2921, we explored the effects of diverse substitutions at the 2-position and 4-position of the phenyl. The potentiating activity results for these analogues are shown in Table 3. Chlorine or fluorine substitution at the 4-position slightly decreased the potentiating activity when compounds 17a and 17b were compared with FS292 and compounds 22a and 22b with 22c. Removal of the *ortho*-methyl group induced a significant potentiating activity decrease when compounds 17d and 17e were compared with FS2921. As can be seen from compounds 17c/17d/17h/17i/17j, removing the substitution at the 4-position of the phenyl also reduced compound potentiating activity. When an ethyl group (17f), chlorine (17g), or methoxycarbonyl group (22c) was introduced to replace the *ortho*-methyl group of FS2921, the activity decreased moderately. Similar results were observed in compounds 17l/17n/22b when compared with compound 17b. When a phenyl group was added to the *ortho*-position, compound 17j showed a loss in activity. However, compound 17k was found to be more effective, suggesting that a bulky group at the 4-position was tolerated. Increased potentiating activity was also observed in the compound with a 2,4-dichlorophenyl moiety (17m).

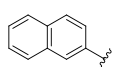
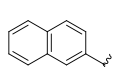
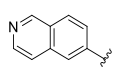
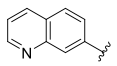
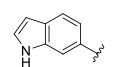
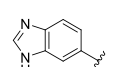
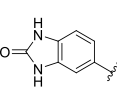
The SAR results indicated that the methyl or chlorine groups were preferable substitutions at the 2-position on the phenyl. Combined with the predicted Log BB, the introduction at the 2-position of some polar groups such as hydroxyl/amino/ester led to a decrease in activity and a decrease in brain permeability. The introduction of substituents at the 4-position of the phenyl is critical to activity. This position can also accommodate larger substitutions.

Next, we changed the methyl group of the pyrazol moiety to a trifluoromethyl group to gain BBB permeability. Bearing the 3-methyl-5-(trifluoromethyl)-1H-pyrazol moiety, the potentiation of compound 20a increased by 2-fold compared to that of compound 17b. However, compound 20b with a *para*-bromine group showed a slight decrease in enhancement potentiating activity. Nevertheless, when the two methyl groups on the pyrazol ring were both changed to trifluoromethyl groups, some opposite results were observed. Compared to compounds 17a/b, compounds 20c/d seemed to be unaffected by trifluoromethyl groups, but the predicted Log BB improved. Compound 20e was found to exhibit a high potentiating activity with an enhanced  $\Delta I/I_{\text{NMDA}}$  value of 10.7  $\pm$  3.5. Moreover, compound 20h ( $\Delta I/I_{\text{NMDA}}$  = 13.8  $\pm$  4.9) showed potentiating activity that was more than 4 fold that of FS2921 and possessed micromolar potency (EC<sub>50</sub> = 12.5  $\mu$ M) (Table 7). Compounds 20d and 20f were observed to slightly enhance currents. When one *meta*-chlorine of compound 20h was moved to the *para*-position (20g), the potentiation was retained but greatly reduced. As can be seen from compounds 20h/20i/20j, the *meta*-methoxyl group was just as potent as the *meta*-fluorine group but was significantly weaker than the *meta*-chlorine group. By comparing compound 20c with 20j and 20g with 20f, *meta*-substituents seemed to be more positive than *ortho*-substituents.

After transforming the furan moiety of FS2921 to a thiophene moiety, we explored a new scaffold of thiophene-2-carboxamide that possessed increased stability and lower toxicity. Compound 32a exhibited a slight decrease in activity compared with FS2921. Unexpectedly, as can be seen with compound 32b, the potentiating activity of currents was eliminated. Compound 32c displayed a significant improvement in potentiation ( $\Delta I/I_{\text{NMDA}}$  = 10.1  $\pm$  0.8), of which EC<sub>50</sub> was determined to be 7.75  $\mu$ M (Table 7). When a phenyl or pyridine group was introduced to the *para*-position (compounds 32d/32e/32n/32o), the potencies of all analogues

Table 6. Chemical Structures and In Vitro Activity of 5-((3,5-Dimethyl-1H-pyrazol-1-yl)methyl)-N-(aromatic Ring)-thiophene-2-carboxamides



Compound	X	Ar	$\Delta I/I_{\text{NMDA}}$ (mean $\pm$ SEM) <sup>a</sup>	LogBB (BBB_level) <sup>b</sup>	PSA <sup>c</sup>
16a	O		2.9 $\pm$ 1.1	-0.6 (3)	74.3
16b	O		3.2 $\pm$ 0.3	-0.4 (2)	60.8
33a	S		1.8 $\pm$ 0.7	-0.2 (2)	51.9
33b	S		-0.2 $\pm$ 0.4	-0.5 (3)	65.0
33c	S		1.1 $\pm$ 0.5	-0.5 (2)	64.4
33d	S		8.9 $\pm$ 2.9	-0.5 (2)	65.8
33e	S		0.1 $\pm$ 0.4	-0.8 (3)	79.7
33f	S		0.3 $\pm$ 2.4	-1.6 (3)	111.6

<sup>a</sup>Values are the increased folds of the test compound (30  $\mu\text{M}$ ) coupled with NMDA (100  $\mu\text{M}$ ) over NMDA (100  $\mu\text{M}$ ) alone. <sup>b</sup>Log of the brain/blood partition coefficient (Log BB) using the Maestro 11.5 *Qikprop* module; 0: very high; 1: high; 2: medium; 3: low; 4: undefined. <sup>c</sup>Polar surface area using the Maestro 11.5 *Qikprop* module.

Table 7.  $\text{EC}_{50}$  and  $E_{\text{max}}$  on the Primary Neuron of Selected Compounds

compound	$\text{EC}_{50}$ ( $\mu\text{M}$ ) <sup>a</sup>	$E_{\text{max}}$
FS2921	8.8	3.8 $\pm$ 0.7
20h	12.5	13.8 $\pm$ 4.9
32c	7.8	10.2 $\pm$ 4.1
32h	2.4	14.3 $\pm$ 4.8
32o	3.6	12.8 $\pm$ 2.2
33d	9.0	10.5 $\pm$ 2.7

<sup>a</sup>NMDAR  $\text{EC}_{50}$  values were determined in the presence of saturating glutamate. The values are the mean of at least five experiments. The  $\text{EC}_{50}$  of each compound is expressed relative to the maximal response that it induces.

were retained. Moreover, compound 32o exhibited a significant increase with potentiating activity and potency ( $\Delta I/I = 14.3 \pm 4.8$  and  $\text{EC}_{50} = 3.6 \mu\text{M}$ ) (Table 7). Next, as

shown in compounds 32f-j, the collocation of *para*-substitutions and *meta*-substitutions was investigated, where the fluorine, chlorine, methyl, or ethoxyl group all showed potential. Among them, compound 32h provided superior potentiating activity with a  $\Delta I/I_{\text{NMDA}}$  value of  $12.5 \pm 5.7$  and an improved  $\text{EC}_{50}$  value of  $2.4 \mu\text{M}$  (Table 7). When one of the two chlorine substitutions of compound 32h was replaced by fluorine, the potentiation of currents was reduced significantly, as can be seen in compounds 32g/32i. When substitutions were introduced to both *meta*-positions, it was observed that *meta*-fluorine groups were more potent than *meta*-methoxyl groups and *meta*-chlorine groups by comparing compounds 32k-m.

We proceeded with our exploration of the SAR by replacing the substituted phenyl with different aromatic rings. When a pyridin-3-yl moiety (16a) replaced the benzene moiety of FS2921, the activity was retained. The same result was observed with the naphthalen-2-yl moiety (16b). However, for

the thiophene-2-carboxamide scaffold, a naphthalene-2-yl moiety induced a slight decrease in potentiating activity by comparing compound **33a** with **16b**. When a quinolone moiety replaced the naphthalene moiety, the potentiation of currents was reduced significantly as shown in compounds **33b** and **33c**. Benzo-heterocycles were also introduced to replace the substituted phenyl, such as indole (**33d**), benzimidazole (**33e**), or benzimidazolone (**33f**). The activity for compound **33d** increased significantly with  $\Delta I/I_{\text{NMDA}} = 8.9 \pm 2.9$ , but compounds **33e** and **33f** exhibited a large decrease in potentiating activity. The  $\text{EC}_{50}$  of compound **33d** was determined to be  $9.0 \mu\text{M}$  (Table 7).

It was exciting to observe that most of these analogues exhibited NMDA potentiating behaviors like FS2921. Some of these compounds showed a more significant potentiation to NMDAR currents than FS2921 and were selected for  $\text{EC}_{50}$  determination. As shown in Table 7, among these compounds, compound **32h** had the best  $\text{EC}_{50}$  value of  $2.44 \mu\text{M}$ , and the other compounds (**20h/32c/32o/33d**) were observed to exhibit micromolar activity as well. Therefore, these five compounds were selected for further evaluation of *in vivo* activities and safety profiles.

**Effects of the Selected Derivatives of FS2921 in the FST.** To demonstrate the potential antidepressant effects of NMDAR PAMs, we further investigated several novel analogues of FS2921 in the FST (Figure 6). Because

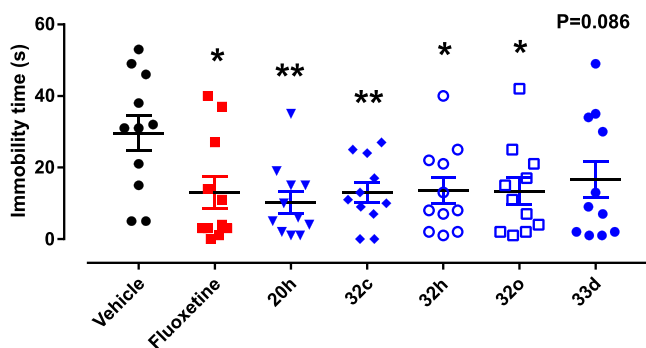


**Figure 6.** Effects of the selected compounds in the ICR mice FST by single i.p. treatment. Values are expressed as mean  $\pm$  SEM from 10–12 independent experiments. The *p* value was obtained by comparing it with the control group (\**p* < 0.05, \*\**p* < 0.01).

intracerebroventricular administration is complicated and requires evaluating the blood–brain barrier effect, we used intraperitoneal (i.p.) administrations in the following behavioral experiments. Based on the *in vitro* data, compounds **20h/32c/32h/32o/33d** were chosen for the tests in ICR mice, with fluoxetine as the positive drug at the same dose of 30 mg/kg. The results showed that compounds **20h** and **32c** significantly decreased the immobility time compared with the vehicle group. Similarly, the compounds **32h** and **32o** moderately reduced the immobility duration compared with the vehicle group, while compound **33d** did not show significant effects.

To differentiate the *in vivo* efficacy of the selected derivatives, we further investigated compounds **20h/32c/32h/32o** at lower concentrations in the FST. Each compound was tested at two doses (3 and 10 mg/kg), and each experiment was performed three times with intraperitoneal administration. Duloxetine, which is considered a more effective antidepressant drug than fluoxetine in clinical practice, was used as the positive control. Administration of duloxetine

caused a robust decrease in the immobility time, demonstrating its extraordinary antidepressant effect. Compounds **20h** and **32h** significantly shortened the immobility time at two doses (Figure 7). However, compounds **32c** and **32o** did not change the immobility time compared with the vehicle group (Figure S4).

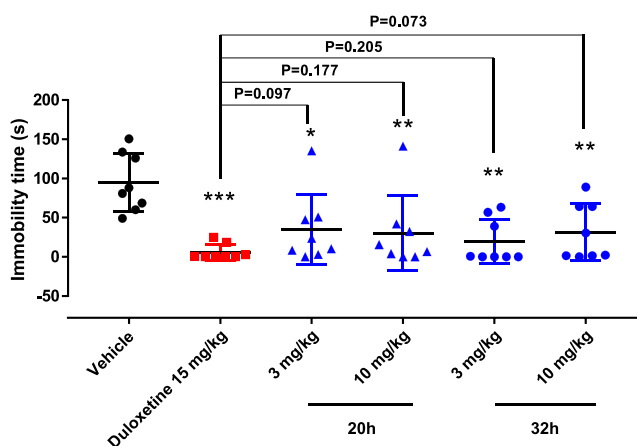


**Figure 7.** Effects of the compounds **20h** and **32h** in the ICR mice FST with treatment repeated three times. Values are expressed as mean  $\pm$  SEM from eight independent experiments. The *p* value is obtained by comparing it with the control group (\**p* < 0.05, \*\**p* < 0.01).

**Influence of the Selected FS2921 Analogues on Locomotion of ICR Mice.** Spontaneous locomotor activity tests are used to investigate the influence of antidepressants on the spontaneous locomotor activity in animals. It is considered that hypoactivity or hyperactivity induced by candidate compounds should be determined to avoid potential psychotic side effects. Compounds **20h/32c/32h/32o/33d** were investigated at a dose of 10 mg/kg by intraperitoneal injection. The results showed that none of the analogues caused hyperlocomotion or hypolocomotion of the treated mice (Figure S5).

Monoamine neurotransmitter antagonists can attenuate hyperlocomotion induced by dopamine receptor direct agonists such as apomorphine. To determine whether these compounds affected the function of monoamine neurotransmitters, we investigated the compounds **20h/32c/32h/32o/33d** in APO (apomorphine)-induced climbing tests. The results showed that none of these analogues affected APO-induced climbing; by contrast, risperidone (an inhibitor of  $\text{D}_2$  receptors and  $5\text{-HT}_2\text{A}$  receptors) significantly inhibited the APO-induced climbing behavior (Figure S6).

**Effects of the Compounds **20h** and **32h** on Additional Targets.** We detected the influence of the compounds **20h** and **32h** on native AMPA receptors and  $\gamma$ -aminobutyric acid (GABA) receptors were detected (Figure S3). The primary hippocampal neurons cultured for 7–9 days were used. Similar to FS2921, these two derivatives did not have any influence on the currents of AMPA receptors induced by  $10 \mu\text{M}$  AMPA. Likewise, the responses induced by  $10 \mu\text{M}$  GABA did not significantly differ from those in the presence of the test compounds ( $30 \mu\text{M}$ ).

Several common antidepressant drug targets were also explored to determine if the potential antidepressant effects of compound **32h** was related to other targets. Binding affinities

Table 8. PK and Brain Penetration Properties of Compounds 20h and 32h in ICR Mice<sup>a</sup>

parameter	20h		32h	
	3 mg/kg (i.v.)	10 mg/kg (p.o.)	3 mg/kg (i.v.)	10 mg/kg (p.o.)
$C_{\max}$ (ng/mL)		989.0		760.0
$t_{\max}$ (h)		2.0		0.5
$t_{1/2}$ (h)	5.0	5.7	2.8	2.9
AUC <sub>0-t</sub> (h·ng/mL)	1751.0	4217.0	1448.0	3051.0
CL (L/h)	1.8		2.0	
MRT (h)	3.4	4.7	4.0	4.2
$V_{\text{dss}}$ (L/kg)	12.7		8.3	
F (%)		72.2		63.3
brain concentration at 0.5 h (ng/mL)	73.6 ± 19.3	93.4 ± 10.4	160.2 ± 13.4	280.7 ± 28.5
plasma concentration at 0.5 h (ng/mL)	506.5 ± 75.4	580.2 ± 24.4	388.7 ± 50.4	760.2 ± 79.3
brain/plasma ratio at 0.5 h	0.14	0.16	0.41	0.37
brain concentration at 2.0 h (ng/mL)	49.0 ± 10.9	148.2 ± 13.6	85.5 ± 29.7	173.8 ± 12.2
plasma concentration at 2.0 h (ng/mL)	304.2 ± 49.2	988.8 ± 20.0	239.3 ± 52.8	451.0 ± 38.3
brain/plasma ratio at 2.0 h	0.16	0.15	0.34	0.38

<sup>a</sup>Values are expressed as mean ± SD from male ICR mice ( $n = 6/\text{treatment group}$ ).

Table 9. Pharmacokinetics Study of Compound 32h in Rats<sup>a</sup>

PK profiles of compound 32h in plasma							
dose (mg/kg)	$C_{\max}$ (ng/mL)	$t_{1/2}$ (min)	$t_{\max}$ (min)	CL (L/h/kg)	$V_{\text{ss}}$ (L/kg)	AUC <sub>0-t</sub> (h·ng/mL)	F (%)
3, i.v.	2347.8 ± 476.17	102.2 ± 7.8		1.67 ± 0.22	1.27 ± 0.22	1816.88 ± 252.26	
10, p.o.	190.2 ± 122.2	67.8 ± 35.8	33.3 ± 11.6			502.7 ± 201.3	8.32
brain penetration analysis of compound 32h							
dose (mg/kg)	time (min)	brain conc (ng/g)	plasma conc (ng/mL)	brain/plasma ratio			
3, i.v.	20	2190.2 ± 274.6	1489.2 ± 208.7	1.5			
3, i.v.	80	353.6 ± 99.0	238.8 ± 26.0	1.5			

<sup>a</sup>Values are expressed as mean ± standard deviation (SD) from male Sprague–Dawley rats ( $n = 3/\text{treatment group}$ ).

of compound 32h tested by a radioligand binding assay showed that the  $K_i/IC_{50}$  values were all greater than 10  $\mu\text{M}$  for the main GPCRs ( $D_2$ ,  $D_3$ ,  $\alpha_1$ , 5-HT<sub>1A</sub>, 5-HT<sub>1B</sub>, 5-HT<sub>2A</sub>, 5-HT<sub>2C</sub>, and 5-HT<sub>6</sub>) or transporters (DAT, NET, and SERT) (Table S3 in the Supporting Information). The additional antitarget results indicated that compound 32h had no influence on these targets and that the antidepressant effects seen *in vivo* could not come from other CNS-relevant receptors.

#### Pharmacokinetic Profiles and Brain Penetration Properties of Compounds 20h/32c/32o/32h in Mice.

Pharmacokinetics profiles of the selected compounds were extensively studied in ICR mice by i.v. administration at 3 mg/kg and p.o. administration at 10 mg/kg. The plasma concentration–time curves are shown in Figure S7 in the Supporting Information. Compound 32h showed a rapid distribution ( $t_{\max} = 0.5 \pm 0.0$  h) compared with compound 20h ( $t_{\max} = 2.0 \pm 0.0$  h) at a dose of 10 mg/kg (p.o.). However, the half-life of compound 32h via p.o. ( $t_{1/2} = 2.9 \pm 0.2$  h.) administration was shorter than that of compound 20h ( $t_{1/2} = 5.7 \pm 0.7$  h); nevertheless, compound 32h still showed an effective blood plasma concentration ( $C_{\max} = 760 \pm 86$  ng/mL) comparable to that of compound 20h ( $C_{\max} = 989 \pm 22$  ng/mL). Finally, the oral bioavailabilities of compounds 20h and 32h were 72.3 and 62.3%, respectively. Further tests for their brain penetration properties were performed at 0.5 and 2.0 h, and the brain/plasma ratios were calculated. The results showed that the brain/plasma ratio of compound 20h was lower than 0.2 at both time points after one single administration (10 mg/kg p.o. or 3 mg/kg i.v.). The BBB

permeability of compound 32h was found to be prominent in that a single oral administration resulted in a brain/plasma ratio higher than 0.3, and the brain concentration of compound 32h rapidly reached its highest level of  $280.7 \pm 28.5$  ng/mL in half an hour. Notably, considering the brain concentration at 2.0 h ( $C_{\text{brain}/2.0\text{h}} = 148.2 \pm 13.6$  ng/mL) after a single oral administration as  $C_{\max}$  of the brain concentration, compound 20h seemed to provide a moderate brain exposure (Table 8).

Given the favorable potential antidepressant effects of compounds 20h and 32h by intraperitoneal injection, *in vivo* PK profiles of compounds 32c and 32o should be explored to clarify why these two compounds did not show significant efficacy in the FST. For compound 32c, despite the high  $C_{\text{brain}}/C_{\text{plasma}}$  ratio, the concentrations in plasma and brain were rather low. The high CL (13.6 L/h/kg) led to a short  $t_{1/2}$  and an AUC<sub>0-t</sub> of 105.94 h·ng/mL. It was difficult for compound 32c to maintain an effective drug concentration. In our experiments, compound 32o showed poor water solubility, which made this compound difficult to inject intravenously. After the intravenous injection, compound 32o might precipitate in plasma; thus, low concentrations were detected after the i.v. administration compared with p.o. administration. Taking into account the poor water solubility, intraperitoneal injection of compound 32o in the FST might face the same problem as i.v. administration, which could explain its inefficiency *in vivo*. However, after p.o. administration, rather high concentrations were detected, revealing that compound 32o had a high permeability value. Additionally, compound

Table 10. Cytotoxicity and hERG Channel Inhibition of the Selected Compounds<sup>a</sup>

compounds	inhibition (%)							
	VERO		L929		HEK293		hERG	
	120 $\mu$ M	60 $\mu$ M	120 $\mu$ M	60 $\mu$ M	120 $\mu$ M	60 $\mu$ M	100 $\mu$ M	30 $\mu$ M
20h	95.8 $\pm$ 0.3	96.2 $\pm$ 0.2	90.6 $\pm$ 0.1	84.3 $\pm$ 0.5	73.6 $\pm$ 7.6	42.0 $\pm$ 4.4	68.4 $\pm$ 7.3	49.1 $\pm$ 5.3
32c	8.7 $\pm$ 1.2	-1.5 $\pm$ 1.4	23.9 $\pm$ 1.0	11.5 $\pm$ 1.5	34.4 $\pm$ 3.6	16.3 $\pm$ 1.7	47.6 $\pm$ 6.3	33.4 $\pm$ 8.5
32h	22.6 $\pm$ 1.3	21.9 $\pm$ 1.5	-4.6 $\pm$ 1.4	0.5 $\pm$ 1.3	-14.0 $\pm$ 2.3	-5.2 $\pm$ 0.9	45.0 $\pm$ 9.1	35.4 $\pm$ 6.7
32o	-7.5 $\pm$ 1.3	-3.8 $\pm$ 1.3	28.6 $\pm$ 1.7	27.5 $\pm$ 1.3	18.0 $\pm$ 1.9	6.5 $\pm$ 0.8	53.4 $\pm$ 13.8	44.2 $\pm$ 5.1
33d	-0.4 $\pm$ 2.0	-3.2 $\pm$ 2.3	25.5 $\pm$ 1.3	2.8 $\pm$ 1.6	2.5 $\pm$ 0.4	-7.4 $\pm$ 1.2	46.7 $\pm$ 11.4	33.6 $\pm$ 11.6

<sup>a</sup>Values are expressed as mean  $\pm$  SEM from three independent experiments

32o exhibited a short  $t_{1/2}$  and definitely a low  $C_{\text{brain}}/C_{\text{plasma}}$  ratio (Table S4 in the Supporting Information).

**Pharmacokinetic Profiles and Brain Distribution Study of Compound 32h in Rats.** A pharmacokinetics study of compound 32h was also performed in Sprague–Dawley rats for further evaluation. The concentrations in plasma and cerebrospinal fluid were determined at 10 time points after i.v. administration at 3 mg/kg and p.o. administration at 10 mg/kg (Figure S8 in the Supporting Information). Compound 32h displayed suitable *in vivo* PK profiles with a low clearance and a reasonable half-life; however, it exhibited different oral bioavailabilities across species. In contrast to the concentration in plasma, the level in cerebrospinal fluid (CSF) was too low to be detected. The results of brain penetration showed that the  $C_{\text{brain}}/C_{\text{plasma}}$  ratio at 20/80 min reached 1.5 in rats after i.v. administration at 3 mg/kg. Generally, compounds with a brain/plasma ratio greater than 0.3–0.5 are considered to have sufficiently good CNS diffusion, and compounds with a value greater than 1 freely cross the BBB. Accordingly, compound 32h has a satisfactory CNS distribution.

**Cytotoxicity and hERG Channel Inhibition of the Selected Compounds.** For further druggability studies of the selected compounds, a CCK8 assay was applied to detect cytotoxicity. The results are summarized in Table 9 for three representative mammalian cell lines at 60 and 120  $\mu$ M of each compound. Unexpectedly, compound 20h exhibited significant cytotoxicity with  $IC_{50}$  values of  $23.2 \pm 1.4$ ,  $29.7 \pm 1.2$ , and  $84.8 \pm 29.6 \mu$ M for VERO, L929, and HEK293, respectively. The compounds 32h, 32o, and 33d showed no significant cytotoxicity. Moreover, compound 32c exhibited slight cytotoxicity at high concentrations (Table 10).

The inhibition of the hERG channel of the selected compounds was further tested by patch-clamp assays to predict cardiovascular toxicity. Unwanted inhibition of the hERG channel can induce serious cardiac arrhythmias, such as long QT syndrome characterized by prolonged QT intervals and torsades de pointes. The results of compounds 32c/32h/33d exhibited negligible affinities toward the hERG channel with inhibitions of  $46.7 \pm 11.4$ ,  $47.6 \pm 6.3$ , and  $45.0 \pm 9.1\%$ , respectively, at a 100  $\mu$ M dose (Table 10). Compound 20h at a dose of 30  $\mu$ M showed a higher hERG inhibition compared with other compounds (50%,  $49.1 \pm 5.3\%$ ). Compound 32o showed moderate inhibition of  $44.2 \pm 5.1\%$  at 30  $\mu$ M and  $53.4 \pm 13.8\%$  at 100  $\mu$ M. Taken together, considering the low  $EC_{50}$  in primary neurons, compound 32h ( $EC_{50} = 2.44 \mu$ M) displayed a good safety profile with low cytotoxicity and cardiotoxicity.

**Acute Toxicity and Effect on Mouse Body Weight.** The acute toxicities of compounds 20h and 32h were

investigated in terms of  $LD_{50}$  values. Both compounds showed quite low acute toxicities, even at the highest tested dose (1500 mg/kg, dissolved in PEG400), and were not lethal in any of the mice 24 h after administration by i.p. injection. Then, successive p.o. administrations of compounds 20h and 32h were performed for 28 days, and body weight was recorded every day. Only a slight reduction in body weight was observed for each compound compared with the vehicle (Figure S9 in the Supporting Information). Nevertheless, weight gain trends and daily behavior of the drug administration groups were unaffected. Taken together, these results suggested that both compounds displayed a remarkable safety profile.

## CONCLUSIONS

We aimed to develop novel NMDAR PAMs with improved *in vivo* activity and drug properties for further development as clinical antidepressants. Starting with virtual screens, the scaffold of furan-2-carboxamide was identified to possess PAM effects on NMDA responses of brain slides and cultured neurons. Further studies determined FS2921 as a functionally selective GluN1/GluN2A PAM versus GluN1/GluN2B and GluN1/GluN2D. FS2921 exhibited a weak NAM effect for GluN1/GluN2C but did not show any influence on native AMPA receptors and GABA receptors. Subsequently, a series of novel derivatives were designed and synthesized based on the discovered core scaffolds. Several selected candidates, including the compound 32h, exhibited favorable *in vitro* activity with  $\Delta I/I_{\text{NDMA}} = 12.5 \pm 5.7$  and  $EC_{50} = 2.4 \mu$ M. It was also found that the compound 32h was as efficacious as duloxetine in FST. Furthermore, the PK/PD studies of the compound 32h in mice and rats displayed superior profiles, including moderate drug exposure and excellent brain penetration properties. In addition, the compound 32h exhibited excellent safety profiles in cytotoxicity, hERG inhibition, and long-term drug administration. The excellent potency, exquisite target selectivity, and *in vivo* PK/PD profile of the compound 32h supported it as an excellent lead compound for further optimizations to discover a promising pharmacotherapeutic for the treatment of depression.

## EXPERIMENTAL SECTION

**Structure-Based Virtual Screening and Docking.** As shown in Figure 2A, the GluN2A and GluN1 ligand-binding domains' (LBDs) crystal structure (PDB ID: 5KDT) was selected for the study *in silico*. Approximately 300,000 compounds from the SPECS chemical library and PKU-CNCL database were prepared to generate conformations by the LigPrep module of the Schrodinger suite (Schrodinger, NY, USA). Then, energy-minimized conformations were docked into the GNE0723 binding site of the crystal structure prepared by the Protein Preparation Wizard module. Then, three predicted binding poses were generated for each compound. According to the score obtained

by the extra precision (XP) scoring function of the Glide module, the top 1000 compounds were retained, among which 361 compounds were selected for the binding pose filter with a  $\pi$ - $\pi$  interaction with Tyr144. The remaining compounds were structurally clustered into 26 clusters based on the Tanimoto coefficients computed using the ECFP\_6 fingerprint. Lastly, eight candidate compounds were purchased for further evaluation by patch-clamp experiments on mice brain slices.

For induced-docking studies, the prepared crystal structure (PDB ID: 5KDT) was used in the Induced Docking module with XP. For ligand preparation, conformations of GNE-0723 and FS2921 were generated and energy-minimized by the LigPrep module. Images depicting the proposed binding modes were generated using Maestro 11.5 (Figure 4).

**General Chemistry.** All commercially available reagents and solvents were used without further purification. Reactions were monitored by thin-layer chromatography (TLC) on precoated glass silica gel plates (GF254, 0.25 mm, Yantai Xinde Chemical Co., Ltd.) using a  $\text{CH}_2\text{Cl}_2/\text{MeOH}/50\%$  aq  $\text{NH}_4\text{OH}$  system or an EtOAc/Petroleum ether system. Column chromatographic purification was carried out using silica gel. Melting points were determined using an X-4 micro melting point apparatus.  $^1\text{H}$  NMR and  $^{13}\text{C}$  NMR spectra were recorded on a Bruker Avance III 400 spectrometer using chloroform-*d* or DMSO-*d*<sub>6</sub> as the solvent. *J* values were reported in hertz (Hz). Chemical shifts were given in  $\delta$  values (ppm), using tetramethylsilane (TMS) as the internal standard. Signal multiplicities are characterized as the following abbreviation: s (singlet), d (doublet), t (triplet), q (quartet), m (multiplet), and br (broad signal). All final test compounds' purity is determined by high-performance liquid chromatography (HPLC), and all final test compounds display purity higher than 95%. HPLC methods used the following: Waters LC-20 AD spectrometer; Waters Xbridge BEH Amide column (4.6  $\times$  250 mm, 5  $\mu\text{m}$  i.d.); mobile phase,  $\text{H}_2\text{O}$  aq/ acetonitrile (30/70; Thermo Fisher Scientific Inc., USA) at a flow rate of 1 mL/min. The column temperature was 25  $^\circ\text{C}$ . The detection wavelength was 254 nm.

**General Procedure A: Synthesis of Pyrazol-Compounds 14, 22a/b, and 30.** Properly substituted parazoles (1 mmol) was solved in dry  $\text{CH}_3\text{CN}$  and followed with  $\text{K}_2\text{CO}_3$  (2 mmol). To the mixture was added the solution of intermediates 13 or 29 (1.5 mmol) in  $\text{CH}_3\text{CN}$ . The resulting suspension was stirred under 60  $^\circ\text{C}$  for 8 h, and then evaporated under reduced pressure. The residue was treated with water/ $\text{CH}_2\text{Cl}_2$ . The organic layer was evaporated to remove the solvent for further purification. The final product was obtained through silica gel column chromatography by elution with EtOAc/Petroleum ether.

**General Procedure B: Hydrolysis of Methyl Esters to Obtain Carboxylic Acids 15, 19a/b, 23a-d, and 31.** To a solution of methyl esters (1 mmol) in methanol, NaOH (1.5 mmol) was added. The mixture was stirred at room temperature overnight. Then the solvent was removed under reduced pressure and redissolved in water/EtOAc. The aqueous layer was added 1 M HCl to pH 4, and then washed with  $\text{CH}_2\text{Cl}_2$ . The combined organic layer was evaporated to remove the solvent for the next step without further purification.

**General Procedure C: Coupling of Carboxamides 9a-c, 16a/b, 17a-n, 20a-k, 22a-d, 32a-o, and 33a-f.** A mixture of Furan-2-carboxylic acid or thiophene-2-carboxylic acid (1 mmol), DIPEA (2 mmol), and HATU (1.2 mmol) in  $\text{CH}_2\text{Cl}_2$  (10 mL) were stirred at 0  $^\circ\text{C}$  for 20 min. Properly substituted aniline (2 mmol) was added to the solvent, and the reaction was stirred at room temperature overnight. The resulting mixture was washed with water and dried over  $\text{Na}_2\text{SO}_4$ . Then, the solvent was removed under reduced pressure for further purification. The residue was purified through silica gel column chromatography by elution with a  $\text{CH}_2\text{Cl}_2/\text{MeOH}/50\%$  aq  $\text{NH}_4\text{OH}$  system to give the target products.

***N*-(4-Bromo-2-methylphenyl)furan-2-carboxamide (9a).** Compound 9a was prepared with general procedure C using starting materials 7a and 8. The final product was obtained as a white solid in 93% yield. M.p.: 105–107  $^\circ\text{C}$ .  $^1\text{H}$  NMR (400 MHz, DMSO-*d*<sub>6</sub>)  $\delta$

9.82 (s, 1H), 7.94 (d, 1H), 7.50 (d, *J* = 2.0 Hz, 1H), 7.45–7.37 (m, 1H), 7.34–7.29 (m, 2H), 6.70 (dd, *J* = 3.4, 1.7 Hz, 1H), 2.23 (s, 3H).  $^{13}\text{C}$  NMR (101 MHz, DMSO-*d*<sub>6</sub>)  $\delta$  156.73, 147.86, 146.12, 136.77, 135.50, 133.23, 129.30, 128.78, 118.79, 115.16, 112.58, 18.06. HRMS (ESI): calcd for  $\text{C}_{12}\text{H}_{11}\text{BrNO}_2$  [ $\text{M} + \text{H}$ ]<sup>+</sup> *m/z* 279.9973, found 279.9975; purity:  $\geq 98\%$  by HPLC analysis.

***N*-(4-Bromo-2-methylphenyl)-5-methylfuran-2-carboxamide (9b).** Compound 9b was prepared with general procedure C using starting materials 7b and 8. The final product was obtained as a white solid in 96% yield. M.p.: 138–140  $^\circ\text{C}$ .  $^1\text{H}$  NMR (400 MHz, DMSO-*d*<sub>6</sub>)  $\delta$  9.67 (s, 1H), 7.49 (d, *J* = 2.0 Hz, 1H), 7.39 (dd, *J* = 8.5, 2.2 Hz, 1H), 7.30 (d, *J* = 8.5 Hz, 1H), 7.20 (d, *J* = 3.3 Hz, 1H), 6.32 (d, *J* = 3.2 Hz, 1H), 2.38 (s, 3H), 2.22 (s, 3H).  $^{13}\text{C}$  NMR (101 MHz, DMSO-*d*<sub>6</sub>)  $\delta$  156.74, 155.51, 146.33, 136.75, 135.66, 133.19, 129.26, 128.72, 118.64, 116.33, 108.94, 18.09, 14.03. HRMS (ESI): calcd for  $\text{C}_{13}\text{H}_{13}\text{BrNO}_2$  [ $\text{M} + \text{H}$ ]<sup>+</sup> *m/z* 294.0130, found 294.0125; purity:  $\geq 99\%$  by HPLC analysis.

***N*-(4-Bromo-2-methylphenyl)-5-chlorofuran-2-carboxamide (9c).** Compound 9c was prepared with general procedure C using starting materials 7c and 8. The final compound was obtained as a white solid in 89% yield. M.p.: 122–124  $^\circ\text{C}$ .  $^1\text{H}$  NMR (400 MHz, DMSO-*d*<sub>6</sub>)  $\delta$  9.92 (s, 1H), 7.51 (d, *J* = 1.7 Hz, 1H), 7.44–7.34 (m, 2H), 7.27 (d, *J* = 8.5 Hz, 1H), 6.75 (d, *J* = 3.6 Hz, 1H), 2.21 (s, 3H).  $^{13}\text{C}$  NMR (101 MHz, DMSO-*d*<sub>6</sub>)  $\delta$  155.69, 147.42, 138.28, 137.02, 135.22, 133.29, 129.35, 128.96, 119.07, 117.45, 109.95, 18.07. HRMS (ESI): calcd for  $\text{C}_{12}\text{H}_{10}\text{ClBrNO}_2$  [ $\text{M} + \text{H}$ ]<sup>+</sup> *m/z* 313.9683, found 313.9690; purity:  $\geq 98\%$  by HPLC analysis.

**Methyl 5-(Hydroxymethyl)furan-2-carboxylate (11).** To a solution of starting material 10 in dry methanol (10 mL) was added concentrated sulfuric acid (2 mL) at 0  $^\circ\text{C}$ . After slow addition, the mixture was stirred for 10 h at room temperature. Then, to the mixture was added 2 N  $\text{NaHCO}_3$  until the pH becomes 7. After that, the mixture was extracted with dichloromethane three times, and the organic phase was combined and dried over  $\text{Na}_2\text{SO}_4$ . Then, the solvent was removed under reduced pressure for further purification. The residue was purified through silica gel column chromatography by elution with EtOAc/petroleum ether (1:2). The final compound was obtained as a pale yellow oil in 94% yield.  $^1\text{H}$  NMR (400 MHz,  $\text{CDCl}_3$ )  $\delta$  7.13 (d, *J* = 3.4 Hz, 1H), 6.42 (dd, *J* = 3.4, 0.7 Hz, 1H), 4.70–4.65 (m, 2H), 3.89 (s, 3H), 2.69 (s, 1H).  $^{13}\text{C}$  NMR (101 MHz, chloroform-*d*)  $\delta$  159.23, 158.47, 143.97, 118.91, 109.42, 57.49, 51.96. MS (ESI): calcd for  $\text{C}_7\text{H}_9\text{O}_4$  [ $\text{M} + \text{H}$ ]<sup>+</sup> *m/z* 157, found 157.

**Methyl 5-(Chloromethyl)furan-2-carboxylate (12).** A solution of compound 11 (1 mmol) in a mixture of  $\text{CH}_2\text{Cl}_2$  (9.5 mL) and DMF (0.5 mL) was treated with  $\text{SOCl}_2$  (1.5 mmol). The mixture was stirred for 1 h at room temperature. Then, the reaction was treated with saturated  $\text{NaHCO}_3$  solution. The residue was purified through silica gel column chromatography by elution with EtOAc/petroleum ether (1:4). The final compound was obtained as a colorless oil in 86% yield.  $^1\text{H}$  NMR (400 MHz,  $\text{CDCl}_3$ )  $\delta$  7.13 (d, *J* = 3.5 Hz, 1H), 6.49 (d, *J* = 3.5 Hz, 1H), 4.60 (s, 2H), 3.90 (s, 3H).  $^{13}\text{C}$  NMR (101 MHz,  $\text{CDCl}_3$ )  $\delta$  158.78, 154.13, 144.80, 118.80, 111.39, 52.04, 36.65. MS (ESI): calcd for  $\text{C}_7\text{H}_8\text{ClO}_3$  [ $\text{M} + \text{H}$ ]<sup>+</sup> *m/z* 175, found 175.

**Methyl 5-(Iodomethyl)furan-2-carboxylate (13).** To a solution of compound 12 (1 mmol) in acetone (10 mL) was added NaI (1.5 mmol). The mixture was refluxed for 10 h and cooled to r.t. Then, the reaction was treated with EtOAc/water. The organic layer was evaporated to remove the solvent for the next step without further purification.

**Methyl 5-((3,5-Dimethyl-1H-pyrazol-1-yl)methyl)furan-2-carboxylate (14).** Compound 14 was prepared with general procedure A using 3,5-dimethyl-1H-pyrazole and intermediate 13. The final compound was obtained as a colorless oil in 66% yield.  $^1\text{H}$  NMR (400 MHz,  $\text{CDCl}_3$ )  $\delta$  7.07 (d, *J* = 2.8 Hz, 1H), 6.17 (d, *J* = 2.8 Hz, 1H), 5.82 (s, 1H), 5.20 (s, 2H), 3.85 (s, 3H), 2.26 (s, 3H), 2.19 (s, 3H). MS (ESI): calcd for  $\text{C}_{12}\text{H}_{15}\text{N}_2\text{O}_3$  [ $\text{M} + \text{H}$ ]<sup>+</sup> *m/z* 235, found 235.

**5-((3,5-Dimethyl-1H-pyrazol-1-yl)methyl)furan-2-carboxylic Acid (15).** Compound 15 was prepared with general procedure B using starting material intermediate 26. The final compound was obtained as a white solid for the next step without further purification.

5-((3,5-Dimethyl-1H-pyrazol-1-yl)methyl)-N-(pyridin-3-yl)furan-2-carboxamide (**16a**). Compound **16a** was prepared with general procedure C using pyridin-3-amine and intermediate **15**. The final compound was obtained as a white solid in 65% yield. M.p.: 144–146 °C. <sup>1</sup>H NMR (400 MHz, DMSO-*d*<sub>6</sub>) δ 10.36 (s, 1H), 8.90 (s, 1H), 8.31 (d, *J* = 4.3 Hz, 1H), 8.14 (d, *J* = 8.3 Hz, 1H), 7.38 (dd, *J* = 9.7, 3.4 Hz, 2H), 6.47 (d, *J* = 2.5 Hz, 1H), 5.85 (s, 1H), 5.29 (s, 2H), 2.28 (s, 3H), 2.08 (s, 3H). <sup>13</sup>C NMR (101 MHz, DMSO-*d*<sub>6</sub>) δ 156.82, 154.41, 146.95, 146.88, 145.09, 142.41, 139.58, 135.67, 127.84, 123.99, 116.42, 110.77, 105.71, 45.52, 13.73, 11.08. HRMS (ESI): calcd for C<sub>16</sub>H<sub>17</sub>N<sub>4</sub>O<sub>2</sub> [M + H]<sup>+</sup> *m/z* 297.1352, found 297.1354; purity: ≥96% by HPLC analysis.

5-((3,5-Dimethyl-1H-pyrazol-1-yl)methyl)-N-(naphthalen-2-yl)furan-2-carboxamide (**16b**). Compound **16b** was prepared with general procedure C using naphthalen-2-amine and intermediate **15**. The final compound was obtained as a white solid in 45% yield. M.p.: 138–140 °C. <sup>1</sup>H NMR (400 MHz, DMSO-*d*<sub>6</sub>) δ 10.32 (s, 1H), 8.37 (s, 1H), 7.96–7.74 (m, 4H), 7.56–7.33 (m, 3H), 6.49 (d, *J* = 3.4 Hz, 1H), 5.86 (s, 1H), 5.31 (s, 2H), 2.31 (s, 3H), 2.09 (s, 3H). <sup>13</sup>C NMR (101 MHz, DMSO-*d*<sub>6</sub>) δ 156.73, 154.21, 147.36, 146.86, 139.60, 136.61, 133.74, 130.46, 128.68, 127.92, 127.82, 126.89, 125.31, 121.31, 117.10, 115.93, 110.69, 105.71, 45.56, 13.76, 11.11. HRMS (ESI): calcd for C<sub>21</sub>H<sub>20</sub>N<sub>3</sub>O<sub>2</sub> [M + H]<sup>+</sup> *m/z* 346.1556, found 346.1549; purity: ≥96% by HPLC analysis.

5-((3,5-Dimethyl-1H-pyrazol-1-yl)methyl)-N-(4-fluoro-2-methylphenyl)furan-2-carboxamide (**17a**). Compound **17a** was prepared with general procedure C using 4-fluoro-2-methylaniline and intermediate **15**. The final compound was obtained as a white solid in 47% yield. M.p.: 120–122 °C. <sup>1</sup>H NMR (400 MHz, DMSO-*d*<sub>6</sub>) δ 9.73 (s, 1H), 7.37–7.29 (m, 1H), 7.26 (d, *J* = 3.0 Hz, 1H), 7.14 (dd, *J* = 9.6, 2.4 Hz, 1H), 7.04 (td, *J* = 8.6, 2.7 Hz, 1H), 6.47 (d, *J* = 3.3 Hz, 1H), 5.85 (s, 1H), 5.27 (s, 2H), 2.30 (s, 3H), 2.21 (s, 3H), 2.08 (s, 3H). <sup>13</sup>C NMR (101 MHz, DMSO-*d*<sub>6</sub>) δ 160.47 (d, *J* = 242.0 Hz), 156.81, 153.88, 147.39, 146.83, 139.59, 137.03 (d, *J* = 8.3 Hz), 132.21 (d, *J* = 2.8 Hz), 128.86 (d, *J* = 8.8 Hz), 117.09 (d, *J* = 22.2 Hz), 115.60, 113.10 (d, *J* = 22.0 Hz), 110.66, 105.65, 45.46, 18.32, 13.74, 11.11. HRMS (ESI): calcd for C<sub>18</sub>H<sub>19</sub>FN<sub>3</sub>O<sub>2</sub> [M + H]<sup>+</sup> *m/z* 328.1461, found 328.1463; purity: ≥96% by HPLC analysis.

N-(4-Chloro-2-methylphenyl)-5-((3,5-dimethyl-1H-pyrazol-1-yl)methyl)furan-2-carboxamide (**17b**). Compound **17b** was prepared with general procedure C using 4-chloro-2-methylaniline and intermediate **15**. The final compound was obtained as a white solid in 49% yield. M.p.: 133–135 °C. <sup>1</sup>H NMR (400 MHz, CDCl<sub>3</sub>) δ 7.94 (d, *J* = 9.2 Hz, 1H), 7.88 (s, 1H), 7.28 (s, 0H), 7.19 (s, 2H), 7.14 (d, *J* = 2.9 Hz, 1H), 6.33 (d, *J* = 2.7 Hz, 1H), 5.87 (s, 1H), 5.23 (s, 2H), 2.30 (s, 3H), 2.28 (s, 3H), 2.23 (s, 3H). <sup>13</sup>C NMR (101 MHz, CDCl<sub>3</sub>) δ 155.72, 152.46, 148.32, 147.38, 139.12, 133.77, 130.34, 130.24, 130.03, 126.82, 123.56, 116.22, 110.54, 105.97, 45.80, 17.43, 13.49, 11.07. HRMS (ESI): calcd for C<sub>18</sub>H<sub>19</sub>N<sub>3</sub>O<sub>2</sub>Cl [M + H]<sup>+</sup> *m/z* 344.1166, found 344.1159; purity: ≥96% by HPLC analysis.

5-((3,5-Dimethyl-1H-pyrazol-1-yl)methyl)-N-(*o*-tolyl)furan-2-carboxamide (**17c**). Compound **17c** was prepared with general procedure C using *o*-toluidine and intermediate **15**. The final compound was obtained as a white solid in 55% yield. M.p.: 98–100 °C. <sup>1</sup>H NMR (400 MHz, CDCl<sub>3</sub>) δ 8.03–7.90 (m, 2H), 7.32–7.20 (m, 2H), 7.16–7.04 (m, 2H), 6.32 (s, 1H), 5.87 (s, 1H), 5.22 (s, 2H), 2.30 (s, 6H), 2.23 (s, 3H). <sup>13</sup>C NMR (101 MHz, CDCl<sub>3</sub>) δ 155.80, 152.31, 148.28, 147.64, 139.16, 135.15, 130.49, 128.55, 126.87, 125.12, 122.41, 115.94, 110.48, 105.94, 45.81, 17.57, 13.51, 11.08. HRMS (ESI): calcd for C<sub>18</sub>H<sub>20</sub>N<sub>3</sub>O<sub>2</sub> [M + H]<sup>+</sup> *m/z* 310.1556, found 310.1555; purity: ≥97% by HPLC analysis.

5-((3,5-Dimethyl-1H-pyrazol-1-yl)methyl)-N-phenylfuran-2-carboxamide (**17d**). Compound **17d** was prepared with general procedure C using aniline and intermediate **15**. The final compound was obtained as a white solid in 75% yield. M.p.: 124–126 °C. <sup>1</sup>H NMR (400 MHz, DMSO-*d*<sub>6</sub>) δ 10.10 (s, 1H), 7.72 (d, *J* = 8.6 Hz, 2H), 7.41–7.28 (m, 3H), 7.10 (t, *J* = 7.4 Hz, 1H), 6.46 (d, *J* = 3.5 Hz, 1H), 5.85 (s, 1H), 5.28 (s, 2H), 2.29 (s, 3H), 2.09 (s, 3H). <sup>13</sup>C NMR (101 MHz, DMSO-*d*<sub>6</sub>) δ 156.53, 154.08, 147.37, 146.83, 139.57, 138.93, 129.10, 124.21, 120.84, 115.77, 110.62, 105.69, 45.54, 13.75,

11.10. HRMS (ESI): calcd for C<sub>17</sub>H<sub>18</sub>N<sub>3</sub>O<sub>2</sub> [M + H]<sup>+</sup> *m/z* 296.1399, found 296.1401; purity: ≥98% by HPLC analysis.

N-(4-Bromophenyl)-5-((3,5-dimethyl-1H-pyrazol-1-yl)methyl)furan-2-carboxamide (**17e**). Compound **17e** was prepared with general procedure C using 4-bromoaniline and intermediate **15**. The final compound was obtained as a white solid in 62% yield. M.p.: 168–170 °C. <sup>1</sup>H NMR (400 MHz, CDCl<sub>3</sub>) δ 8.33 (s, 1H), 7.53 (d, *J* = 8.4 Hz, 2H), 7.42 (d, *J* = 8.5 Hz, 2H), 7.12 (d, *J* = 3.2 Hz, 1H), 6.28 (d, *J* = 2.9 Hz, 1H), 5.85 (s, 1H), 5.18 (s, 2H), 2.26 (s, 3H), 2.21 (s, 3H). <sup>13</sup>C NMR (101 MHz, CDCl<sub>3</sub>) δ 155.83, 152.38, 148.37, 147.37, 139.20, 136.51, 131.98 (2C), 121.62 (2C), 117.11, 116.36, 110.79, 106.08, 77.26, 45.75, 13.47, 11.11. HRMS (ESI): calcd for C<sub>17</sub>H<sub>17</sub>BrN<sub>3</sub>O<sub>2</sub> [M + H]<sup>+</sup> *m/z* 374.0504, found 374.0505; purity: ≥96% by HPLC analysis.

N-(4-Bromo-2-ethylphenyl)-5-((3,5-dimethyl-1H-pyrazol-1-yl)methyl)furan-2-carboxamide (**17f**). Compound **17f** was prepared with general procedure C using 4-bromo-2-aniline and intermediate **15**. The final compound was obtained as a white solid in 68% yield. M.p.: 155–157 °C. <sup>1</sup>H NMR (400 MHz, CDCl<sub>3</sub>) δ 7.90 (d, *J* = 8.7 Hz, 2H), 7.33 (d, *J* = 7.0 Hz, 2H), 7.14 (d, *J* = 3.4 Hz, 1H), 6.34 (d, *J* = 3.4 Hz, 1H), 5.85 (s, 1H), 5.22 (s, 2H), 2.61 (q, *J* = 7.6 Hz, 2H), 2.29 (s, 3H), 2.21 (s, 3H), 1.25 (t, *J* = 7.6 Hz, 4H). <sup>13</sup>C NMR (101 MHz, CDCl<sub>3</sub>) δ 155.80, 152.45, 148.33, 147.43, 139.10, 136.35, 133.62, 131.38, 129.75, 124.27, 118.32, 116.28, 110.63, 105.94, 45.80, 24.07, 13.57, 13.51, 11.09. HRMS (ESI): calcd for C<sub>19</sub>H<sub>21</sub>BrN<sub>3</sub>O<sub>2</sub> [M + H]<sup>+</sup> *m/z* 402.0817, found 402.0818; purity: ≥96% by HPLC analysis.

N-(4-Bromo-2-chlorophenyl)-5-((3,5-dimethyl-1H-pyrazol-1-yl)methyl)furan-2-carboxamide (**17g**). Compound **17g** was prepared with general procedure C using 4-bromo-2-chloroaniline and intermediate **15**. The final compound was obtained as a white solid in 58% yield. M.p.: 186–188 °C. <sup>1</sup>H NMR (400 MHz, CDCl<sub>3</sub>) δ 8.51 (s, 1H), 8.40 (d, *J* = 8.9 Hz, 1H), 7.53 (s, 1H), 7.39 (d, *J* = 8.9 Hz, 1H), 7.16 (d, *J* = 3.1 Hz, 1H), 6.36 (d, *J* = 2.9 Hz, 1H), 5.86 (s, 1H), 5.23 (s, 2H), 2.33 (s, 3H), 2.21 (s, 3H). <sup>13</sup>C NMR (101 MHz, CDCl<sub>3</sub>) δ 155.42, 153.08, 148.42, 146.90, 139.19, 133.45, 131.48, 130.91, 123.39, 122.14, 116.88, 116.34, 110.77, 105.96, 45.69, 13.51, 11.11. HRMS (ESI): calcd for C<sub>17</sub>H<sub>16</sub>ClN<sub>3</sub>O<sub>2</sub> [M + H]<sup>+</sup> *m/z* 408.0114, found 408.0112; purity: ≥98% by HPLC analysis.

5-((3,5-Dimethyl-1H-pyrazol-1-yl)methyl)-N-(2-(methylamino)phenyl)furan-2-carboxamide (**17h**). Compound **17h** was prepared with general procedure C using N<sup>1</sup>-methylbenzene-1,2-diamine and intermediate **15**. The final compound was obtained as a white solid in 38% yield. M.p.: 135 ~ 137 °C. <sup>1</sup>H NMR (400 MHz, DMSO-*d*<sub>6</sub>) δ 9.41 (s, 1H), 7.26 (s, 1H), 7.18–7.04 (m, 2H), 6.68–6.55 (m, 2H), 6.47 (d, *J* = 2.9 Hz, 1H), 5.85 (s, 1H), 5.26 (s, 2H), 5.13 (d, *J* = 4.5 Hz, 1H), 2.71 (d, *J* = 4.8 Hz, 3H), 2.30 (s, 3H), 2.09 (s, 3H). <sup>13</sup>C NMR (101 MHz, DMSO-*d*<sub>6</sub>) δ 157.20, 153.53, 147.74, 146.76, 145.32, 139.55, 127.75, 127.52, 122.81, 115.83, 115.33, 110.75, 110.58, 105.64, 45.48, 30.28, 13.75, 11.13. HRMS (ESI): calcd for C<sub>18</sub>H<sub>21</sub>N<sub>4</sub>O<sub>2</sub> [M + H]<sup>+</sup> *m/z* 325.1665, found 325.1671; purity: ≥97% by HPLC analysis.

5-((3,5-Dimethyl-1H-pyrazol-1-yl)methyl)-N-(2-(2-hydroxyethyl)phenyl)furan-2-carboxamide (**17i**). Compound **17i** was prepared with general procedure C using 2-(2-aminophenyl)ethan-1-ol and intermediate **15**. The final compound was obtained as a white solid in 38% yield. M.p.: 93–95 °C. <sup>1</sup>H NMR (400 MHz, DMSO-*d*<sub>6</sub>) δ 10.23 (s, 1H), 7.60 (d, *J* = 7.9 Hz, 1H), 7.33–7.21 (m, 2H), 7.18 (d, 1H), 7.17–7.12 (m, 1H), 6.56–6.45 (m, 1H), 5.85 (s, 1H), 5.53–5.33 (m, 1H), 5.27 (s, 2H), 3.70 (t, *J* = 5.7 Hz, 2H), 2.78 (t, *J* = 5.6 Hz, 2H), 2.31 (s, 3H), 2.09 (s, 3H). <sup>13</sup>C NMR (101 MHz, DMSO-*d*<sub>6</sub>) δ 156.43, 153.82, 147.62, 146.91, 139.66, 136.46, 134.56, 130.86, 126.96, 125.84, 125.32, 115.41, 110.79, 105.64, 62.68, 45.38, 35.44, 13.75, 11.08. HRMS (ESI): calcd for C<sub>19</sub>H<sub>22</sub>N<sub>3</sub>O<sub>3</sub> [M + H]<sup>+</sup> *m/z* 340.1661, found 340.1664; purity: ≥97% by HPLC analysis.

N-([1,1'-Biphenyl]-2-yl)-5-((3,5-dimethyl-1H-pyrazol-1-yl)methyl)furan-2-carboxamide (**17j**). Compound **17j** was prepared with general procedure C using [1,1'-biphenyl]-4-amine and intermediate **15**. The final compound was obtained as a white solid in 38% yield. M.p.: 97 ~ 99 °C. <sup>1</sup>H NMR (400 MHz, DMSO-*d*<sub>6</sub>) δ

9.46 (s, 1H), 7.63 (d,  $J = 7.8$  Hz, 1H), 7.49–7.27 (m, 8H), 7.10 (d,  $J = 2.9$  Hz, 1H), 6.43 (d,  $J = 3.2$  Hz, 1H), 5.84 (s, 1H), 5.19 (s, 2H), 2.21 (s, 3H), 2.08 (s, 3H).  $^{13}\text{C}$  NMR (101 MHz, DMSO- $d_6$ )  $\delta$  156.90, 153.77, 147.38, 146.82, 139.52, 139.08, 137.47, 134.40, 130.77, 129.12 (2C), 128.92 (2C), 128.35, 127.85, 127.38, 126.88, 115.62, 110.78, 105.64, 45.36, 13.74, 11.07. HRMS (ESI): calcd for  $\text{C}_{23}\text{H}_{22}\text{N}_3\text{O}_2$   $[\text{M} + \text{H}]^+$   $m/z$  372.1712, found 372.1717; purity:  $\geq 97\%$  by HPLC analysis.

*N*-([1,1'-Biphenyl]-4-yl)-5-((3,5-dimethyl-1H-pyrazol-1-yl)methyl)furan-2-carboxamide (17k). Compound 17k was prepared with general procedure C using [1,1'-biphenyl]-2-amine and intermediate 15. The final compound was obtained as a white solid in 38% yield. M.p.: 178–180 °C.  $^1\text{H}$  NMR (400 MHz, DMSO- $d_6$ )  $\delta$  10.23 (s, 1H), 7.85 (d,  $J = 8.6$  Hz, 2H), 7.67 (d,  $J = 8.7$  Hz, 4H), 7.45 (t,  $J = 7.6$  Hz, 2H), 7.40–7.29 (m, 2H), 6.47 (d,  $J = 3.3$  Hz, 1H), 5.86 (s, 1H), 5.30 (s, 2H), 2.30 (s, 3H), 2.09 (s, 3H).  $^{13}\text{C}$  NMR (101 MHz, DMSO- $d_6$ )  $\delta$  156.55, 154.15, 147.38, 146.87, 140.13, 139.57, 138.48, 135.86, 129.35 (2C), 127.54, 127.31 (2C), 126.75 (2C), 121.12 (2C), 115.90, 110.66, 105.72, 45.56, 13.75, 11.10. HRMS (ESI): calcd for  $\text{C}_{23}\text{H}_{22}\text{N}_3\text{O}_2$   $[\text{M} + \text{H}]^+$   $m/z$  372.1712, found 372.1714; purity:  $\geq 98\%$  by HPLC analysis.

*N*-(4-Chloro-2-(hydroxymethyl)phenyl)-5-((3,5-dimethyl-1H-pyrazol-1-yl)methyl)furan-2-carboxamide (17l). Compound 17l was prepared with general procedure C using (2-amino-5-chlorophenyl)methanol and intermediate 15. The final compound was obtained as a white solid in 44% yield. M.p.: 131–133 °C.  $^1\text{H}$  NMR (400 MHz, DMSO- $d_6$ )  $\delta$  10.04 (s, 1H), 7.75 (d,  $J = 8.6$  Hz, 1H), 7.46 (d,  $J = 2.3$  Hz, 1H), 7.35 (dd,  $J = 8.6, 2.4$  Hz, 1H), 7.23 (d,  $J = 3.4$  Hz, 1H), 6.51 (d,  $J = 3.4$  Hz, 1H), 5.84 (s, 1H), 5.75 (t,  $J = 5.5$  Hz, 1H), 5.27 (s, 2H), 4.57 (d,  $J = 5.4$  Hz, 2H), 2.31 (s, 3H), 2.08 (s, 3H).  $^{13}\text{C}$  NMR (101 MHz, DMSO- $d_6$ )  $\delta$  156.22, 154.14, 147.18, 146.91, 139.66, 137.03, 134.72, 129.36, 127.58, 127.48, 125.69, 116.16, 111.06, 105.63, 60.94, 45.36, 13.75, 11.10. HRMS (ESI): calcd for  $\text{C}_{18}\text{H}_{19}\text{N}_3\text{O}_3\text{Cl}$   $[\text{M} + \text{H}]^+$   $m/z$  360.1115, found 360.1119; purity:  $\geq 96\%$  by HPLC analysis.

*N*-(2,4-Dichlorophenyl)-5-((3,5-dimethyl-1H-pyrazol-1-yl)methyl)furan-2-carboxamide (17m). Compound 17m was prepared with general procedure C using 2,4-dichloroaniline and intermediate 15. The final compound was obtained as a white solid in 63% yield. M.p.: 175–177 °C.  $^1\text{H}$  NMR (400 MHz,  $\text{CDCl}_3$ )  $\delta$  8.53 (s, 1H), 8.47 (d,  $J = 8.9$  Hz, 1H), 7.42 (s, 1H), 7.19 (d,  $J = 3.3$  Hz, 1H), 6.38 (d,  $J = 3.2$  Hz, 1H), 5.87 (s, 1H), 5.25 (s, 2H), 2.35 (s, 3H), 2.23 (s, 3H).  $^{13}\text{C}$  NMR (101 MHz,  $\text{CDCl}_3$ )  $\delta$  155.48, 153.06, 148.45, 146.93, 139.20, 133.00, 129.18, 128.77, 128.02, 123.24, 121.88, 116.87, 110.75, 105.96, 45.72, 13.50, 11.10. HRMS (ESI): calcd for  $\text{C}_{17}\text{H}_{16}\text{Cl}_2\text{N}_3\text{O}_2$   $[\text{M} + \text{H}]^+$   $m/z$  364.0620, found 364.0623; purity:  $\geq 98\%$  by HPLC analysis.

*N*-(4-Chloro-2-fluorophenyl)-5-((3,5-dimethyl-1H-pyrazol-1-yl)methyl)furan-2-carboxamide (17n). Compound 17n was prepared with general procedure C using 2-fluoro-4-chloroaniline and intermediate 15. The final compound was obtained as a white solid in 66% yield. M.p.: 131–133 °C.  $^1\text{H}$  NMR (400 MHz, DMSO- $d_6$ )  $\delta$  9.86 (s, 1H), 7.79–7.40 (m, 2H), 7.29 (d,  $J = 10.7$  Hz, 2H), 6.50 (s, 1H), 5.85 (s, 1H), 5.28 (s, 2H), 2.30 (s, 3H), 2.08 (s, 3H).  $^{13}\text{C}$  NMR (101 MHz, DMSO- $d_6$ )  $\delta$  160.14 (d,  $J = 246.4$  Hz), 156.69, 154.22, 146.91, 146.86, 139.60, 131.31 (d,  $J = 3.5$  Hz), 130.72 (d,  $J = 11.1$  Hz), 129.87 (d,  $J = 9.1$  Hz), 117.20 (d,  $J = 25.9$  Hz), 116.28, 115.14 (d,  $J = 22.1$  Hz), 110.83, 105.66, 45.43, 13.75, 11.11. HRMS (ESI): calcd for  $\text{C}_{17}\text{H}_{16}\text{ClFN}_3\text{O}_2$   $[\text{M} + \text{H}]^+$   $m/z$  348.0915, found 348.0913; purity:  $\geq 95\%$  by HPLC analysis.

Methyl 5-((3-Methyl-5-(trifluoromethyl)-1H-pyrazol-1-yl)methyl)furan-2-carboxylate (18a) or Methyl 5-((3,5-Bis(trifluoromethyl)-1H-pyrazol-1-yl)methyl)furan-2-carboxylate (18b). Compound 18a/18b was prepared with general procedure A using 3-methyl-5-(trifluoromethyl)-1H-pyrazole or 3,5-bis(trifluoromethyl)-1H-pyrazole and intermediate 25. The final compound was obtained as a colorless oil without further purification for the next step.

5-((3-Methyl-5-(trifluoromethyl)-1H-pyrazol-1-yl)methyl)furan-2-carboxylic Acid (19a) or 5-((3,5-Bis(trifluoromethyl)-1H-pyrazol-1-yl)methyl)furan-2-carboxylic Acid (19b). Compound 19a or 19b

was prepared with general procedure B using intermediate 18a or 18b. The final compound was obtained as a white solid without further purification for the next step.

*N*-(4-Chloro-2-methylphenyl)-5-((5-methyl-3-(trifluoromethyl)-1H-pyrazol-1-yl)methyl)furan-2-carboxamide (20a). Compound 20a was prepared with general procedure C using 4-chloro-2-methylaniline and intermediate 19a. The final compound was obtained as a white solid in 60% yield. M.p.: 127–129 °C.  $^1\text{H}$  NMR (400 MHz, DMSO- $d_6$ )  $\delta$  9.76 (s, 1H), 7.42–7.34 (m, 2H), 7.34–7.24 (m, 2H), 6.63 (d,  $J = 3.4$  Hz, 1H), 6.57 (s, 1H), 5.52 (s, 2H), 2.43 (s, 3H), 2.21 (s, 3H).  $^{13}\text{C}$  NMR (101 MHz, DMSO- $d_6$ )  $\delta$  156.54, 152.33, 147.73, 142.03, 140.34 (q,  $J = 37.2$  Hz), 136.30, 134.92, 130.47, 130.36, 128.34, 126.39, 122.00 (q,  $J = 268.2$  Hz), 115.80, 111.68, 104.55 (d,  $J = 2.5$  Hz), 46.51, 18.05, 11.19. HRMS (ESI): calcd for  $\text{C}_{18}\text{H}_{16}\text{F}_3\text{N}_3\text{O}_2$   $[\text{M} + \text{H}]^+$   $m/z$  398.0883, found 398.0873; purity:  $\geq 98\%$  by HPLC analysis.

*N*-(4-Bromo-2-methylphenyl)-5-((5-methyl-3-(trifluoromethyl)-1H-pyrazol-1-yl)methyl)furan-2-carboxamide (20b). Compound 20b was prepared with general procedure C using 4-bromo-2-methylaniline and intermediate 19a. The final compound was obtained as a white solid in 57% yield. M.p.: 98–100 °C.  $^1\text{H}$  NMR (400 MHz, DMSO- $d_6$ )  $\delta$  9.75 (s, 1H), 7.57–7.46 (m, 1H), 7.45–7.36 (m, 1H), 7.37–7.25 (m, 2H), 6.63 (d,  $J = 3.4$  Hz, 1H), 6.56 (s, 1H), 5.52 (s, 2H), 2.43 (s, 3H), 2.21 (s, 3H).  $^{13}\text{C}$  NMR (101 MHz, DMSO- $d_6$ )  $\delta$  156.48, 152.34, 147.72, 142.03, 140.35 (q,  $J = 37.2$  Hz), 136.62, 135.38, 133.26, 129.34, 128.61, 122.00 (q,  $J = 268.1$  Hz), 118.82, 115.82, 111.68, 104.55, 46.51, 17.9, 11.19. HRMS (ESI): calcd for  $\text{C}_{18}\text{H}_{16}\text{BrF}_3\text{N}_3\text{O}_2$   $[\text{M} + \text{H}]^+$   $m/z$  442.0378, found 442.0383; purity:  $\geq 96\%$  by HPLC analysis.

5-((3,5-Bis(trifluoromethyl)-1H-pyrazol-1-yl)methyl)-*N*-(4-fluoro-2-methylphenyl)furan-2-carboxamide (20c). Compound 20c was prepared with general procedure C using 4-fluoro-2-methylaniline and intermediate 19b. The final compound was obtained as a white solid in 55% yield. M.p.: 162–164 °C.  $^1\text{H}$  NMR (400 MHz,  $\text{CDCl}_3$ )  $\delta$  8.12 (s, 1H), 7.94–7.90 (m, 2H), 7.83 (s, 1H), 7.21 (d,  $J = 4.0$  Hz, 1H), 6.97–6.92 (m, 1H), 6.63 (d,  $J = 4.0$  Hz, 1H), 5.55 (s, 2H), 2.32 (s, 3H).  $^{13}\text{C}$  NMR (101 MHz,  $\text{CDCl}_3$ )  $\delta$  161.15, 158.72, 155.50, 148.61, 148.48, 130.88, 130.85, 124.42, 124.34, 117.24, 117.02, 115.96, 113.50, 113.28, 113.00, 106.86, 77.33, 77.02, 76.70, 48.36, 48.34, 17.47. HRMS (ESI): calcd for:  $\text{C}_{19}\text{H}_{12}\text{F}_7\text{N}_3\text{O}_4$   $[\text{M} + \text{H}]^+$   $m/z$  436.0896, found 436.0894; purity:  $\geq 97\%$  by HPLC analysis.

5-((3,5-Bis(trifluoromethyl)-1H-pyrazol-1-yl)methyl)-*N*-(4-chloro-2-methylphenyl)furan-2-carboxamide (20d). Compound 20d was prepared with general procedure C using 4-chloro-2-methylaniline and intermediate 19b. The final compound was obtained as a white solid in 48% yield. M.p.: 145–147 °C.  $^1\text{H}$  NMR (400 MHz,  $\text{CDCl}_3$ )  $\delta$  8.03 (d,  $J = 6.0$  Hz, 2H), 7.90 (s, 1H), 7.23 (m, 3H), 6.97 (s, 1H), 6.64 (d,  $J = 4.0$  Hz, 2H), 5.55 (s, 2H), 2.31 (s, 3H).  $^{13}\text{C}$  NMR (101 MHz,  $\text{CDCl}_3$ )  $\delta$  155.32, 148.67, 148.42, 133.68, 133.24, 130.31, 130.08, 129.95, 126.91, 123.20, 124.68, 121.45, 120.47, 118.81, 116.13, 113.09, 106.88, 48.33, 17.14. HRMS (ESI): calcd for:  $\text{C}_{18}\text{H}_{12}\text{ClF}_6\text{N}_3\text{O}_2$   $[\text{M} + \text{H}]^+$   $m/z$  452.0600, found 452.0600; purity:  $\geq 97\%$  by HPLC analysis.

5-((3,5-Bis(trifluoromethyl)-1H-pyrazol-1-yl)methyl)-*N*-(4-bromo-2-methylphenyl)furan-2-carboxamide (20e). Compound 20e was prepared with general procedure C using 4-bromo-2-methylaniline and intermediate 19b. The final compound was obtained as a white solid in 68% yield. M.p.: 130–132 °C.  $^1\text{H}$  NMR (400 MHz, DMSO- $d_6$ )  $\delta$  9.72 (s, 1H), 7.65 (s, 1H), 7.50 (s, 1H), 7.40 (d, 1H), 7.37–7.32 (m, 2H), 6.72 (d,  $J = 2.6$  Hz, 1H), 5.75 (s, 2H), 2.21 (s, 3H).  $^{13}\text{C}$  NMR (101 MHz, DMSO- $d_6$ )  $\delta$  156.38, 150.46, 148.07, 141.26 (q,  $J = 40.2$  Hz), 136.39, 135.32, 133.26, 133.20 (q,  $J = 40.2$  Hz), 129.34, 128.40, 120.86 (q,  $J = 269.0$  Hz), 119.38 (q,  $J = 269.8$  Hz), 118.76, 115.79, 112.69, 108.22, 48.88, 17.86. HRMS (ESI): calcd for  $\text{C}_{18}\text{H}_{13}\text{BrF}_6\text{N}_3\text{O}_2$   $[\text{M} + \text{H}]^+$   $m/z$  496.0095, found 496.0103; purity:  $\geq 96\%$  by HPLC analysis.

5-((3,5-Bis(trifluoromethyl)-1H-pyrazol-1-yl)methyl)-*N*-(2,4-dichlorophenyl)furan-2-carboxamide (20f). Compound 20f was prepared with general procedure C using 2,4-dichloroaniline and intermediate 19b. The final compound was obtained as an off-white

solid in 63% yield. M.p.: 123–125 °C. <sup>1</sup>H NMR (400 MHz, CDCl<sub>3</sub>) δ 8.58 (s, 1H), 8.50 (d, *J* = 12.0 Hz, 1H), 7.45 (d, *J* = 4.0 Hz, 1H), 7.3 (dd, *J* = 2.0, 9.0 Hz, 1H), 7.25 (d, *J* = 4.0 Hz, 1H), 6.97 (s, 1H), 6.65 (d, *J* = 4.0 Hz, 1H), 5.57 (s, 2H). <sup>13</sup>C NMR (101 MHz, CDCl<sub>3</sub>) δ 155.19, 149.21, 147.93, 132.86, 130.65, 129.43, 128.88, 127.99, 123.43, 121.91, 121.60, 119.11, 116.68, 116.64, 113.06, 106.82, 48.33. HRMS (ESI): calcd for: C<sub>17</sub>H<sub>9</sub>Cl<sub>2</sub>F<sub>6</sub>N<sub>3</sub>O<sub>2</sub> [M + H]<sup>+</sup> *m/z* 472.0054, found 472.0056; purity: ≥96% by HPLC analysis.

**5-((3,5-Bis(trifluoromethyl)-1H-pyrazol-1-yl)methyl)-N-(3,4-dichlorophenyl)furan-2-carboxamide (20g).** Compound 20g was prepared with general procedure C using 3,4-dichloroaniline and intermediate 19b. The final compound was obtained as a white solid in 55% yield. M.p.: 143–145 °C. <sup>1</sup>H NMR (400 MHz, DMSO-*d*<sub>6</sub>) δ 10.39 (s, 1H), 8.07 (d, *J* = 4.0 Hz, 1H), 7.69 (d, *J* = 8.0 Hz, 2H), 7.62 (d, *J* = 8.0 Hz, 1H), 7.61, 7.60, 7.42 (d, *J* = 4.0 Hz, 1H), 6.72 (d, *J* = 4.0 Hz, 1H), 5.76 (s, 1H). <sup>13</sup>C NMR (101 MHz, DMSO-*d*<sub>6</sub>) δ 156.45, 151.07, 147.59, 139.04, 133.00, 131.37, 131.11, 125.80, 121.92, 120.96, 120.71, 120.27, 116.48, 112.76, 108.39, 107.13, 48.93. HRMS (ESI): calcd for: C<sub>17</sub>H<sub>9</sub>Cl<sub>2</sub>F<sub>6</sub>N<sub>3</sub>O<sub>2</sub> [M + H]<sup>+</sup> *m/z* 472.0054, found 472.0057; purity: ≥98% by HPLC analysis.

**5-((3,5-Bis(trifluoromethyl)-1H-pyrazol-1-yl)methyl)-N-(3,5-dichlorophenyl)furan-2-carboxamide (20h).** Compound 20h was prepared with general procedure C using 3,5-dichloroaniline and intermediate 19b. The final compound was obtained as a white solid in 51% yield. M.p.: 148–150 °C. <sup>1</sup>H NMR (400 MHz, CDCl<sub>3</sub>) δ 8.11 (s, 1H), 7.62 (d, *J* = 2.0 Hz, 2H), 7.24 (d, *J* = 4.0 Hz, 1H), 7.16 (t, *J* = 4.0 Hz, 1H), 6.99 (s, 1H), 6.62 (d, *J* = 4.0 Hz, 1H), 5.55 (s, 2H). <sup>13</sup>C NMR (101 MHz, CDCl<sub>3</sub>) δ 155.34, 149.04, 147.71, 138.94, 135.39 (2C), 133.64, 133.24, 124.68, 121.45, 120.47, 118.16 (2C), 116.86, 113.21, 107.06, 48.31. HRMS (ESI): calcd for: C<sub>17</sub>H<sub>9</sub>Cl<sub>2</sub>F<sub>6</sub>N<sub>3</sub>O<sub>2</sub> [M + H]<sup>+</sup> *m/z* 472.0054, found 472.0053; HPLC purity >97% by HPLC analysis.

**5-((3,5-Bis(trifluoromethyl)-1H-pyrazol-1-yl)methyl)-N-(3,5-dimethoxyphenyl)furan-2-carboxamide (20i).** Compound 20i was prepared with general procedure C using 3,5-dimethoxy aniline and intermediate 19b. The final compound was obtained as a white solid in 41% yield. M.p.: 123–125 °C. <sup>1</sup>H NMR (400 MHz, CDCl<sub>3</sub>) δ 8.00 (s, 1H), 7.20 (d, *J* = 4.0 Hz, 1H), 6.98 (s, 1H), 6.89 (d, *J* = 4.0 Hz, 2H), 6.60 (d, *J* = 4.0 Hz, 1H), 6.30 (t, *J* = 4.0 Hz, 1H), 5.55 (s, 2H), 3.83 (s, 6H). <sup>13</sup>C NMR (101 MHz, CDCl<sub>3</sub>) δ 161.13 (2C), 155.42, 148.62, 148.34, 138.84, 124.68, 121.45, 116.02 (2C), 112.99, 107.16, 98.15 (2C), 97.25, 77.22, 55.41 (2C), 48.42. HRMS (ESI): calcd for: C<sub>19</sub>H<sub>16</sub>F<sub>6</sub>N<sub>3</sub>O<sub>4</sub> [M + H]<sup>+</sup> *m/z* 464.1045, found 464.1045; purity: ≥98% by HPLC analysis.

**5-((3,5-Bis(trifluoromethyl)-1H-pyrazol-1-yl)methyl)-N-(4-fluoro-3-methylphenyl)furan-2-carboxamide (20j).** Compound 20j was prepared with general procedure C using 4-fluoro-3-methyl aniline and intermediate 19b. The final compound was obtained as a white solid in 49% yield. M.p.: 132–134 °C. <sup>1</sup>H NMR (400 MHz, CDCl<sub>3</sub>) δ 7.97 (s, 1H), 7.50 (dd, *J* = 4.0, 8.0 Hz, 1H), 7.39 (m, 1H), 7.20 (d, *J* = 4.0 Hz, 1H), 7.01 (m, 2H), 6.60 (d, *J* = 4.0 Hz, 1H), 5.55 (s, 2H), 2.31 (s, 3H). <sup>13</sup>C NMR (101 MHz, CDCl<sub>3</sub>) δ 159.48, 155.39, 148.57, 148.37, 132.72, 125.70, 125.52, 123.23, 123.18, 120.49, 119.10, 119.02, 115.97, 115.47, 115.24, 113.01, 48.40, 14.70. HRMS (ESI): calcd for: C<sub>18</sub>H<sub>13</sub>F<sub>7</sub>N<sub>3</sub>O<sub>2</sub> [M + H]<sup>+</sup> *m/z* 436.0885, found 436.0893; purity: ≥96% by HPLC analysis.

**Methyl 2-(5-((3,5-Dimethyl-1H-pyrazol-1-yl)methyl)furan-2-carboxamido)-5-fluorobenzoate (22a).** Compound 22a was prepared with general procedure C using methyl 2-amino-5-fluorobenzoate and intermediate 15. The final compound was obtained as an off-white solid in 49% yield. M.p.: 168–170 °C. <sup>1</sup>H NMR (400 MHz, CDCl<sub>3</sub>) δ 11.81 (bs, 1H), 8.87–8.84 (m, 1H), 7.76 (d, *J* = 8.0 Hz, 1H), 7.33–7.28 (m, 1H), 7.19 (s, 1H), 6.41 (s, 1H), 5.86 (s, 1H), 5.25 (s, 2H), 3.99 (s, 3H), 2.43 (s, 3H), 2.24 (s, 3H). <sup>13</sup>C NMR (101 MHz, CDCl<sub>3</sub>) δ 167.59, 156.34, 153.19, 148.34, 147.64, 139.68, 137.52, 122.38, 121.85, 121.63, 117.09, 116.85, 116.43, 110.86, 105.75, 52.61, 45.66, 13.48, 11.04. HRMS (ESI): calcd for C<sub>19</sub>H<sub>19</sub>FN<sub>3</sub>O<sub>4</sub> [M + H]<sup>+</sup> *m/z* 372.1360, found 372.1356; purity: ≥98% by HPLC analysis.

**Methyl 5-Chloro-2-(5-((3,5-dimethyl-1H-pyrazol-1-yl)methyl)furan-2-carboxamido)benzoate (22b).** Compound 22b was pre-

pared with general procedure C using methyl 2-amino-5-chlorobenzoate and intermediate 15. The final compound was obtained as an off-white solid in 43% yield. M.p.: 180–182 °C. <sup>1</sup>H NMR (400 MHz, CDCl<sub>3</sub>) δ 11.86 (s, 1H), 8.81 (d, *J* = 9.1 Hz, 1H), 8.02 (s, 1H), 7.51 (d, *J* = 9.1 Hz, 1H), 7.17 (d, *J* = 3.1 Hz, 1H), 6.37 (d, *J* = 2.6 Hz, 1H), 5.84 (s, 1H), 5.25 (s, 2H), 3.97 (s, 3H), 2.41 (s, 3H), 2.21 (s, 3H). <sup>13</sup>C NMR (101 MHz, CDCl<sub>3</sub>) δ 167.53, 156.36, 153.36, 148.33, 139.73, 139.60, 134.50, 130.49, 127.80, 121.87, 116.63, 116.46, 110.86, 105.72, 77.23, 52.63, 45.69, 13.54, 11.05. HRMS (ESI): calcd for C<sub>19</sub>H<sub>19</sub>ClN<sub>3</sub>O<sub>4</sub> [M + H]<sup>+</sup> *m/z* 388.1064, found 388.1068; purity: ≥97% by HPLC analysis.

**Methyl 5-Bromo-2-(5-((3,5-dimethyl-1H-pyrazol-1-yl)methyl)furan-2-carboxamido)benzoate (22c).** Compound 22c was prepared with general procedure C using methyl 2-amino-5-bromobenzoate and intermediate 15. The final compound was obtained as an off-white solid in 37% yield. M.p.: 174–176 °C. <sup>1</sup>H NMR (400 MHz, DMSO-*d*<sub>6</sub>) δ 9.92 (s, 1H), 7.78 (s, 2H), 7.29 (d, *J* = 3.3 Hz, 1H), 6.49 (d, *J* = 3.4 Hz, 1H), 5.85 (s, 1H), 5.28 (s, 2H), 3.71 (s, 3H), 2.30 (s, 3H), 2.24 (s, 3H), 2.08 (s, 3H). <sup>13</sup>C NMR (101 MHz, DMSO-*d*<sub>6</sub>) δ 165.67, 156.66, 154.08, 147.25, 146.84, 139.73, 139.61, 136.84, 134.65, 130.43, 130.39, 119.06, 115.98, 110.77, 105.66, 52.79, 45.46, 18.24, 13.75, 11.12. HRMS (ESI): calcd for C<sub>19</sub>H<sub>19</sub>BrN<sub>3</sub>O<sub>4</sub> [M + H]<sup>+</sup> *m/z* 432.0715, found 432.0716; purity: ≥97% by HPLC analysis.

**Methyl-2-(5-((3,5-bis(trifluoromethyl)-1H-pyrazol-1-yl)methyl)furan-2-carboxamido)-5-fluorobenzoate (22d).** Compound 22d was prepared with general procedure C using methyl 2-amino-5-bromobenzoate and intermediate 19b. The final compound was obtained as a white solid in 40% yield. M.p.: 116–118 °C. <sup>1</sup>H NMR (400 MHz, CDCl<sub>3</sub>) δ 11.82 (s, 1H), 8.84 (dd, *J* = 5.0, 19.0 Hz, 1H), 7.76 (dd, *J* = 4.0, 8.0 Hz, 1H), 7.33–7.28 (m, 1H), 7.22 (d, *J* = 4.0 Hz, 1H), 6.97 (s, 1H), 6.57 (d, *J* = 4.0 Hz, 1H), 5.60 (s, 2H), 3.99 (s, 3H). <sup>13</sup>C NMR (101 MHz, CDCl<sub>3</sub>) δ 167.37, 158.79, 156.36, 156.00, 149.33, 148.57, 137.27, 122.40, 121.70, 121.48, 117.15, 116.91, 116.88, 116.81, 116.14, 112.53, 106.69, 52.58, 48.57. HRMS (ESI): calcd for C<sub>19</sub>H<sub>13</sub>F<sub>7</sub>N<sub>3</sub>O<sub>4</sub> [M + H]<sup>+</sup> *m/z* 480.0783, found 480.0789; purity: ≥98% by HPLC analysis.

**5-Fluoro-2-(5-((3,5-dimethyl-1H-pyrazol-1-yl)methyl)furan-2-carboxamido)benzoic Acid (23a).** Compound 23a was prepared with general procedure B using intermediate 22a. The final compound was obtained as a white solid without further purification for the next step.

**5-Chloro-2-(5-((3,5-dimethyl-1H-pyrazol-1-yl)methyl)furan-2-carboxamido)benzoic Acid (23b).** Compound 23b was prepared with general procedure B using intermediate 22b. The final compound was obtained as a white solid without further purification for the next step.

**5-Bromo-2-(5-((3,5-dimethyl-1H-pyrazol-1-yl)methyl)furan-2-carboxamido)benzoic Acid (23c).** Compound 23c was prepared with general procedure B using intermediate 22c. The final compound was obtained as a white solid without further purification for the next step.

**5-Fluoro-2-(5-((3,5-bis(trifluoromethyl)-1H-pyrazol-1-yl)methyl)furan-2-carboxamido)benzoic Acid (23d).** Compound 23d was prepared with general procedure B using intermediate 22d. The final compound was obtained as a white solid without further purification for the next step.

**N-(4-Chloro-2-((4-hydroxybutyl)carbamoyl)phenyl)-5-((3,5-dimethyl-1H-pyrazol-1-yl)methyl)furan-2-carboxamide (24a).** Compound 24a was prepared with general procedure C using 4-aminobutan-1-ol and intermediate 23b. The final compound was obtained as a white solid in 86% yield. M.p.: 175–177 °C. <sup>1</sup>H NMR (400 MHz, DMSO-*d*<sub>6</sub>) δ 12.44 (s, 1H), 8.94 (s, 1H), 8.60 (d, *J* = 8.8 Hz, 1H), 7.89 (s, 1H), 7.59 (d, *J* = 8.2 Hz, 1H), 7.18 (s, 1H), 6.61 (s, 1H), 5.81 (s, 1H), 5.26 (s, 2H), 4.18–4.00 (m, 1H), 3.18 (d, *J* = 4.7 Hz, 2H), 2.44 (s, 3H), 2.05 (s, 3H), 1.55 (q, 2H), 1.37 (q, 2H), 0.92 (t, *J* = 6.9 Hz, 3H). <sup>13</sup>C NMR (101 MHz, DMSO-*d*<sub>6</sub>) δ 167.32, 155.81, 154.36, 147.45, 139.92, 138.19, 132.19, 128.18, 127.12, 122.28, 122.14, 116.67, 111.66, 105.41, 49.05, 45.12, 39.52, 31.23, 20.15, 14.11, 13.71, 11.05. HRMS (ESI): calcd for C<sub>22</sub>H<sub>26</sub>ClN<sub>4</sub>O<sub>4</sub> [M + H]<sup>+</sup> *m/z* 445.1643, found 445.1641; purity: ≥96% by HPLC analysis.

*N*-(4-Chloro-2-((3-hydroxypropyl)carbamoyl)phenyl)-5-((3,5-dimethyl-1*H*-pyrazol-1-yl)methyl)furan-2-carboxamide (**24b**). Compound **24b** was prepared with general procedure C using 3-aminopropan-1-ol and intermediate **23b**. The final compound was obtained as a white solid in 88% yield. M.p.: 190–192 °C. <sup>1</sup>H NMR (400 MHz, DMSO-*d*<sub>6</sub>) δ 11.60 (s, 1H), 10.64 (s, 1H), 8.51 (d, *J* = 8.9 Hz, 1H), 8.00 (s, 1H), 7.75 (d, *J* = 8.0 Hz, 2H), 7.67 (d, *J* = 9.0 Hz, 1H), 7.43 (t, *J* = 7.6 Hz, 2H), 7.27–7.12 (m, 2H), 6.63 (d, *J* = 2.5 Hz, 1H), 5.78 (s, 1H), 5.25 (s, 2H), 2.38 (s, 3H), 2.03 (s, 3H). <sup>13</sup>C NMR (101 MHz, DMSO-*d*<sub>6</sub>) δ 166.28, 155.79, 154.40, 147.26, 146.96, 139.87, 138.68, 137.52, 132.43, 129.09, 129.02, 127.45, 124.98, 123.97, 122.96, 121.54, 116.99, 111.82, 105.40, 45.04, 13.74, 11.15. HRMS (ESI): calcd for C<sub>21</sub>H<sub>24</sub>ClN<sub>4</sub>O<sub>4</sub> [M + H]<sup>+</sup> *m/z* 431.1486, found 431.1483; purity: ≥95% by HPLC analysis.

*N*-(2-(Benzylcarbamoyl)-4-chlorophenyl)-5-((3,5-dimethyl-1*H*-pyrazol-1-yl)methyl)furan-2-carboxamide (**24c**). Compound **24b** was prepared with general procedure C using phenylmethanamine and intermediate **23b**. The final compound was obtained as a white solid in 79% yield. M.p.: 210–212 °C. <sup>1</sup>H NMR (400 MHz, DMSO-*d*<sub>6</sub>) δ 12.42 (s, 1H), 9.53 (t, *J* = 5.2 Hz, 1H), 8.62 (d, *J* = 9.0 Hz, 1H), 7.99 (s, 1H), 7.62 (d, *J* = 9.0 Hz, 1H), 7.37 (s, 4H), 7.28 (s, 1H), 7.19 (d, *J* = 2.5 Hz, 1H), 6.72–6.52 (m, 1H), 5.77 (s, 1H), 5.25 (s, 2H), 4.54 (d, *J* = 5.4 Hz, 2H), 2.38 (s, 3H), 2.05 (s, 3H). <sup>13</sup>C NMR (101 MHz, DMSO-*d*<sub>6</sub>) δ 167.46, 155.85, 154.41, 147.40, 146.95, 139.92, 139.15, 138.36, 132.48, 128.85 (2C), 128.30, 127.81 (2C), 127.44, 127.21, 122.39, 121.77, 116.78, 111.69, 105.44, 45.11, 43.19, 13.74, 11.06. HRMS (ESI): calcd for C<sub>25</sub>H<sub>24</sub>ClN<sub>4</sub>O<sub>3</sub> [M + H]<sup>+</sup> *m/z* 463.1512, found 463.1512; purity: ≥96% by HPLC analysis.

*N*-(4-Chloro-2-(phenylcarbamoyl)phenyl)-5-((3,5-dimethyl-1*H*-pyrazol-1-yl)methyl)furan-2-carboxamide (**24d**). Compound **24b** was prepared with general procedure C using aniline and intermediate **23b**. The final compound was obtained as an off-white solid in 75% yield. M.p.: 228–230 °C. <sup>1</sup>H NMR (400 MHz, DMSO-*d*<sub>6</sub>) δ 12.42 (s, 1H), 9.08–8.84 (m, 1H), 8.59 (d, *J* = 9.0 Hz, 1H), 7.89 (s, 1H), 7.60 (d, *J* = 9.0 Hz, 1H), 7.18 (d, *J* = 2.9 Hz, 1H), 6.60 (d, *J* = 2.8 Hz, 1H), 5.83 (s, 1H), 5.27 (s, 2H), 4.53 (t, *J* = 4.9 Hz, 1H), 3.51 (q, *J* = 5.7 Hz, 2H), 3.41–3.35 (m, 2H), 2.44 (s, 3H), 2.06 (s, 3H), 1.73 (p, *J* = 6.4 Hz, 2H). <sup>13</sup>C NMR (101 MHz, DMSO-*d*<sub>6</sub>) δ 167.40, 155.82, 154.41, 147.41, 146.98, 139.98, 138.14, 132.22, 128.24, 127.12, 122.27, 122.17, 116.70, 111.64, 105.47, 59.05, 45.13, 37.32, 32.39, 13.74, 11.09. HRMS (ESI): calcd for C<sub>24</sub>H<sub>22</sub>ClN<sub>4</sub>O<sub>3</sub> [M + H]<sup>+</sup> *m/z* 449.1380, found 449.1380; purity: ≥95% by HPLC analysis.

*N*-(4-Chloro-2-((*n*-butyl)carbamoyl)phenyl)-5-((3,5-dimethyl-1*H*-pyrazol-1-yl)methyl)furan-2-carboxamide (**24e**). Compound **24b** was prepared with general procedure C using butan-1-amine and intermediate **23b**. The final compound was obtained as a white solid in 90% yield. M.p.: 142–144 °C. <sup>1</sup>H NMR (400 MHz, DMSO-*d*<sub>6</sub>) δ 12.45 (s, 1H), 8.97 (s, 1H), 8.60 (d, *J* = 9.0 Hz, 1H), 7.90 (s, 1H), 7.61 (d, *J* = 9.0 Hz, 1H), 7.19 (s, 1H), 6.61 (s, 1H), 5.83 (s, 1H), 5.27 (s, 2H), 4.46 (t, *J* = 4.6 Hz, 1H), 3.45 (q, *J* = 5.6 Hz, 2H), 2.45 (s, 3H), 2.06 (s, 3H), 1.67–1.55 (m, 2H), 1.55–1.43 (m, 2H). <sup>13</sup>C NMR (101 MHz, DMSO-*d*<sub>6</sub>) δ 167.31, 155.82, 154.40, 147.40, 146.97, 139.97, 138.18, 132.25, 128.20, 127.11, 122.26, 122.10, 116.74, 111.70, 105.44, 60.89, 45.10, 30.48, 30.48, 25.87, 13.75, 11.08. HRMS (ESI): calcd for C<sub>22</sub>H<sub>26</sub>N<sub>4</sub>O<sub>4</sub>Cl [M + H]<sup>+</sup> *m/z* 429.1693, found 429.1698; purity: ≥95% by HPLC analysis.

*Methyl 5-Formylthiophene-2-carboxylate* (**26**). To a mixture of starting material 5-formylthiophene-2-carboxylic acid (**25**, 2 mmol) and MeI (2.5 mmol) in DMF 20 mL, NaHCO<sub>3</sub> (5 mmol) was added. Then, the reaction was stirred for 20 h at r.t. The mixture was filtered to remove solids, and the residue was concentrated in vacuo. The residue was diluted with EtOAc (10 mL) and washed with water (3 × 8 mL). The organic layers were dried over Na<sub>2</sub>SO<sub>4</sub> and purified through silica gel column chromatography by elution with EtOAc/Petroleum ether (1:5). The final compound was obtained as a pale yellow oil in 98% yield. <sup>1</sup>H NMR (400 MHz, CDCl<sub>3</sub>) δ 9.99 (s, 1H), 7.86 (d, *J* = 4.0 Hz, 1H), 7.75 (d, *J* = 3.9 Hz, 1H), 3.96 (s, 3H). <sup>13</sup>C NMR (101 MHz, CDCl<sub>3</sub>) δ 183.31, 161.95, 147.78, 140.96, 135.03, 133.36, 52.79. MS (ESI): calcd for C<sub>7</sub>H<sub>7</sub>O<sub>3</sub>S [M + H]<sup>+</sup> *m/z* 171, found 171.

*Methyl 5-(Hydroxymethyl)thiophene-2-carboxylate* (**27**). To a solution of intermediate **26** (1 mmol) in EtOH (10 mL) was added NaBH<sub>3</sub>CN (0.5 mmol) at 0 °C. The mixture was stirred for 2 h from 0 °C to r.t. The reaction was diluted with 20 mL of water and washed with EtOAc (3 × 10 mL). Combined organic layers were dried over Na<sub>2</sub>SO<sub>4</sub> and purified through silica gel column chromatography by elution with EtOAc/Petroleum ether (1:2). The final compound was obtained as a colorless oil in 98% yield. <sup>1</sup>H NMR (400 MHz, CDCl<sub>3</sub>) δ 7.69 (d, *J* = 3.8 Hz, 1H), 7.00 (dt, *J* = 3.8, 0.9 Hz, 1H), 4.86 (d, *J* = 5.6 Hz, 2H), 3.89 (s, 3H), 2.30 (t, *J* = 6.0 Hz, 1H). <sup>13</sup>C NMR (101 MHz, CDCl<sub>3</sub>) δ 162.73, 151.83, 133.56, 132.75, 125.32, 60.22, 52.18. MS (ESI): calcd for C<sub>7</sub>H<sub>8</sub>O<sub>3</sub>S [M + H]<sup>+</sup> *m/z* 173, found 173.

*Methyl 5-(Chloromethyl)thiophene-2-carboxylate* (**28**). Compound **28** was prepared using the same procedure as for compound **12** to afford the product as a pale yellow oil. <sup>1</sup>H NMR (400 MHz, CDCl<sub>3</sub>) δ 7.67 (d, *J* = 3.8 Hz, 1H), 7.09 (dt, *J* = 3.8, 0.8 Hz, 1H), 4.78 (d, *J* = 0.8 Hz, 2H), 3.90 (s, 3H). <sup>13</sup>C NMR (101 MHz, CDCl<sub>3</sub>) δ 162.30, 147.14, 134.14, 133.30, 127.88, 52.28, 39.82. MS (ESI): calcd for C<sub>7</sub>H<sub>7</sub>ClO<sub>2</sub>S [M + H]<sup>+</sup> *m/z* 191, found 191.

*Methyl 5-(Iodomethyl)thiophene-2-carboxylate* (**29**). Compound **28** was prepared using the same procedure as for compound **13** to afford a crude product as a brown oil. The final product was directly used in the next step without further purification.

*Methyl 5-((3,5-Dimethyl-1*H*-pyrazol-1-yl)methyl)thiophene-2-carboxylate* (**30**). Compound **30** was prepared with general procedure A using intermediate **29**. The final compound was obtained as an off-white solid in 69% yield. <sup>1</sup>H NMR (400 MHz, CDCl<sub>3</sub>) δ 7.62 (dd, *J* = 3.8, 1.0 Hz, 1H), 6.85 (dd, *J* = 3.8, 0.9 Hz, 1H), 5.84 (s, 1H), 5.33 (d, *J* = 1.0 Hz, 2H), 3.84 (d, *J* = 1.1 Hz, 3H), 2.23 (d, *J* = 1.0 Hz, 6H). <sup>13</sup>C NMR (101 MHz, CDCl<sub>3</sub>) δ 162.40, 148.33, 147.42, 138.95, 133.48, 132.99, 125.87, 106.01, 52.12, 47.78, 13.51, 11.04. MS (ESI): calcd for C<sub>12</sub>H<sub>15</sub>N<sub>2</sub>O<sub>2</sub>S [M + H]<sup>+</sup> *m/z* 251, found 251.

*5-((3,5-Dimethyl-1*H*-pyrazol-1-yl)methyl)thiophene-2-carboxylic Acid* (**31**). Compound **31** was prepared with general procedure B using intermediate **30**. The final compound was obtained as an off-white solid in 73% yield. <sup>1</sup>H NMR (400 MHz, DMSO-*d*<sub>6</sub>) δ 13.05 (s, 1H), 7.58 (d, *J* = 3.7 Hz, 1H), 7.02 (dd, *J* = 3.8, 1.0 Hz, 1H), 5.84 (s, 1H), 5.39 (d, *J* = 0.9 Hz, 2H), 2.21 (d, *J* = 0.8 Hz, 3H), 2.10 (s, 3H). <sup>13</sup>C NMR (101 MHz, DMSO-*d*<sub>6</sub>) δ 163.17, 148.14, 147.11, 139.20, 134.40, 133.46, 127.06, 105.78, 47.33, 13.79, 11.03. HRMS (ESI): calcd for C<sub>11</sub>H<sub>13</sub>N<sub>2</sub>O<sub>2</sub>S [M + H]<sup>+</sup> *m/z* 237, found 237.

*N*-(4-Bromo-2-methylphenyl)-5-((3,5-dimethyl-1*H*-pyrazol-1-yl)methyl)thiophene-2-carboxamide (**32a**). Compound **32a** was prepared with general procedure C using 4-bromo-2-methylaniline and intermediate **31**. The final compound was obtained as a white solid in 66% yield. M.p.: 97–99 °C. <sup>1</sup>H NMR (400 MHz, DMSO-*d*<sub>6</sub>) δ 9.90 (s, 1H), 7.81 (d, *J* = 3.1 Hz, 1H), 7.50 (s, 1H), 7.40 (d, *J* = 8.1 Hz, 1H), 7.25 (d, *J* = 8.4 Hz, 1H), 7.07 (d, *J* = 2.7 Hz, 1H), 5.85 (s, 1H), 5.40 (s, 2H), 2.23 (s, 3H), 2.21 (s, 3H), 2.11 (s, 3H). <sup>13</sup>C NMR (101 MHz, DMSO-*d*<sub>6</sub>) δ 160.17, 147.03, 146.52, 139.22, 139.12, 137.03, 135.76, 133.27, 129.47, 129.33, 129.03, 126.94, 118.94, 105.76, 47.36, 18.05, 13.81, 11.07. HRMS (ESI): calcd for C<sub>18</sub>H<sub>19</sub>BrN<sub>3</sub>O<sub>2</sub>S [M + H]<sup>+</sup> *m/z* 404.0432, found 404.0435; purity: ≥98% by HPLC analysis.

*N*-(4-Chloro-2-methylphenyl)-5-((3,5-dimethyl-1*H*-pyrazol-1-yl)methyl)thiophene-2-carboxamid (**32b**). Compound **32b** was prepared with general procedure C using 4-chloro-2-methylaniline and intermediate **31**. The final compound was obtained as a white solid in 56% yield. M.p.: 110–112 °C. <sup>1</sup>H NMR (400 MHz, DMSO-*d*<sub>6</sub>) δ 9.90 (s, 1H), 7.81 (d, *J* = 3.6 Hz, 1H), 7.36 (s, 1H), 7.34–7.24 (m, 2H), 7.07 (d, *J* = 3.5 Hz, 1H), 5.85 (s, 1H), 5.40 (s, 2H), 2.24 (s, 3H), 2.21 (s, 3H), 2.11 (s, 3H). <sup>13</sup>C NMR (101 MHz, DMSO-*d*<sub>6</sub>) δ 160.23, 147.04, 146.52, 139.23, 139.11, 136.68, 135.31, 130.57, 130.37, 129.45, 128.72, 126.93, 126.39, 105.76, 47.36, 18.12, 13.81, 11.07. HRMS (ESI): calcd for C<sub>18</sub>H<sub>19</sub>ClN<sub>3</sub>O<sub>2</sub>S [M + H]<sup>+</sup> *m/z* 360.0937, found 360.0933; purity: ≥98% by HPLC analysis.

*5-((3,5-Dimethyl-1*H*-pyrazol-1-yl)methyl)-*N*-(4-fluoro-2-methylphenyl)thiophene-2-carboxamide* (**32c**). Compound **32c** was prepared with general procedure C using 4-fluoro-2-methylaniline and

intermediate **31**. The final compound was obtained as a white solid in 61% yield. M.p.: 124–126 °C. <sup>1</sup>H NMR (400 MHz, DMSO-*d*<sub>6</sub>) δ 9.88 (s, 1H), 7.80 (d, *J* = 3.3 Hz, 1H), 7.34–7.23 (m, 1H), 7.19–7.10 (m, 1H), 7.11–6.98 (m, 2H), 5.85 (s, 1H), 5.40 (s, 2H), 2.24 (s, 3H), 2.21 (s, 3H), 2.11 (s, 3H). <sup>13</sup>C NMR (101 MHz, DMSO-*d*<sub>6</sub>) δ 160.53 (d), 160.35, 147.03, 146.35, 139.37, 139.10, 137.28 (d, *J* = 8.4 Hz), 132.54 (d, *J* = 2.7 Hz), 129.26, 129.11 (d, *J* = 8.9 Hz), 126.91, 117.09 (d, *J* = 22.1 Hz), 113.11 (d, *J* = 22.1 Hz), 105.75, 47.36, 18.32, 13.80, 11.06. HRMS (ESI): calcd for C<sub>18</sub>H<sub>19</sub>FN<sub>3</sub>OS [M + H]<sup>+</sup> *m/z* 344.1233, found 344.1230; purity: ≥97% by HPLC analysis.

**5-((3,5-Dimethyl-1H-pyrazol-1-yl)methyl)-N-(3-methyl-[1,1'-biphenyl]-4-yl)thiophene-2-carboxamide (32d)**. Compound **32d** was prepared with general procedure C using 3-methyl-[1,1'-biphenyl]-4-amine and intermediate **31**. The final compound was obtained as a white solid in 59% yield. M.p.: 70–72 °C. <sup>1</sup>H NMR (400 MHz, DMSO-*d*<sub>6</sub>) δ 9.92 (s, 3H), 7.84 (d, *J* = 4.0 Hz, 1H), 7.67 (d, *J* = 8.0 Hz, 1H), 7.58 (s, 1H), 7.52–7.45 (m, 2H), 7.39–7.36 (m, 2H), 7.09 (d, *J* = 4.0 Hz, 1H), 5.86 (s, 1H), 5.40 (s, 2H), 2.29 (s, 3H), 2.25 (s, 3H), 2.11 (s, 3H). <sup>13</sup>C NMR (101 MHz, DMSO-*d*<sub>6</sub>) δ 160.25, 147.04, 146.38, 140.17, 139.56, 139.13, 138.35, 135.75, 134.65, 129.37, 129.31, 129.10, 127.79, 127.50, 127.03, 126.95, 124.77, 105.77, 47.37, 18.50, 13.82, 11.09. HRMS (ESI): calcd for C<sub>24</sub>H<sub>24</sub>N<sub>3</sub>OS [M + H]<sup>+</sup> *m/z* 402.1640, found 402.1633; purity: ≥97% by HPLC analysis.

**5-((3,5-Dimethyl-1H-pyrazol-1-yl)methyl)-N-(2-methyl-4-(pyridin-3-yl)phenyl)thiophene-2-carboxamide (32e)**. Compound **32e** was prepared with general procedure C using 2-methyl-4-(pyridin-3-yl)aniline and intermediate **31**. The final compound was obtained as a white solid in 58% yield. M.p.: 74–76 °C. <sup>1</sup>H NMR (400 MHz, DMSO-*d*<sub>6</sub>) δ 9.94 (s, 1H), 8.92 (d, *J* = 2.0 Hz, 1H), 8.57 (dd, *J* = 2.0, 4.0 Hz, 1H), 8.10 (d, *J* = 8.0 Hz, 1H), 7.84 (d, *J* = 4.0 Hz, 1H), 7.66 (s, 1H), 7.58 (d, *J* = 12.0 Hz, 1H), 7.50–7.47 (m, 1H), 7.42 (d, *J* = 12.0 Hz, 1H), 7.10 (d, *J* = 4.0 Hz, 1H), 5.86 (s, 1H), 5.41 (s, 2H), 2.30 (s, 3H), 2.24 (s, 3H), 2.11 (s, 3H). <sup>13</sup>C NMR (101 MHz, DMSO-*d*<sub>6</sub>) δ 160.25, 148.83, 148.02, 147.05, 146.47, 139.47, 139.14, 136.44, 135.57, 135.14, 134.87, 134.41, 129.40, 129.31, 127.60, 126.96, 124.97, 124.31, 105.77, 47.37, 18.47, 13.82, 11.09. HRMS (ESI): calcd for C<sub>23</sub>H<sub>23</sub>N<sub>4</sub>OS [M + H]<sup>+</sup> *m/z* 403.1593, found 403.1586; purity: ≥98% by HPLC analysis.

**5-((3,5-Dimethyl-1H-pyrazol-1-yl)methyl)-N-(4-fluoro-3-methylphenyl)thiophene-2-carboxamide (32f)**. Compound **32f** was prepared with general procedure C using 4-fluoro-3-methyl aniline and intermediate **31**. The final compound was obtained as a white solid in 57% yield. M.p.: 154–156 °C. <sup>1</sup>H NMR (400 MHz, CDCl<sub>3</sub>) δ 7.74 (s, 1H), 7.45 (m, 2H), 7.44, 7.32 (m, 1H), 6.98 (d, *J* = 4.0 Hz, 1H), 6.88 (d, *J* = 4.0 Hz, 1H), 5.88 (s, 1H), 5.35 (s, 2H), 2.28 (s, 6H), 2.26 (s, 3H). <sup>13</sup>C NMR (101 MHz, CDCl<sub>3</sub>) δ 159.72, 148.43, 145.54, 139.08, 138.60, 133.22, 128.63, 126.01, 125.56, 125.37, 123.64, 119.43, 115.36, 106.08, 47.68, 14.69, 14.65, 13.52, 11.09. HRMS (ESI): calcd for C<sub>18</sub>H<sub>19</sub>FN<sub>3</sub>OS [M + H]<sup>+</sup> *m/z* 344.1233, found 344.1226; purity: ≥98% by HPLC analysis.

**N-(3-Chloro-4-fluorophenyl)-5-((3,5-dimethyl-1H-pyrazol-1-yl)methyl)thiophene-2-carboxamide (32g)**. Compound **32g** was prepared with general procedure C using 3-chloro-4-fluoroaniline and intermediate **31**. The final compound was obtained as a white solid in 74% yield. M.p.: 163–165 °C. <sup>1</sup>H NMR (400 MHz, DMSO-*d*<sub>6</sub>) δ 10.34 (s, 1H), 7.98 (dd, *J* = 4.0, 8.0 Hz, 1H), 7.84 (d, *J* = 4.0 Hz, 1H), 7.65 (m, 1H), 7.41 (t, *J* = 8.0 Hz, 1H), 7.08 (d, *J* = 4.0 Hz, 1H), 5.85 (s, 1H), 5.41 (s, 2H), 2.23 (s, 3H), 2.11 (s, 3H). <sup>13</sup>C NMR (101 MHz, DMSO-*d*<sub>6</sub>) δ 160.26, 152.66, 147.07 (d, *J* = 28 Hz), 139.16 (d, *J* = 36 Hz), 136.42, 129.82, 126.99, 122.18, 121.00 (d, *J* = 28 Hz), 119.62, 119.43, 117.45, 117.23, 105.79, 47.37, 13.81, 11.06. HRMS (ESI): calcd for C<sub>17</sub>H<sub>16</sub>ClFN<sub>3</sub>OS [M + H]<sup>+</sup> *m/z* 363.0687, found 363.0680; purity: ≥96% by HPLC analysis.

**N-(3,4-Dichlorophenyl)-5-((3,5-dimethyl-1H-pyrazol-1-yl)methyl)thiophene-2-carboxamide (32h)**. Compound **32h** was prepared with general procedure C using 3,4-dichloroaniline and intermediate **31**. The final compound was obtained as a white solid in 70% yield. M.p.: 162–164 °C. <sup>1</sup>H NMR (400 MHz, DMSO-*d*<sub>6</sub>) δ 10.41 (s, 1H), 8.06 (d, *J* = 3.2 Hz, 1H), 7.86 (d, *J* = 4.0 Hz, 1H), 7.70

(dd, *J* = 4.0, 8.0 Hz, 1H), 7.62 (d, *J* = 8.0 Hz, 1H), 7.07 (d, *J* = 4.0 Hz, 1H), 5.86 (s, 1H), 5.41 (s, 2H), 2.23 (s, 3H), 2.11 (s, 3H). <sup>13</sup>C NMR (101 MHz, DMSO-*d*<sub>6</sub>) δ 160.38, 147.39, 139.33, 139.17, 138.94, 131.36, 131.09, 130.04, 127.03, 125.64, 121.82, 120.62, 113.46, 105.79, 47.36, 13.81, 11.07. HRMS (ESI): calcd for C<sub>17</sub>H<sub>16</sub>Cl<sub>2</sub>N<sub>3</sub>OS [M + H]<sup>+</sup> *m/z* 380.0391, found 380.0385; purity: ≥97% by HPLC analysis.

**N-(3-Fluoro-4-chlorophenyl)-5-((3,5-dimethyl-1H-pyrazol-1-yl)methyl)thiophene-2-carboxamide (32i)**. Compound **32i** was prepared with general procedure C using 3-fluoro-4-chloroaniline and intermediate **31**. The final compound was obtained as a white solid in 54% yield. M.p.: 246 ~ 248 °C. <sup>1</sup>H NMR (400 MHz, DMSO-*d*<sub>6</sub>) δ 10.42 (bs, 1H), 7.86 (d, *J* = 4.0 Hz, 1H), 7.82 (d, *J* = 2.0 Hz, 1H), 7.32–7.15 (m, 1H), 7.09 (d, *J* = 4.0 Hz, 1H), 5.86 (s, 1H), 5.41 (s, 2H), 2.23 (s, 3H), 2.11 (s, 3H). <sup>13</sup>C NMR (101 MHz, DMSO-*d*<sub>6</sub>) δ 160.51, 147.63, 147.10, 141.57, 139.18, 138.70, 134.46, 130.23, 127.07, 123.31, 118.65, 105.80, 47.36, 13.81, 11.06. HRMS (ESI): calcd for C<sub>17</sub>H<sub>16</sub>Cl<sub>2</sub>N<sub>3</sub>OS [M + H]<sup>+</sup> *m/z* 380.0391, found 380.0385; purity: ≥98% by HPLC analysis.

**N-(3,4-Diethoxyphenyl)-5-((3,5-dimethyl-1H-pyrazol-1-yl)methyl)thiophene-2-carboxamide (32j)**. Compound **32j** was prepared with general procedure C using 3,4-diethoxyaniline and intermediate **31**. The final compound was obtained as a white solid in 44% yield. M.p.: 223–225 °C. <sup>1</sup>H NMR (400 MHz, DMSO-*d*<sub>6</sub>) δ 10.47 (s, 1H), 7.86 (d, *J* = 4.0 Hz, 1H), 7.50–7.44 (m, 2H), 7.09 (d, *J* = 4.0 Hz, 1H), 6.99–6.93 (m, 1H), 5.86 (s, 1H), 5.41 (s, 2H), 2.23 (s, 3H), 2.11 (s, 3H). <sup>13</sup>C NMR (101 MHz, DMSO-*d*<sub>6</sub>) δ 160.52, 147.57, 147.10, 141.75, 139.18, 138.78, 130.17, 127.03, 105.80, 103.50, 103.21, 101.07, 47.36, 13.81, 11.06. HRMS (ESI): calcd for C<sub>17</sub>H<sub>16</sub>F<sub>2</sub>N<sub>3</sub>OS [M + H]<sup>+</sup> *m/z* 348.0982, found 347.0977; purity: ≥99% by HPLC analysis.

**N-(3,5-Dichlorophenyl)-5-((3,5-dimethyl-1H-pyrazol-1-yl)methyl)thiophene-2-carboxamide (32k)**. Compound **32k** was prepared with general procedure C using 3,5-dichloroaniline and intermediate **31**. The final compound was obtained as a white solid in 39% yield. M.p.: 239–241 °C. <sup>1</sup>H NMR (400 MHz, DMSO-*d*<sub>6</sub>) δ 10.44 (s, 1H), 7.87–7.84 (m, 2H), 7.58–7.51 (m, 2H), 7.09 (d, *J* = 4.0 Hz, 1H), 5.85 (s, 1H), 5.41 (s, 2H), 2.23 (s, 3H), 2.11 (s, 3H). <sup>13</sup>C NMR (101 MHz, DMSO-*d*<sub>6</sub>) δ 160.41, 147.38, 147.09, 139.17, 138.95, 130.94, 130.03, 127.00, 117.48, 113.94, 108.83, 108.58, 105.80, 101.81, 47.37, 13.81, 11.06. HRMS (ESI): calcd for C<sub>17</sub>H<sub>16</sub>Cl<sub>2</sub>N<sub>3</sub>OS [M + H]<sup>+</sup> *m/z* 364.0687, found 364.0686; purity: ≥97% by HPLC analysis.

**N-(3,5-Difluorophenyl)-5-((3,5-dimethyl-1H-pyrazol-1-yl)methyl)thiophene-2-carboxamide (32l)**. Compound **32l** was prepared with general procedure C using 3,5-difluoroaniline and intermediate **31**. The final compound was obtained as a white solid in 67% yield. M.p.: 194–196 °C. <sup>1</sup>H NMR (400 MHz, CDCl<sub>3</sub>) δ 7.76 (s, 1H), 7.45 (d, *J* = 4.0 Hz, 1H), 6.88 (d, *J* = 4.0 Hz, 1H), 6.86 (d, *J* = 2.0 Hz, 2H), 6.28 (t, *J* = 2.0 Hz, 1H), 5.88 (s, 1H), 5.36 (s, 2H), 3.80 (s, 6H), 2.28 (s, 3H), 2.26 (s, 3H). <sup>13</sup>C NMR (101 MHz, CDCl<sub>3</sub>) δ 161.05 (2C), 159.80, 148.43, 145.69, 139.52, 139.12, 138.90, 128.53, 126.01, 106.08, 98.29 (2C), 97.14, 55.38 (2C), 47.67, 13.52, 11.08. HRMS (ESI): calcd for C<sub>19</sub>H<sub>22</sub>N<sub>3</sub>O<sub>3</sub>S [M + H]<sup>+</sup> *m/z* 372.1382, found 372.1375; purity: ≥96% by HPLC analysis.

**N-(3,5-Dimethoxyphenyl)-5-((3,5-Dimethyl-1H-pyrazol-1-yl)methyl)thiophene-2-carboxamide (32m)**. Compound **32m** was prepared with general procedure C using 3,5-dimethoxyaniline and intermediate **31**. The final compound was obtained as a white solid in 77% yield. M.p.: 146–148 °C. <sup>1</sup>H NMR (400 MHz, CDCl<sub>3</sub>) δ 7.77 (bs, 2H), 7.43 (dd, *J* = 2.0, 12.0 Hz, 1H), 6.93 (dd, *J* = 4.0, 8.0 Hz, 1H), 6.87–6.83 (m, 2H), 5.88 (s, 1H), 5.35 (s, 2H), 4.15–4.06 (m, 4H), 2.28 (s, 3H), 2.26 (s, 3H), 1.47–1.43 (m, 6H). <sup>13</sup>C NMR (101 MHz, CDCl<sub>3</sub>) δ 159.69, 148.92, 148.38, 145.58, 145.29, 139.11, 139.03, 131.44, 128.35, 125.99, 113.90, 112.33, 106.86, 106.05, 64.95, 64.45, 47.68, 14.86, 14.71, 13.51, 11.08. HRMS (ESI): calcd for C<sub>21</sub>H<sub>26</sub>N<sub>3</sub>O<sub>3</sub>S [M + H]<sup>+</sup> *m/z* 400.1695, found 400.1691; purity: ≥96% by HPLC analysis.

**N-([1,1'-Biphenyl]-4-yl)-5-((3,5-dimethyl-1H-pyrazol-1-yl)methyl)thiophene-2-carboxamide (32n)**. Compound **32n** was

prepared with general procedure C using [1,1'-biphenyl]-4-amine and intermediate 31. The final compound was obtained as a white solid in 56% yield. M.p.: 188 ~ 190 °C. <sup>1</sup>H NMR (400 MHz, CDCl<sub>3</sub>) δ 8.14 (bs, 1H), 7.70–7.67 (m, 2H), 7.60–7.57 (m, 4H), 7.49 (d, *J* = 4.0 Hz, 1H), 7.45 (t, *J* = 8.0 Hz, 2H), 7.35 (t, *J* = 8.0 Hz, 1H), 6.85 (d, *J* = 4.0 Hz, 1H), 5.89 (s, 1H), 5.35 (s, 2H), 2.29 (s, 3H), 2.27 (s, 3H). <sup>13</sup>C NMR (101 MHz, CDCl<sub>3</sub>) δ 159.75, 148.45, 145.63, 140.43, 139.11, 138.80, 137.38, 137.01, 128.79, 128.68, 127.66, 127.16, 126.84, 126.04, 120.50, 106.10, 77.35, 77.03, 76.71, 47.71, 13.54, 11.11. HRMS (ESI): calcd for C<sub>23</sub>H<sub>22</sub>N<sub>3</sub>OS [M + H]<sup>+</sup> *m/z* 388.1484, found 388.1479; purity: ≥96% by HPLC analysis.

**5-((3,5-Dimethyl-1H-pyrazol-1-yl)methyl)-N-(4-(pyridin-3-yl)phenyl)thiophene-2-carboxamide (32o).** Compound 32o was prepared with general procedure C using 4-(pyridin-3-yl)aniline and intermediate 31. The final compound was obtained as a white solid in 57% yield. M.p.: 191–193 °C. <sup>1</sup>H NMR (400 MHz, DMSO-*d*<sub>6</sub>) δ 10.32 (s, 1H), 8.91 (d, *J* = 4.0 Hz, 1H), 8.55 (dd, *J* = 2.0, 4.0 Hz, 1H), 8.08 (m, 1H), 7.90 (d, *J* = 4.0 Hz, 1H), 7.80 (dd, *J* = 8.0, 48.0 Hz, 1H), 7.47 (dd, *J* = 2.0, 4.0 Hz, 1H), 7.09 (d, *J* = 4.0 Hz, 1H), 5.86 (s, 1H), 5.76 (s, 1H), 5.41 (s, 2H), 2.24 (s, 3H), 2.11 (s, 3H). <sup>13</sup>C NMR (101 MHz, DMSO-*d*<sub>6</sub>) δ 160.24, 148.59, 147.81, 147.07, 146.87, 139.69, 139.31, 139.16, 135.51, 134.08, 132.62, 129.59, 127.59, 126.95, 124.30, 121.16, 105.79, 55.38, 47.40, 13.82, 11.08. HRMS (ESI): calcd for C<sub>22</sub>H<sub>21</sub>N<sub>4</sub>OS [M + H]<sup>+</sup> *m/z* 389.1436, found 389.1427; purity: ≥99% by HPLC analysis.

**5-((3,5-Dimethyl-1H-pyrazol-1-yl)methyl)-N-(naphthalen-2-yl)thiophene-2-carboxamide (33a).** Compound 33a was prepared with general procedure C using naphthalen-2-amine and intermediate 31. The final compound was obtained as an off-white solid in 73% yield. M.p.: 197–199 °C. <sup>1</sup>H NMR (400 MHz, DMSO-*d*<sub>6</sub>) δ 10.56 (s, 1H), 9.21 (s, 1H), 8.43 (m, 2H), 8.12 (d, *J* = 8.0 Hz, 1H), 7.97 (d, *J* = 4.0 Hz, 1H), 7.94 (dd, *J* = 2.0, 10.0 Hz, 1H), 7.7 (d, *J* = 6.0 Hz, 1H), 7.11 (d, *J* = 4.0 Hz, 1H), 5.86 (s, 1H), 5.43 (s, 2H), 2.25 (s, 3H), 2.12 (s, 3H). <sup>13</sup>C NMR (101 MHz, DMSO-*d*<sub>6</sub>) δ 160.68, 151.96, 147.35, 147.09, 143.52, 140.85, 139.31, 139.18, 136.55, 130.09, 128.93, 127.06, 125.64, 122.39, 120.67, 114.66, 105.80, 47.13, 13.82, 11.08. HRMS (ESI): calcd for C<sub>21</sub>H<sub>20</sub>N<sub>3</sub>OS [M + H]<sup>+</sup> *m/z* 362.1327, found 362.1320; purity: ≥98% by HPLC analysis.

**5-((3,5-Dimethyl-1H-pyrazol-1-yl)methyl)-N-(isoquinolin-6-yl)thiophene-2-carboxamide (33b).** Compound 33b was prepared with general procedure C using isoquinolin-6-amine and intermediate 31. The final compound was obtained as an off-white solid in 73% yield. M.p.: 195–198 °C. <sup>1</sup>H NMR (400 MHz, DMSO-*d*<sub>6</sub>) δ 12.40 (bs, 1H), 10.19 (s, 1H), 8.18 (s, 1H), 8.07 (s, 1H), 7.88 (d, *J* = 4.0 Hz, 1H), 7.56 (d, *J* = 8.0 Hz, 1H), 7.43 (d, *J* = 8.0 Hz, 1H), 7.07 (d, *J* = 4.0 Hz, 1H), 5.86 (s, 1H), 5.40 (s, 2H), 2.24 (s, 3H), 2.12 (s, 3H). <sup>13</sup>C NMR (101 MHz, DMSO-*d*<sub>6</sub>) δ 160.01, 147.02, 146.30, 142.71, 140.22, 139.13, 133.75, 129.05, 126.87, 116.41, 105.77, 49.07, 47.41, 13.82, 11.08. HRMS (ESI): calcd for C<sub>20</sub>H<sub>19</sub>N<sub>4</sub>OS [M + H]<sup>+</sup> *m/z* 363.1280, found 363.1275; purity: ≥98% by HPLC analysis.

**5-((3,5-Dimethyl-1H-pyrazol-1-yl)methyl)-N-(quinolin-7-yl)thiophene-2-carboxamide (33c).** Compound 33c was prepared with general procedure C using quinolin-7-amine and intermediate 31. The final compound was obtained as a white solid in 79% yield. M.p.: 285–287 °C. <sup>1</sup>H NMR (400 MHz, DMSO-*d*<sub>6</sub>) δ 11.06 (bs, 1H), 10.09 (s, 1H), 7.96 (s, 1H), 7.87 (d, *J* = 4.0 Hz, 1H), 7.48 (d, *J* = 8.0 Hz, 1H), 7.29 (t, *J* = 2.0 Hz, 1H), 7.21 (dd, *J* = 2.0, 8.0 Hz, 1H), 7.06 (d, *J* = 4.0 Hz, 1H), 6.38–6.37 (m, 1H), 5.86 (s, 1H), 5.40 (s, 2H), 2.24 (s, 3H), 2.11 (s, 3H). <sup>13</sup>C NMR (101 MHz, DMSO-*d*<sub>6</sub>) δ 159.85, 147.00, 146.10, 140.49, 139.12, 136.24, 133.07, 128.83, 126.86, 125.71, 124.79, 120.15, 113.83, 105.77, 103.95, 101.41, 47.41, 13.83, 11.09. HRMS (ESI): calcd for C<sub>20</sub>H<sub>19</sub>N<sub>4</sub>OS [M + H]<sup>+</sup> *m/z* 363.1280, found 363.1271; purity: ≥99% by HPLC analysis.

**5-((3,5-Dimethyl-1H-pyrazol-1-yl)methyl)-N-(1H-indol-6-yl)thiophene-2-carboxamide (33d).** Compound 33d was prepared with general procedure C using 1H-indol-6-amine and intermediate 31. The final compound was obtained as a white solid in 79% yield. M.p.: 191 ~ 194 °C. <sup>1</sup>H NMR (400 MHz, DMSO-*d*<sub>6</sub>) δ 10.39 (s, 1H), 8.34 (s, 1H), 7.93–7.77 (m, 5H), 7.51–7.41 (m, 2H), 7.09 (d, *J* = 4.0 Hz, 1H), 5.87 (s, 1H), 5.42 (s, 2H), 2.25 (s, 3H), 2.12 (s, 3H). <sup>13</sup>C NMR

(101 MHz, DMSO-*d*<sub>6</sub>) δ 160.36, 147.05, 146.79, 139.80, 139.16, 136.77, 133.75, 130.45, 129.53, 128.71, 127.93, 127.85, 127.01, 126.91, 125.33, 121.28, 117.09, 105.79, 47.39, 13.83, 11.09. HRMS (ESI): calcd for C<sub>19</sub>H<sub>19</sub>N<sub>4</sub>OS [M + H]<sup>+</sup> *m/z* 351.1280, found 351.1273; purity: ≥96% by HPLC analysis.

**N-(1H-Benzo[d]imidazol-5-yl)-5-((3,5-dimethyl-1H-pyrazol-1-yl)methyl)thiophene-2-carboxamide (33e).** Compound 33e was prepared with general procedure C using 1H-benzo[d]imidazol-6-amine and intermediate 31. The final compound was obtained as a white solid in 83% yield. M.p.: 304–306 °C. <sup>1</sup>H NMR (400 MHz, DMSO-*d*<sub>6</sub>) δ 10.62 (s, 1H), 10.55 (s, 1H), 10.09 (s, 1H), 7.85 (d, *J* = 4.0 Hz, 1H), 7.48 (s, 1H), 7.20 (dd, *J* = 2.0, 8.0 Hz, 1H), 7.04 (d, *J* = 4.0 Hz, 1H), 6.86 (d, *J* = 12.0 Hz, 1H), 5.85 (s, 1H), 5.39 (s, 2H), 2.23 (s, 3H), 2.11 (s, 3H). <sup>13</sup>C NMR (101 MHz, DMSO-*d*<sub>6</sub>) δ 160.16, 147.05, 146.76, 140.11, 139.80, 139.15, 138.64, 135.82, 129.48, 129.38, 127.33, 126.94, 126.76, 121.08, 105.79, 47.40, 13.83, 11.08. HRMS (ESI): calcd for C<sub>18</sub>H<sub>18</sub>N<sub>5</sub>OS [M + H]<sup>+</sup> *m/z* 351.1280, found 351.1273; purity: ≥98% by HPLC analysis.

**5-((3,5-Dimethyl-1H-pyrazol-1-yl)methyl)-N-(2-oxo-2,3-dihydro-1H-benzod[imidazol-5-yl]thiophene-2-carboxamide (33f).** Compound 33f was prepared with general procedure C using 5-amino-1,3-dihydro-2H-benzo[d]imidazol-2-one and intermediate 31. The final compound was obtained as a white solid in 84% yield. M.p.: 199–201 °C. <sup>1</sup>H NMR (400 MHz, DMSO-*d*<sub>6</sub>) δ 10.51 (s, 1H), 8.86 (dd, *J* = 2.0, 4.0 Hz, 1H), 8.48 (s, 1H), 8.29 (d, *J* = 8.0 Hz, 1H), 7.97–7.90 (m, 3H), 7.47 (dd, *J* = 2.0, 4.0 Hz, 1H), 7.11 (d, *J* = 4.0 Hz, 1H), 5.87 (s, 1H), 5.43 (s, 2H), 2.25 (s, 3H), 2.12 (s, 3H). <sup>13</sup>C NMR (101 MHz, DMSO-*d*<sub>6</sub>) δ 160.54, 151.43, 148.77, 147.15, 147.09, 140.04, 139.51, 139.18, 136.01, 129.88, 128.83, 127.01, 125.11, 121.47, 120.75, 117.75, 105.80, 47.40, 13.83, 11.09. HRMS (ESI): calcd for C<sub>18</sub>H<sub>18</sub>N<sub>5</sub>O<sub>2</sub>S [M + H]<sup>+</sup> *m/z* 368.1181, found 368.1175; purity: ≥97% by HPLC analysis.

**Animals.** Male adult C57BL/6 mice (6–8 weeks old) and ICR mice (6–8 weeks old) were obtained from Beijing Vital River Lab Animal Technology Co., Ltd. All animals were housed in cages under artificial lighting from 7:00 AM to 7:00 PM, with free access to food and water. Animals were assigned to different experimental groups randomly, each kept in a separate cage. All experimental procedures were approved by the Peking University Institutional Animal Care and Use Committee.

**Cell Culture and Transfection.** HEK-293 cells were incubated in Dulbecco's modified Eagle medium (DMEM) supplemented with 10% fetal bovine serum (FBS) at 37 °C under 5% CO<sub>2</sub>. For electrophysiological recording, cells were plated onto coverslips in 35 mm dishes 2 days before. Then, cells were transiently transfected with cDNA of GluN1/GluN2A, GluN1/GluN2B, GluN1/GluN2C, and GluN1/GluN2D using Lipofectamine 2000 (Invitrogen) 16–24 h following the manufacturer's instructions. 200 mM AP-5 was added in the medium when replacing DMEM to inhibit cell death. After 18–24 h of transfection, coverslips were prepared in an external solution for recording.

**Culture of Cortical Neurons.** The primary cortical culture was obtained from embryos of embryonic day 18 (E18) ICR mice embryos of either sex after decapitation. Hippocampal regions were gently removed and digested with 0.25% trypsin for 30 min at 37 °C followed by trituration with a pipette in plating medium (DMEM with 10% FBS). Dissociated neurons were plated onto poly-D-lysine coated coverslips in 35 mm dishes at a density of 1 × 10<sup>6</sup> cells per dish. After 4 h, the medium was displaced by neurobasal medium supplemented with 2% B27 and 0.5 mmol/L GlutaMAX-I. Neurons were obtained at 37 °C under 5% CO<sub>2</sub>, and half the medium was replaced every 3 days. After being cultured for 7–9 days, cortical neurons were harvested and used for electrophysiological experiments in Figure 4. After being cultured for 12–15 days, cortical neurons were harvested and used for electrophysiological experiments in Figure 5 and evaluations of all derivatives.

The cultured hippocampal neurons used for the tests on AMPARs and GABARs were obtained from embryos of embryonic day 18 (E18) ICR mice embryos of either sex after decapitation. The neurons

were cultured for 7–9 days as the protocol mentioned above before tests.

**Slice Preparations.** C57BL/6 mice were anesthetized and decapitated, and brains were dissected and placed into ice-cold slice solution of the following: 110 mM choline chloride, 2.5 mM KCl, 1.25 mM  $\text{NaH}_2\text{PO}_4$ , 25 mM  $\text{NaHCO}_3$ , 0.5 mM  $\text{CaCl}_2$ , 7 mM  $\text{MgCl}_2$ , 25 mM glucose, 0.6 mM ascorbic acid, 3.1 mM pyruvic acid (bubbled with 95%  $\text{O}_2$  and 5%  $\text{CO}_2$ , pH 7.4). For epilepsy tissues of patients, brain tissues were put into ice-cold slice solution immediately after surgery. Acute horizontal slices were cut by a vibratome at 350  $\mu\text{m}$  thickness and then transferred to artificial cerebrospinal fluid (ACSF): 125 mM NaCl, 2.5 mM KCl, 2.0 mM  $\text{CaCl}_2$ , 2.0 mM  $\text{MgCl}_2$ , 25 mM  $\text{NaHCO}_3$ , 1.25 mM  $\text{NaH}_2\text{PO}_4$ , 10 mM glucose (bubbled with 95%  $\text{O}_2$  and 5%  $\text{CO}_2$ , pH 7.4). Slices were incubated at 37 °C for 30 min and stored at room temperature before recording. Magnesium was abolished when recording. TTX (500 nM) and strychnine (1 mM) were applied to the recording solution to obtain NMDA-mediated current.

**Electrophysiological Recording.** For whole-cell voltage-clamp recording in primary neuron and transfected cells, cells were held at  $-70$  mV and recorded at room temperature using a HEKA EPC10 amplifier with PatchMaster software (HEKA Elektronik). Patch pipettes were pulled from borosilicate glass to a resistance of 4–6 M $\Omega$  when filled with an internal pipette solution composed of the following: 122 mM CsCl, 1 mM  $\text{CaCl}_2$ , 5 mM  $\text{MgCl}_2$ , 10 mM EGTA, 10 mM HEPES, 4 mM  $\text{Na}_2\text{ATP}$ , 0.3 mM Tris-GTP, 14 mM Tris-phosphocreatine, adjusted to pH 7.3 with CsOH. Cells were perfused with the external solution containing: 140 mM NaCl, 2.5 mM KCl, 2 mM  $\text{CaCl}_2$ , 10 mM HEPES, and 10 mM glucose, pH 7.4. NMDA and other compounds were applied via gravity-fed tubes for NMDA current recording until the current reached a steady current value (5–10 s). Data were acquired with PatchMaster software (HEKA) and filtered at 1 kHz with an LIH 8 + 8 computer interface.

For *in vitro* slice recording, the internal solution was the same as for primary cultured neurons. All recordings were performed with a MultiClamp 700B amplifier (Molecular Devices), and data were obtained with clamp 10.6 software, filtered at 2 kHz and sampling rate at 33 kHz with a Digidata 1440A digitizer (Molecular Devices). Slices were incubated in flow ACSF at 32–33 °C. For NMDA current recording, NMDA and other compounds were dissolved in ACSF until a peak current amplitude was obtained (15–30 min). Data were acquired with PatchMaster software (HEKA) and filtered at 1 kHz with an LIH 8 + 8 computer interface.

Potentiating activity for the compound was calculated as  $\Delta I/I_{\text{NMDA}}$  from the following equation:

$$\Delta I/I_{\text{NMDA}} = \frac{I_{\text{compound}} - I_{\text{NMDA}}}{I_{\text{NMDA}}}$$

**In Vivo Efficacy Studies.** *Drugs.* FS2921 and fluoxetine were dissolved in artificial cerebrospinal fluid in a concentration of 10  $\mu\text{M}/\text{L}$ . Selected compounds, fluoxetine and duloxetine, were dissolved in phosphate-buffered saline (PBS) containing 4% DMSO and Tween 80 (2%) at indicated doses.

*Studies with C57BL/6N Mice by Intracerebroventricular Injections.* The cannulas were attached to skulls of C57BL/6N mice (from bregma: AP, +0.8; ML,  $-1.5$ ; DV,  $-2.5$ ) under a stereotaxic surgery and secured by dental cement and screws. For injections, the cannulas were connected to the microinjector through an injection needle and long hose. Drugs were injected into the lateral ventricle for 4  $\mu\text{L}$  over the course of 10 min (at a rate of 0.4  $\mu\text{L}/\text{min}$ ). Mice were not anesthetized for the daily injections and could move around during the intracerebroventricular injections. After injection for 30 min, each mouse was placed in a clear cylindrical tank (40 cm tall  $\times$  20 cm diameter), filled with water (30 cm tall) at  $24 \pm 2$  °C. Mice were judged as immobile when they float motionlessly. Mice were forced to swim freely for 6 min, and the last four minutes was considered when analyzing. Water was changed after every test.

*Studies with ICR Mice by i.p. Administrations.* ICR mice were randomly separated into seven groups ( $n = 10$ ) and administered with selected compounds and fluoxetine by intraperitoneal injection only

once at a dose of 30 mg/kg. The control group has injected the vehicle. After injection for 20 min, each mouse was placed in a clear cylindrical tank (40 cm tall  $\times$  20 cm diameter), filled with water (30 cm tall) at  $24 \pm 2$  °C. Mice were judged as immobile when they float motionlessly. Mice were forced to swim freely for 6 min, and the last four minutes was considered when analyzing. Water was changed after every test. Then, ICR mice ( $n = 10$  in each group) were i.p. administered with the vehicle, duloxetine (15 mg/kg), compound 20e (3 and 10 mg/kg), and compound 32h (3 and 10 mg/kg). As described above, each mouse underwent the FST after injection for 30 min.

*Chronic Social Defeat Stress and Social Interaction Testing.* FS2921 or fluoxetine were dissolved in artificial cerebrospinal fluid in a concentration of 10  $\mu\text{M}/\text{L}$  and injected into the lateral ventricle (from bregma: AP, +0.8; ML,  $-1.5$ ; DV,  $-2.5$ ) of C57BL/6N mice for 4  $\mu\text{L}$  over the course of 10 min (at a rate of 0.4  $\mu\text{L}/\text{min}$ ) for 11 days. Every day after injection of FS2921, fluoxetine, or the vehicle for 30 min, mice were subjected to social defeat stress. Chronic social defeat stress was performed according to previously described protocols.<sup>40</sup> C57BL/6 mice were physically defeated by a novel CD-1 aggressor for 5 min/day and then kept in one side of the cages divided by a transparent, perforated baffle plate, sensory contacting with CD-1 mice on the other side for 24 h for 10 days. CD-1 aggressors were changed daily. On day 11, after injection of the drugs for 30 min, mice were assayed on the social interaction test. The depression level of mice was obtained based on the social interaction ratio.

*Hyperactivity Test.* Mice (10 mice in each group) were dosed with the vehicle and selected compounds (10 mg/kg) by intraperitoneal injection. Animals were placed in Plexiglas cages for evaluating locomotor activity. After the environmental adaptation for 60 min, the total locomotor distance of each animal was recorded for 90 min.

*Apomorphine-Induced Climbing.* Mice (10 mice in each group) were dosed with the vehicle and selected compounds (10 mg/kg) by intraperitoneal injection. Animals were then challenged at 30 min post-injection with 1.0 mg/kg apomorphine in 0.9% NaCl + 0.1% ascorbic acid, placed in cylindrical wire cages (12 cm in diameter, 14 cm in height), and observed for climbing behavior at 10, 20, and 30 min post-dose. The climbing behavior was scored as follows: 3 or 4 paws on the cage floor = 0 scores; 2 and 3 paws on the cage = 1 score; 4 paws on the cage = 2 scores.

**Cytotoxicity Test.** Cytotoxicity of selected compounds was determined using the cell counting kit-8 (CCK8) assay kit (Beyotime, Shanghai, China). Briefly, fibroblasts L929, HEK293, and VERO were cultured in 96-well plates at a density of 1000 cells per well at 37 °C overnight. Then, different amounts of selected compounds were added into cells and incubated for 48 h. According to the manufacturer's instruction, 10  $\mu\text{L}$  of CCK8 detection reagent was added into 100  $\mu\text{L}$  of medium per well. After 1 h, the absorbance was read at 450 nm for CCK8 using a Spark multimode microplate reader. Cell inhibition was calculated as relative absorbance compared to a DMSO-only control.

**Receptor Binding Studies.** *Materials.* The following specific radioligands and tissue sources were used: (a) the serotonin 5-HT<sub>1A</sub> receptor, [<sup>3</sup>H] 8-OH-DPAT, from h5-HT<sub>1A</sub>-CHO cells, (b) the serotonin 5-HT<sub>1B</sub> receptor, [<sup>3</sup>H] GR125743, from h5-HT<sub>1A</sub>-CHO cells, (c) the serotonin 5-HT<sub>2A</sub> receptor, [<sup>3</sup>H] ketanserin in the presence of 4-dione hydrochloride hydrate (35 nM), from h5-HT<sub>2A</sub>-CHO cells, (d) the serotonin 5-HT<sub>2C</sub> receptor, [<sup>3</sup>H] mesulergine, in the presence of spiperone (40 nM), from rat cerebral cortex, (e) the serotonin 5-HT<sub>6</sub> receptor, [<sup>3</sup>H] lysergic acid diethylamide, from h5-HT<sub>6</sub>-CHO cells, (f) the dopamine D2 receptor, [<sup>3</sup>H] N-methylspiperone, from hD<sub>2</sub>-CHO cells, (g) the dopaminergic D3 receptor, [<sup>3</sup>H] N-methylspiperone, from hD<sub>3</sub>-CHO cells, (h) the adrenergic  $\alpha 1$  receptor, [<sup>3</sup>H] prazosin, from rat cerebral cortex, (i) the serotonin transporter (SERT), [<sup>3</sup>H] paroxetine, from hSERT-CHO cells, (j) the dopamine transporter (DAT), [<sup>3</sup>H] WIN35,428, from rat striatum, and (k) the noradrenaline transporter (NET), [<sup>3</sup>H] nisoxetine, from hNET-CHO cells.

**General Procedures for the Binding Assays.** The radioligand competitive binding assay for each receptor was performed as depicted before.<sup>41a–41c</sup> Compound **32h** was dissolved in 50% (v/v) DMSO, and the compound concentration was  $2 \times 10^{-3}$  M; dilution to the initial concentration of the new compound,  $2 \times 10^{-4}$  M, contained 5% DMSO. For one receptor binding assays, total binding (TB) was determined in the presence of the radioligand. Nonspecific binding (NB) was determined in the presence of the radioligand and competitive ligand for the related receptor, whereas compound binding (CB) was determined in the presence of the radioligand and compound **32h**. Each specific binding (SB) was calculated as the total binding (TB) minus the nonspecific binding (NB) at a particular concentration of radioligand. Each percentage of inhibition (%) was calculated as follows: percentage of inhibition (%) =  $[(TB - CB)/(TB - NB)] \times 100$ . Blank binding experiments contained 0.25% (v/v) DMSO were performed; DMSO had no effect. All compounds were tested at least three times over a 6-fold concentration range ( $10^{-5}$  M to  $10^{-10}$  M).  $IC_{50}$  values were determined by nonlinear regression analysis with fitting to the Hill equation curve.  $K_i$  values were calculated using the Cheng and Prusoff equation,  $K_i = IC_{50}/(1 + C/K_d)$ , where  $C$  represents the concentration of the hot ligand used and  $K_d$  is the receptor dissociation constant of each labeled ligand. The  $K_i$  value was derived from at least three independent experiments.

**In Vivo Metabolism Studies. Pharmacokinetics Study in Mice.** The HPLC conditions were as follows: column, Diamonsil C18 (150 mm  $\times$  4.6 mm, 5  $\mu$ m, 120 Å); mobile phase, 0.1% FA in water/acetonitrile (Merck Company, Germany) (v/v, 0–8.0 min, 40:60); flow rate, 0.2 mL/min; column temperature, 40 °C. UV detection, 254 nm. ICR mice ( $n = 6$ /group) were dosed with compounds **20h/32c/32h/32o** via the tail vein for i.v. administration (3 mg/kg) or i.p. administration (10 mg/kg). After the last administration, 80  $\mu$ L of orbital blood was extracted at 0.25, 0.5, 1, 2, 3, 4, 5, 6, 8, and 24 h. After separated by centrifugation (rpm = 18,000, 10 min), the plasma sample (30  $\mu$ L) was prepared for high-pressure liquid chromatography/tandem mass spectrometry (LC–MS/MS) analysis by protein precipitation with acetonitrile (100  $\mu$ L). The plasma samples were analyzed for drug and internal standard via an API 4000 Q trap mass spectrometer (Applied Biosystems, Foster City, CA, USA) coupled with a 1200 series HPLC system (Agilent, Santa Clara, CA, USA). Isocratic elution was used with 80% acetonitrile and 20% water with 0.1% formic acid to separate analytes. The total run time was 3 min, and the flow rate was 0.3 mL/min.

**Blood–Brain Barrier (BBB) Penetration Study in Mice.** At 0.5 and 2 h after the last administration, after euthanizing the mice using CO<sub>2</sub> gas, the blood was collected from the heart immediately and the plasma was separated by centrifugation at 18000 rpm for 10 min at 4 °C. The remaining blood was washed out from the circulation by performing cardiac perfusion with physiological saline containing 10 U/mL heparin. The brain was then removed from the skull and added to three volumes of PBS buffer per weight, homogenized, and stored at –20 °C. The compound concentrations in plasma and brain samples were determined via the LC–MS/MS protocol.

**Pharmacokinetics Study of Compound 32h in Rats.** The same process was performed for the pharmacokinetics study of compound **32h** in rats. The Sprague–Dawley rats ( $n = 3$ /group) were dosed with compounds **32h** via the tail vein for i.v. administration (3 mg/kg) or i.p. administration (10 mg/kg). After the last administration, 80  $\mu$ L of orbital blood and 50  $\mu$ L of CSF were extracted at 10, 20, 40, 80, 160, 320, 640 and 1280 min. The samples were tested with the protocol above.

**hERG Affinity.** Chinese hamster ovary (CHO) cells were stably transfected with hERG cDNA, passaged in Ham's F-12 nutrient mixture supplemented with 10% fetal bovine serum, penicillin (100 U/mL), streptomycin (100  $\mu$ g/mL), and Geneticin (200  $\mu$ g/mL). For whole-cell patch-clamp recordings, CHO cells steadily expressing the hERG channel were seeded on 8 mm  $\times$  8 mm glass coverslips in 35 mm<sup>2</sup> diameter dishes at a density that enabled the germs to be isolated for recording and cultured at 37 °C under 5% CO<sub>2</sub>. Currents were recorded at room temperature using an EPC 10 amplifier with Patchmaster software (HEKA). The total resistance of patch

electrodes was measured to be 3–5 M $\Omega$ . The extracellular solution contained 140 mM, 4 mM KCl, 1.8 mM CaCl<sub>2</sub>, 1 mM MgCl<sub>2</sub>, 10 mM glucose, and 10 mM HEPES with pH adjusted to 7.4 with NaOH. The internal pipette solution contained 130 mM KCl, 1 mM MgCl<sub>2</sub>, 5 mM ethylene glycol-bis( $\beta$ -aminoethyl ether)-*N,N,N,N'*-tetraacetic acid salt (EGTA), 5 mM MgATP, and 10 mM HEPES with the pH adjusted to 7.2 with KOH. Cells were clamped from the holding potential at –80 to –60 mV for 500 ms, and the potential was raised to +30 mV for 2 s, then repolarized to –60 mV for 2 s, and returned back to the initial value at last. The voltage protocol was run once every 10 s. Data were acquired and analyzed using the PatchMaster software (HEKA).

**Statistical Analysis.** All values are presented as mean  $\pm$  SEM or mean  $\pm$  SD. For the calculation of EC<sub>50</sub>, the variable slope model was used with the following equation:  $Y = Y_{\min} + (Y_{\max} - Y_{\min}) / (1 + 10^{((\log EC_{50} - X) \times \text{HillSlope})})$ . Differences between groups were analyzed by two-tailed Student's *t* test. One-way ANOVA followed by post hoc Bonferroni's or Dunnett's multiple comparisons was used to compare more than two groups. Two-way ANOVA followed by post hoc Bonferroni's multiple comparisons test was used for comparison of a series of data collection among groups.

## ■ ASSOCIATED CONTENT

### Supporting Information

The Supporting Information is available free of charge at <https://pubs.acs.org/doi/10.1021/acs.jmedchem.0c02018>.

Figure S1. Effects of FS2921 on NMDA or glycine alone; Figure S2. Whole cell voltage clamp recordings on HEK-293 cells expressing GluN1/GluN2A, GluN1/GluN2B, GluN1/GluN2C or GluN1/GluN2D of FS2921; Figure S3. Effect of FS2921 at native AMPA and GABA receptors; Figure S4. Effects of compounds **32c/32o** in the FST; Figure S5. Effects of selected compounds administered for hyperactivity in mice; Figure S6. Effects of selected compounds on apomorphine (APO)-induced climbing in mice; Figure S7. Plasma concentration–time profiles for compound **20h** and compound **32h**; Figure S8. Concentration–time profiles of compound **32h** in plasma and cerebrospinal fluid; Figure S9. Effects of compounds **20h** and **32h** administered p.o. at 30 mg/kg of the weight of the mice; Table S1. Selected crystal complexes of NMDAR LBD; Table S2. G score and inhibition rate at 10  $\mu$ M of hit compounds; Table S3. Binding affinities of compound **32h** for inhibiting radioligand binding to anti-depressant drug targets; Table S4. PK and brain penetration properties of compounds **32c/32o** in ICR mice (PDF) PDB ID of the co-crystal structure of GNE0723 (PDB) SMILES representation of compounds with key data (CSV)

## ■ AUTHOR INFORMATION

### Corresponding Authors

Zhenming Liu – State Key Laboratory of Natural and Biomimetic Drugs, School of Pharmaceutical Sciences, Peking University, Beijing 100191, China; [orcid.org/0000-0002-8993-4015](https://orcid.org/0000-0002-8993-4015); Phone: +86-10-8280-5281; Email: [zmliu@bjmu.edu.cn](mailto:zmliu@bjmu.edu.cn)

Zhuo Huang – State Key Laboratory of Natural and Biomimetic Drugs, School of Pharmaceutical Sciences, Peking University, Beijing 100191, China; [orcid.org/0000-0001-9198-4778](https://orcid.org/0000-0001-9198-4778); Phone: +86-10-8280-5925; Email: [huangz@hsc.pku.edu.cn](mailto:huangz@hsc.pku.edu.cn)

Liangren Zhang – State Key Laboratory of Natural and Biomimetic Drugs, School of Pharmaceutical Sciences, Peking University, Beijing 100191, China; [orcid.org/0000-0002-7362-9497](https://orcid.org/0000-0002-7362-9497); Phone: +86-10-8280-2567; Email: [liangren@bjmu.edu.cn](mailto:liangren@bjmu.edu.cn)

## Authors

Zhongtang Li – State Key Laboratory of Natural and Biomimetic Drugs, School of Pharmaceutical Sciences, Peking University, Beijing 100191, China

Guanxing Cai – State Key Laboratory of Natural and Biomimetic Drugs, School of Pharmaceutical Sciences, Peking University, Beijing 100191, China

Fan Fang – State Key Laboratory of Natural and Biomimetic Drugs, School of Pharmaceutical Sciences, Peking University, Beijing 100191, China

Wenchao Li – State Key Laboratory of Natural and Biomimetic Drugs, School of Pharmaceutical Sciences, Peking University, Beijing 100191, China

Minghua Fan – State Key Laboratory of Natural and Biomimetic Drugs, School of Pharmaceutical Sciences, Peking University, Beijing 100191, China

Jingjing Lian – State Key Laboratory of Natural and Biomimetic Drugs, School of Pharmaceutical Sciences, Peking University, Beijing 100191, China

Yinli Qiu – Jiangsu Nhwa Pharmaceutical Co., Ltd., Xuzhou, Jiangsu 221116, China

Xiangqing Xu – Jiangsu Nhwa Pharmaceutical Co., Ltd., Xuzhou, Jiangsu 221116, China

Xuehui Lv – State Key Laboratory of Natural and Biomimetic Drugs, School of Pharmaceutical Sciences, Peking University, Beijing 100191, China

Yiyan Li – State Key Laboratory of Natural and Biomimetic Drugs, School of Pharmaceutical Sciences, Peking University, Beijing 100191, China

Ruqiu Zheng – State Key Laboratory of Natural and Biomimetic Drugs, School of Pharmaceutical Sciences, Peking University, Beijing 100191, China

Yuxi Wang – State Key Laboratory of Natural and Biomimetic Drugs, School of Pharmaceutical Sciences, Peking University, Beijing 100191, China

Zhongjun Li – State Key Laboratory of Natural and Biomimetic Drugs, School of Pharmaceutical Sciences, Peking University, Beijing 100191, China; [orcid.org/0000-0003-1642-7773](https://orcid.org/0000-0003-1642-7773)

Guisen Zhang – Jiangsu Key Laboratory of Marine Biological Resources and Environment, Jiangsu Key Laboratory of Marine Pharmaceutical Compound Screening, School of Pharmacy, Jiangsu Ocean University, Lianyungang 222005, China

Complete contact information is available at:

<https://pubs.acs.org/10.1021/acs.jmedchem.0c02018>

## Author Contributions

<sup>||</sup>Z.L., G.C., and F.F. equally contributed to this work.

## Notes

The authors declare no competing financial interest.

## ACKNOWLEDGMENTS

This research was supported by the National Major Scientific and Technological Special Project for Significant New Drugs Development (2018ZX09711002-013-004, 2018ZX09735-

001) and the National Natural Science Foundation of China (NSFC) (81872730).

## ABBREVIATIONS

NMDAR, *N*-methyl-*D*-aspartate receptor; MDD, major depressive disorders; PAM, positive allosteric modulator; FDA, Food and Drug Administration; ERK, extracellular regulated kinase; PFC, prefrontal cortex; LTP, long-term potentiation; LTD, long-term depression; AMPA,  $\alpha$ -amino-3-hydroxy-5-methyl-4-isoxazole-propionic acid; AMPAR,  $\alpha$ -amino-3-hydroxy-5-methyl-4-isoxazole-propionic acid receptor; mTOR, mammalian target of rapamycin; ATD, amino terminal domain; LBD, ligand binding domains; TMD, transmembrane domains; PSA, polar surface area; BBB, blood–brain barrier; Log BB, log of the brain/blood partition coefficient; IC<sub>50</sub>, half-maximal inhibitory concentration; EC<sub>50</sub>, half-maximal effective concentration; PDB, protein data bank; Log *P*, octanol/water partition coefficient; PKUCNCL, Chinese National Compound Library of Peking University; PAINS, pan assay interference compounds; SAR, structure–activity relationship; FST, forced swimming test; CSDS, chronic social defeat stress; ICR, Institute of Cancer Research; APO, apomorphine; D<sub>2</sub>, dopamine 2; D3, dopamine 3; 5-HT<sub>1A</sub>, 5-hydroxytryptamine 1A; 5-HT<sub>1B</sub>, 5-hydroxytryptamine 1B; 5-HT<sub>2A</sub>, 5-hydroxytryptamine 2A; 5-HT<sub>2B</sub>, 5-hydroxytryptamine 2B; 5-HT<sub>2C</sub>, 5-hydroxytryptamine 2C; 5-HT<sub>6</sub>, 5-hydroxytryptamine 6; SER, serotonin transporter; NET, noradrenaline transporter; DAT, dopamine transporter; i.v., intravenous injection; i.p., intraperitoneal injection; C<sub>max</sub>, maximum concentrations; t<sub>max</sub>, distribution half-life; t<sub>1/2</sub>, eliminate half-life; CL, clearance; MRT, mean residence time; V<sub>d</sub>, volume of distribution; *F*, bioavailability; AUC, area under the curve; MRT, mean retention time; LC–MS/MS, liquid chromatography/tandem mass spectrometry; CHO, Chinese hamster ovary; hERG, human ether-a-go-go related gene.

## REFERENCES

- (1) World Health Organization *Depression and other common mental disorders: global health estimates*; World Health Organization, 2017.
- (2) Boku, S.; Nakagawa, S.; Toda, H.; Hishimoto, A. Neural basis of major depressive disorder: Beyond monoamine hypothesis. *Psychiatry Clin. Neurosci.* **2018**, *72*, 3–12.
- (3) Hashimoto, K. Ketamine's antidepressant action: beyond NMDA receptor inhibition. *Expert. Opin. Ther. Targets* **2016**, *20*, 1389–1392.
- (4) Molero, P.; Ramos-Quiroga, J. A.; Martin-Santos, R.; Calvo-Sánchez, E.; Gutiérrez-Rojas, L.; Meana, J. J. Antidepressant Efficacy and Tolerability of Ketamine and Esketamine: A Critical Review. *CNS Drugs* **2018**, *32*, 411–420.
- (5) Krystal, J. H.; Karper, L. P.; Seibyl, J. P.; Freeman, G. K.; Delaney, R.; Bremner, J. D.; Heninger, G. R.; Bowers, M. B., Jr.; Charney, D. S. Subanesthetic effects of the noncompetitive NMDA antagonist, ketamine, in humans. Psychotomimetic, perceptual, cognitive, and neuroendocrine responses. *Arch. Gen. Psychiatry* **1994**, *51*, 199–214.
- (6) Ulbrich, M. H.; Isacoff, E. Y. Rules of engagement for NMDA receptor subunits. *Proc. Natl. Acad. Sci. U. S. A.* **2008**, *105*, 14163–14168.
- (7) Traynelis, S. F.; Wollmuth, L. P.; McBain, C. J.; Menniti, F. S.; Vance, K. M.; Ogden, K. K.; Hansen, K. B.; Yuan, H.; Myers, S. J.; Dingledine, R. Glutamate receptor ion channels: structure, regulation, and function. *Pharmacol. Rev.* **2010**, *62*, 405–496.
- (8) Karakas, E.; Furukawa, H. Crystal structure of a heterotetrameric NMDA receptor ion channel. *Science* **2014**, *344*, 992–997.

- (9) Paoletti, P.; Bellone, C.; Zhou, Q. NMDA receptor subunit diversity: impact on receptor properties, synaptic plasticity and disease. *Nat. Rev. Neurosci.* **2013**, *14*, 383–400.
- (10) Danysz, W.; Parsons, C. G. Glycine and N-methyl-D-aspartate receptors: physiological significance and possible therapeutic applications. *Pharmacol. Rev.* **1998**, *50*, 597–664.
- (11) Simon, R. P.; Swan, J. H.; Griffiths, T.; Meldrum, B. S. Blockade of N-methyl-D-aspartate receptors may protect against ischemic damage in the brain. *Science* **1984**, *226*, 850–852.
- (12) Croucher, M. J.; Collins, J. F.; Meldrum, B. S. Anticonvulsant action of excitatory amino acid antagonists. *Science* **1982**, *216*, 899–901.
- (13) Davies, S. N.; Lodge, D. Evidence for involvement of N-methylaspartate receptors in 'windup' of class 2 neurones in the dorsal horn of the rat. *Brain Res.* **1987**, *424*, 402–406.
- (14) Preskorn, S.; Macaluso, M.; Mehra, D. V.; Zammit, G.; Moskal, J. R.; Burch, R. M. GLYX-13 Clinical Study Group. Randomized proof of concept trial of GLYX-13, an N-methyl-D-aspartate receptor glycine site partial agonist, in major depressive disorder nonresponsive to a previous antidepressant agent. *J. Psychiatr. Pract.* **2015**, *21*, 140–149.
- (15) Moskal, J. R.; Yamamoto, H.; Colley, P. A. The use of antibody engineering to create novel drugs that target N-methyl-D-aspartate receptors. *Curr. Drug Targets* **2001**, *2*, 331–345.
- (16) Zhang, X. L.; Sullivan, J. A.; Moskal, J. R.; Stanton, P. K. A NMDA receptor glycine site partial agonist, GLYX-13, simultaneously enhances LTP and reduces LTD at Schaffer collateral-CA1 synapses in hippocampus. *Neuropharmacology* **2008**, *55*, 1238–1250.
- (17) Moskal, J. R.; Kuo, A. G.; Weiss, C.; Wood, P. L.; O'Connor, H. A.; Kelso, S.; Harris, R. B.; Disterhoft, J. F. GLYX-13: a monoclonal antibody-derived peptide that acts as an N-methyl-D-aspartate receptor modulator. *Neuropharmacology* **2005**, *49*, 1077–1087.
- (18) Moskal, J. R.; Burch, R.; Burgdorf, J. S.; Kroes, R. A.; Stanton, P. K.; Disterhoft, J. F.; Leander, J. D. GLYX-13, an NMDA receptor glycine site functional partial agonist enhances cognition and produces antidepressant effects without the psychotomimetic side effects of NMDA receptor antagonists. *Expert Opin. Invest. Drugs* **2014**, *23*, 243–254.
- (19) Clinicaltrials.gov: NCT03560518; NCT02943577; NCT02943564; NCT02932943; NCT03614156; NCT03002077; NCT02951988.
- (20) Allergan. *Data on Allergan's Rapastinel and NRX-1074 (AGN-241660) presented at the Society for Neuroscience (SfN) Annual Meeting*; Allergan, 2015.
- (21) Burnell, E. S.; Irvine, M.; Fang, G.; Sapkota, K.; Jane, D. E.; Monaghan, D. T. Positive and negative allosteric modulators of N-methyl-d-aspartate (NMDA) Receptors: structure activity relationships and mechanisms of action. *J. Med. Chem.* **2019**, *62*, 3–23.
- (22) Monaghan, D. T.; Irvine, M. W.; Costa, B. M.; Fang, G.; Jane, D. E. Pharmacological modulation of NMDA receptor activity and the advent of negative and positive allosteric modulators. *Neurochem. Int.* **2012**, *61*, 581–592.
- (23) Collingridge, G. L.; Volianskis, A.; Bannister, N.; France, G.; Hanna, L.; Mercier, M.; Tidball, P.; Fang, G.; Irvine, M. W.; Costa, B. M.; Monaghan, D. T.; Bortolotto, Z. A.; Molnár, E.; Lodge, D.; Jane, D. E. The NMDA receptor as a target for cognitive enhancement. *Neuropharmacology* **2013**, *64*, 13–26.
- (24) Malayev, A.; Gibbs, T. T.; Farb, D. H. Inhibition of the NMDA response by pregnenolone sulphate reveals subtype selective modulation of NMDA receptors by sulphated steroids. *Br. J. Pharmacol.* **2002**, *135*, 901–909.
- (25) Horak, M.; Vlcek, K.; Chodounska, H.; Vyklicky, L., Jr. Subtype-dependence of N-methyl-D-aspartate receptor modulation by pregnenolone sulfate. *Neuroscience* **2006**, *137*, 93–102.
- (26) Paul, S. M.; Doherty, J. J.; Robichaud, A. J.; Belfort, G. M.; Chow, B. Y.; Hammond, R. S.; Crawford, D. C.; Linsenbardt, A. J.; Shu, H. J.; Izumi, Y.; Mennerick, S. J.; Zorumski, C. F. The major brain cholesterol metabolite 24(S)-hydroxycholesterol is a potent allosteric modulator of N-methyl-D-aspartate receptors. *J. Neurosci.* **2013**, *33*, 17290–17300.
- (27) Mony, L.; Zhu, S.; Carvalho, S.; Paoletti, P. Molecular basis of positive allosteric modulation of GluN2B NMDA receptors by polyamines. *EMBO J.* **2011**, *30*, 3134–3146.
- (28) Costa, B. M.; Irvine, M. W.; Fang, G.; Eaves, R. J.; Mayo-Martin, M. B.; Skifter, D. A.; Jane, D. E.; Monaghan, D. T. A novel family of negative and positive allosteric modulators of NMDA receptors. *J. Pharmacol. Exp. Ther.* **2010**, *335*, 614–621.
- (29) Sapkota, K.; Irvine, M. W.; Fang, G.; Burnell, E. S.; Bannister, N.; Volianskis, A.; Culley, G. R.; Dravid, S. M.; Collingridge, G. L.; Jane, D. E.; Monaghan, D. T. Mechanism and properties of positive allosteric modulation of N-methyl-d-aspartate receptors by 6-alkyl 2-naphthoic acid derivatives. *Neuropharmacology* **2017**, *125*, 64–79.
- (30) Mullasseril, P.; Hansen, K. B.; Vance, K. M.; Ogden, K. K.; Yuan, H.; Kurtkaya, N. L.; Santangelo, R.; Orr, A. G.; Le, P.; Vellano, K. M.; Liotta, D. C.; Traynelis, S. F. A subunit-selective potentiator of NR2C- and NR2D-containing NMDA receptors. *Nat. Commun.* **2010**, *1*, 90.
- (31) Khatri, A.; Burger, P. B.; Swanger, S. A.; Hansen, K. B.; Zimmerman, S.; Karakas, E.; Liotta, D. C.; Furukawa, H.; Snyder, J. P.; Traynelis, S. F. Structural determinants and mechanism of action of a GluN2C-selective NMDA receptor positive allosteric modulator. *Mol. Pharmacol.* **2014**, *86*, 548–560.
- (32) Hackos, D. H.; Lupardus, P. J.; Grand, T.; Chen, Y.; Wang, T.-M.; Reynen, P.; Gustafson, A.; Wallweber, H. J.; Volgraf, M.; Sellers, B. D.; Schwarz, J. B.; Paoletti, P.; Sheng, M.; Zhou, Q.; Hanson, J. E. Positive allosteric modulators of GluN2A-containing NMDARs with distinct modes of action and impacts on circuit function. *Neuron* **2016**, *89*, 983–999.
- (33) Volgraf, M.; Sellers, B. D.; Jiang, Y.; Wu, G.; Ly, C. Q.; Villemure, E.; Pastor, R. M.; Yuen, P. W.; Lu, A.; Luo, X.; Liu, M.; Zhang, S.; Sun, L.; Fu, Y.; Lupardus, P. J.; Wallweber, H. J.; Liederer, B. M.; Deshmukh, G.; Plise, E.; Tay, S.; Reynen, P.; Herrington, J.; Gustafson, A.; Liu, Y.; Dirksen, A.; Dietz, M. G.; Liu, Y.; Wang, T. M.; Hanson, J. E.; Hackos, D.; SearceLevie, K.; Schwarz, J. B. Discovery of GluN2A-selective NMDA receptor positive allosteric modulators (PAMs): tuning deactivation kinetics via structure-based design. *J. Med. Chem.* **2016**, *59*, 2760–2779.
- (34) Villemure, E.; Volgraf, M.; Jiang, Y.; Wu, G.; Ly, C. Q.; Yuen, P.-w.; Lu, A.; Luo, X.; Liu, M.; Zhang, S.; Lupardus, P. J.; Wallweber, H. J.; Liederer, B. M.; Deshmukh, G.; Plise, E.; Tay, S.; Wang, T.-M.; Hanson, J. E.; Hackos, D. H.; Searce-Levie, K.; Schwarz, J. B.; Sellers, B. D. GluN2A-Selective pyridopyrimidinone series of NMDAR positive allosteric modulators with an improved *in vivo* profile. *ACS Med. Chem. Lett.* **2016**, *8*, 84–89.
- (35) Perszyk, R.; Katzman, B. M.; Kusumoto, H.; Kell, S. A.; Epplin, M. P.; Tahirovic, Y. A.; Moore, R. L.; Menaldino, D.; Burger, P.; Liotta, D. C.; Traynelis, S. F. An NMDAR positive and negative allosteric modulator series share a binding site and are interconverted by methyl groups. *eLife* **2018**, *7*, No. e34711.
- (36) Baell, J. B.; Holloway, G. A. New substructure filters for removal of pan assay interference compounds (PAINS) from screening libraries and for their exclusion in bioassays. *J. Med. Chem.* **2010**, *53*, 2719–2740.
- (37) Schell, M. J.; Brady, R. O., Jr.; Molliver, M. E.; Snyder, S. H. D-serine as a neuromodulator: regional and developmental localizations in rat brain glia resemble NMDA receptors. *J. Neurosci.* **1997**, *17*, 1604–1615.
- (38) Kartvelishvili, E.; Shleper, M.; Balan, L.; Dumin, E.; Wolosker, H. Neuron-derived D-serine release provides a novel means to activate N-methyl-D-aspartate receptors. *J. Biol. Chem.* **2006**, *281*, 14151–14162.
- (39) Li, S.; Uno, Y.; Rudolph, U.; Cobb, J.; Liu, J.; Anderson, T.; Levy, D.; Balu, D. T.; Coyle, J. T. Astrocytes in primary cultures express serine racemase, synthesize d-serine and acquire A1 reactive astrocyte features. *Biochem. Pharmacol.* **2018**, *151*, 245–251.
- (40) Liu, Y.; Li, M.; Fan, M.; Song, Y.; Yu, H.; Zhi, X.; Xiao, K.; Lai, S.; Zhang, J.; Jin, X.; Shang, Y.; Liang, J.; Huang, Z. Chromodomain

Y-like protein-mediated histone crotonylation regulates stress-induced depressive behaviors. *Biol. Psychiatry* **2019**, *85*, 635–649.

(41) (a) Cao, X.; Zhang, Y.; Chen, Y.; Qiu, Y.; Yu, M.; Xu, X.; Liu, X.; Liu, B. F.; Zhang, L.; Zhang, G. Synthesis and biological evaluation of fused tricyclic heterocycle piperazine (piperidine) derivatives as potential multireceptor atypical antipsychotics. *J. Med. Chem.* **2018**, *61*, 10017–10039. (b) Chen, Y.; Wang, S.; Xu, X.; Liu, X.; Yu, M.; Zhao, S.; Liu, S.; Qiu, Y.; Zhang, T.; Liu, B. F.; Zhang, G. Synthesis and biological investigation of coumarin piperazine (piperidine) derivatives as potential multireceptor atypical antipsychotics. *J. Med. Chem.* **2013**, *56*, 4671–4690. (c) Cao, X.; Chen, Y.; Zhang, Y.; Qiu, Y.; Yu, M.; Xu, X.; Liu, X.; Liu, B. F.; Zhang, G. Synthesis and biological evaluation of new 6-hydroxypyridazinone benzisoxazoles: Potential multi-receptor targeting atypical antipsychotics. *Eur. J. Med. Chem.* **2016**, *124*, 713–728.